NTNU

Norwegian University of
Science and Technology

L1 Adaptive Control in Managed Pressure Drilling

Torbjørn Pedersen

Master of Science in Engineering Cybernetics
Submission date: June 2009
Supervisor: Ole Morten Aamo, ITK
Co-supervisor: Glenn-Ole Kaasa, StatoilHydro

Norwegian University of Science and Technology
Department of Engineering Cybernetics

Problem Description

Objective

The goal of the thesis is to evaluate different adaptive pressure control solutions for Managed Pressure Drilling. The candidate will compare robustness and performance of the control solutions with a reference controller using a previously created simulation model.

Main tasks and topics to address

The main tasks of the thesis consist of design and implementation of different adaptive controllers, and a thorough simulation study on robustness and performance under the influence of noise, disturbances and changing system parameters. The project will build upon previously created simulation models and results from the project completed by the candidate during the fall of 2008.

The thesis is divided into multiple parts: theory; controller design and analysis; and a simulation study of robustness and performance. The candidate will also look into different control structures for Managed Pressure Drilling.

1. Theory
    a. Present the necessary background on Managed Pressure Drilling and adaptive control.
2. Controller design and analysis
    a. Determine a system design model.
    b. Implement a reference controller which will be used as a performance benchmark.
    c. Design and implement different adaptive controllers to evaluate the possible benefits and problems of using adaptive control in Managed Pressure Drilling.
    d. Perform an robustness and performance analysis of the controllers.
3. Simulation study
    a. Perform a thorough simulation study to evaluate controller robustness and performance under the influence of noise, changing parameters and disturbances during common drilling operations.
    b. Perform a comprehensive analysis and discussion of the simulation results.

Assignment given: 12. January 2009
Supervisor: Ole Morten Aamo, ITK

Preface

This Master's Thesis was written during the spring of 2009 as the final part of the Master of Science program at the Norwegian University of Science and Technology (NTNU) at the department of Engineering Cybernetics. The work has been time consuming, but very interesting and rewarding.

The project delivery consists of this report and a compact disk. On the compact disk you will find: the simulator developed in Matlab, Simulink models of the system, simulation data, Maple and Matlab scripts, figure files, and parts of the bibliography.

I would like to thank Dr.ing. Glenn-Ole Kaasa from StatoilHydro and Professor Ole Morten Aamo at NTNU for guidance. A special thanks goes to Øyvind Nistad Stamnes from the PhD program at NTNU for great help with the thesis. I would also like to thank my fellow students Eirik and Hans-Kristian for help with the project and LaTeX. Last, but not least, I would like to thank my girlfriend Tuva for proofreading and for being so patient with me.

Torbjørn Pedersen
Trondheim, June 2009

Abstract

The control solution is a crucial part of Managed Pressure Drilling. Existing solutions are often based on Proportional plus Integral (PI) control and have several drawbacks, mainly poor performance for some common drilling operations and a large need for retuning. Better control solutions will reduce costs and improve safety.

This thesis presents a comparison of two adaptive control solutions versus a PI benchmark. Both complexity, tuning, performance and robustness will be compared. The two adaptive solutions considered are the well-known Model-Reference Adaptive Control method, and the recently developed $\mathcal{L}_1$ adaptive control method.

The control solutions are tested on a wide range of common drilling operations, some common controller issues, changing parameters and for two different control setpoints. The adaptive control solutions are shown to give better performance and to have less need for retuning, but not without costs. The main issues of the $\mathcal{L}_1$ adaptive controller is low time-delay margins and high computational demands, but the performance is much better than for the benchmark controller.

The most important recommendation for future work is evaluation of higher order filter designs for the $\mathcal{L}_1$ adaptive controller, because of the potential to both reduce computational needs and to optimize time-delay margins.

Glossary

ACC : American Control Conference
AIAA : American Institute of Aeronautics and Astronautics
CPU : Central Processing Unit
IADC : International Association of Drilling Contractors
IRIS : International Research Institute of Stavanger
MIMO : Multiple-Input and Multiple-Output
MPD : Managed Pressure Drilling
MPT : Mud Pulse Telemetry
MRAC : Model-Reference Adaptive Control
MWT : Measurement While Drilling
ODE : Ordinary Differential Equation
PI-Controller : Proportional plus Integral Controller
RCD : Rotating Control Device
ROP : Rate Of Penetration
SISO : Single-Input and Single-Output
UBO : Underbalanced Operation
UKF : Unscented Kalman Filter

Contents

1 Introduction **1**
- 1.1 Motivation and Goal . . . 1
- 1.2 Layout of the Report . . . 2

2 Theory and background **5**
- 2.1 Background on Managed Pressure Drilling . . . 5
  - 2.1.1 What is Managed Pressure Drilling . . . 5
  - 2.1.2 How does Managed Pressure Drilling work? . . . 6
  - 2.1.3 Benefits of MPD . . . 6
  - 2.1.4 The Well . . . 8
  - 2.1.5 Drilling Operations and Problems . . . 9
- 2.2 Mathematical Model of the Well . . . 11
- 2.3 Control Methods in MPD . . . 12
- 2.4 Adaptive Control . . . 13
- 2.5 Issues in Adaptive Control . . . 13
- 2.6 Model-Reference Adaptive Control . . . 15
- 2.7 $\mathcal{L}_1$ Adaptive Control . . . 16
  - 2.7.1 Introduction . . . 16
  - 2.7.2 Existing Literature . . . 16
  - 2.7.3 Preliminaries . . . 17
  - 2.7.4 Problem Formulation . . . 19
  - 2.7.5 Companion Model Adaptive Control . . . 20
  - 2.7.6 The $\mathcal{L}_1$ Adaptive Controller . . . 20
  - 2.7.7 Design Parameters - How to Achieve the Desired Specifications . . . 22
  - 2.7.8 The Theory of Fast and Robust Adaptation . . . 24
  - 2.7.9 Project Highlights . . . 26

3 Control Design **27**
- 3.1 Proportional plus Integral Controller . . . 27
- 3.2 Model-Reference Adaptive Control . . . 29
  - 3.2.1 System Model . . . 29
  - 3.2.2 The Reference Model . . . 29
  - 3.2.3 The Basic Controller . . . 30
  - 3.2.4 The Update Laws . . . 30
  - 3.2.5 Modifications for Improved Robustness . . . 30
  - 3.2.6 Bottomhole Control . . . 32

3.3 $\mathcal{L}_1$ Adaptive Controller . . . 33
3.3.1 Topside Control . . . 33
3.3.2 Bottomhole Control . . . 37
3.4 Bottomhole Control - Determining an Observer . . . 39
3.5 Topside Control - Determining a Path Generator . . . 39

4 Analysis **41**
4.1 Model-Reference Adaptive Control . . . 41
4.1.1 Stability . . . 41
4.2 $\mathcal{L}_1$ Adaptive Controller . . . 43
4.2.1 Stability . . . 43
4.2.2 Performance . . . 44
4.3 Stability margins . . . 46
4.4 $\mathcal{L}_1$ Time Delay and Gain Margin Analysis . . . 47

5 Simulation **49**
5.1 Simulation Tools . . . 49
5.2 Simulation of Scenarios . . . 50
5.2.1 A Connection . . . 50
5.2.2 Power-loss . . . 52
5.2.3 Reservoir Fluid Loss and Influx . . . 52
5.2.4 Fast Changing Pressure Term . . . 55
5.2.5 Inner Flow Dynamics and Gas in the Choke . . . 55
5.3 Controller Issues . . . 57
5.3.1 Measurement Noise . . . 57
5.3.2 Control Input Saturation . . . 57
5.3.3 Sampling and Numerical Effects . . . 59
5.4 Changing Well Parameters . . . 63
5.4.1 Changing Mud Weight . . . 63
5.4.2 Changing Bulk Modulus . . . 64
5.4.3 Changing Friction Parameters . . . 66
5.5 Control Structure . . . 66
5.5.1 Topside Control . . . 66
5.5.2 Bottomhole Control . . . 66
5.5.3 Comparison of Control Structures . . . 67

6 Discussion **69**
6.1 Controller Complexity . . . 69
6.1.1 The PI Controller . . . 69
6.1.2 The MRAC Controller . . . 69
6.1.3 The $\mathcal{L}_1$ Adaptive Controller . . . 70
6.1.4 Sampling and Numerical Issues . . . 70
6.2 Tuning Aspects . . . 70
6.2.1 The PI Controller . . . 71
6.2.2 The MRAC . . . 71
6.2.3 The $\mathcal{L}_1$ Adaptive Controller . . . 71
6.3 Controller Performance and Robustness . . . 72

6.4 Evaluation of Control Structures . . . 72
6.5 $\mathcal{L}_1$ Highlights . . . 73
6.6 Conclusions . . . 73
6.7 Contributions . . . 74
6.8 Future work . . . 74

A Preliminaries **77**
A.1 Theorems . . . 77

B Tuning **79**
B.1 $\mathcal{L}_1$ Tuning . . . 79
B.1.1 Adaptive Gain Settings for the $\mathcal{L}_1$ Adaptive Controller . . . 79
B.1.2 Selection of Initial Values . . . 82
B.2 MRAC Tuning . . . 83
B.2.1 Different Reference Model Settings for the MRAC . . . 83
B.2.2 Selection of Adaptive Gains . . . 85
B.2.3 Selection of Initial Values . . . 86
B.3 PI Tuning . . . 88
B.3.1 Different Tuning Settings for the PI-Controller . . . 88

C Simulations **93**
C.1 Simulation Overview . . . 93

Bibliography **93**

List of Figures

2.1 Managed Pressure Drilling illustrated 7
2.2 Well pressure limits 8
2.3 Simplified well schematic 9
2.4 Illustration of the MRAC scheme 15
2.5 $\mathcal{L}_1$ gain: Interconnected system 18
2.6 Illustration of the CMAC scheme 20
2.7 Time-delay margins and λ versus increased bandwidth 25

3.1 Closed loop with $\mathcal{L}_1$ adaptive controller 35

4.1 Finding time-delay and gain margins 46

5.1 Connection scenario: Tracking performance 51
5.2 Connection scenario: Control input 51
5.3 Power loss scenario: Tracking performance 52
5.4 Loss scenario - High flow: Tracking performance 53
5.5 Loss scenario - Low flow: Tracking performance 54
5.6 Kick scenario: Tracking performance 54
5.7 Fast ΔP term: Tracking performance 55
5.8 Slow inner flow dynamics: Tracking performance 56
5.9 Noise: $\mathcal{L}_1$ adaptive controller 58
5.10 $\mathcal{L}_1$ adaptive controller: Step-size 60
5.11 Sampling 1 sec: Tracking performance 61
5.12 Sampling 2 sec: Tracking performance 61
5.13 Sampling, dynamics and control hold: Tracking performance 62
5.14 Changing bulk modulus: Tracking performance 64
5.15 Changing bulk modulus: Control input 65
5.16 Ideal conversion: Control structure 67
5.17 Observer: Control structure 68

B.1 Tuning of L1: Adaptive gains - Tracking performance 80
B.2 Tuning of L1: Adaptive gains - Control input usage 80
B.3 Tuning of L1: Adaptive gains - parameter σ 81
B.4 Tuning of L1: Adaptive gains - parameter ω 81
B.5 Tuning of L1: Adaptive gains - State estimate 82
B.6 Tuning of MRAC: Reference systems - Tracking performance 83
B.7 Tuning of MRAC: Reference systems - Control input 84

B.8 Tuning of MRAC: Adaptive gains - Tracking performance 85
B.9 Tuning of MRAC: Initial values - Tracking performance 86
B.10 Tuning of MRAC: Initial values - Control input 87
B.11 Tuning of PI controller: Tracking performance 89
B.12 Tuning of PI controller: Control input usage 90

Chapter 1

Introduction

1.1 Motivation and Goal

The control solution is a crucial part of MPD. Existing solutions are mostly based on conventional PI control. One of the main drawbacks of PI solutions is that performance degrades during critical and common operations such as a connection or movements of the drill string. A second main drawback is the large need for manual tuning of the controllers, which means that the performance degrades during drilling without continuous re-tuning.

The PI-Controller depends heavily on integral action to compensate for friction loss in the well. Only a small proportional term can be used, to prevent generating pressure pulses by fast changes in the control input. The result is that conventional control will react slowly to fast pressure changes and have poor disturbance attenuation in these cases (Kaasa 2007).

Better control solutions will lead to reduced costs in drilling due to higher efficiency and reduced drilling time. They make new reservoirs drillable and contribute to safety by increasing safety margins through increased control and early detection and mitigation of potential hazards.

The measurement signals available for control in MPD are often not dependable. We might lose measurements, or the value of the measurements might be altered while passing through database systems which perform filter operations on the signals. We therefore look for controllers which do not need many measurement signals.

We thus look for robust adaptive controllers which require few signals. I have chosen to look into $\mathcal{L}_1$ adaptive control since it offers to be both a robust controller, needs little tuning and uses few measurement signals. The control method is very new and there are few reports of actual use, so I think it is of great interest to evaluate if the controller is as good as the developers claim. It is also of personal interest to the author, on the background of having been to an adaptive control workshop where this control architecture was presented and much discussed. We come back to why it is interesting to evaluate $\mathcal{L}_1$ adaptive control in the theory and background chapter and see some

interesting highlights.

The goal of this project is to evaluate the usefulness of adaptive control in MPD, and especially $\mathcal{L}_1$ adaptive control. To evaluate the $\mathcal{L}_1$ controller we will compare it with a PI controller and a more known adaptive control technique: MRAC. MRAC, which is evaluated in Pedersen (2008), is selected because it is in many ways similar to $\mathcal{L}_1$ control, except for some key areas. The PI controller is a natural choice as reference controller. The widespread use in the industry is not without reason, and it is interesting to see how much we can gain by using adaptive control. The main focus will be the comparison of the $\mathcal{L}_1$ adaptive controller and the PI controller.

Both the need for tuning, complexity, robustness and performance of the controllers will be evaluated.

It is also of great interest to evaluate different control structures for MPD. I will look at both a topside scheme controlling the bottomhole pressure indirectly by controlling the choke pressure, and a direct bottomhole scheme controlling the bit pressure.

1.2 Layout of the Report

The remainder of this thesis is structured into five parts and some additional appendices.

1. **Chapter 2: Theory and Background** - I start with presenting some background theory on some important topics for this thesis. This chapter includes:
    - MPD - The background concepts for Managed Pressure Drilling. How does it work and why do we need better controllers?
    - Mathematical model - Presentation of the model used for the derivations of controllers in later chapters.
    - Control structure - Different control structures for MPD.
    - Adaptive control - What can be gained by using adaptive controllers, and what are the main challenges with adaptive control.
    - MRAC - What is the background and main concept of Model-Reference Adaptive Control?
    - $\mathcal{L}_1$ adaptive control - What is $\mathcal{L}_1$ adaptive control and how does it work?
2. **Chapter 3: Control Design** - In the third chapter, control design and controller construction is completed. The chapter is divided into four main sections:
    - Proportional-Integral Controller - A standard PI controller is first introduced to be used as the benchmark.
    - MRAC - Derivation of the MRAC, including reference system, control equation and update laws.

- $\mathcal{L}_1$ adaptive control - An $\mathcal{L}_1$ controller is derived for both topside and bottomhole control, and several decisions are made about design parameters.
- Control structure - Simple designs for both topside and bottomhole control are constructed. We select an observer for estimating parameters and bit pressure.

3. **Chapter 4: Analysis** - The next part is controller analysis. We look into stability and margins of the controllers. The sections are divided into:
   - MRAC - Derivation of stability.
   - $\mathcal{L}_1$ adaptive control - Stability and performance.
   - Time-delay margins of the controllers.
4. **Chapter 5: Simulation** - In the fifth chapter I present scenarios and simulation results. We compare $\mathcal{L}_1$ adaptive controller versus MRAC and the benchmark controller. We will look into:
   - Scenarios - Some common drilling scenarios are evaluated.
   - Controller issues - The effects of noise, saturation, sampling and numerical issues.
   - Parameter changes - Some important system parameters are changed to evaluate robustness.
   - Control structure - The control strategies are evaluated.
5. **Chapter 6: Discussion** - In the final part we discuss the findings from chapter 4 and 5 and look into what more can be done in future work. The discussion includes:
   - Tuning and complexity - Do we have to perform continuous retuning of controllers when parameters are changing, and how complex does the controller grow?
   - Performance - How good is controller performance versus the PI benchmark?
   - Robustness - How well do the controllers handle changing parameters and disturbances?
   - Control structure - What are the strengths of the different control strategies and do they have a large impact on performance?
   - $\mathcal{L}_1$ adaptive control highlights.
   - Final conclusions and contributions of this thesis.
   - Recommendations for future work.
6. **Appendices** - The appendices includes:
   - Additional theorems and preliminaries.

- Controller tuning.
- Simulation tables.

Chapter 2

Theory and background

This chapter presents the necessary background to understand the problem, the challenges and the technology evaluated and used in this thesis. The chapter is in no way a complete summary of any of the areas presented, but is meant to be a quick introduction to give basic understanding.

Since the background of this project is very similar to my previous project on MRAC in MPD (Pedersen 2008), the introductory parts on MPD and MRAC are much the same. However, all the sections have been revised and the focus on MRAC has been downplayed. Completely new in this introduction is the part on $\mathcal{L}_1$ adaptive control.

2.1 Background on Managed Pressure Drilling

2.1.1 What is Managed Pressure Drilling

The definition of Managed Pressure Drilling, taken from the IADC UBO and MPD Subcommittee is (Hannegan 2006):

"Managed Pressure Drilling (MPD) means an adaptive drilling process used to control precisely the annular pressure profile throughout the wellbore. The objectives are to ascertain the downhole pressure environment limits and to manage the annular hydraulic pressure profile accordingly."

We will in the next sections take a closer look at what this really means, and what can be gained by using MPD rather than conventional drilling methods.

The IADC UBO and MPC subcommittee has also created a UBO and MPD glossary[1]. This could be a good starting point to get into the terminology of MPD and all the TLAs (three letter abbreviations) of drilling.

[1]The document can be found at www.iadc.org/committees/ubo_mpd/completed_documents.html

2.1.2 How does Managed Pressure Drilling work?

What takes MPD beyond conventional drilling is the ability to control the pressure in the well without changing the mud density. This is accomplished by sealing the top drive with a rotating control device (RCD), the use of a control valve and an extra pump. As indicated in figure 2.1 the annulus is sealed to create a pressurized system.

While drilling there are some pressure constraints which must be satisfied, mainly the pore pressure and the fracture pressure. Falling below the pore pressure will result in influx from the reservoir. This is unwanted, because during drilling the right equipment to handle large influx is not in place and a large amount of influx may even result in a blowout (uncontrollable kick). Breaking the fracture pressure can result in lost circulation: a large loss of mud to the reservoir and possible damage to the production formation. If the drilling-fluid pressure is too low to maintain the structural integrity of the drilled hole, we can get pipe sticking or even a wall collapse leading to a loss of the entire well (Azar & Samuel 2007).

In figure 2.2 you see the upper and lower limits added to two reservoirs. Changes during extraction can make these limits very tight, leaving only a narrow window for drilling. Precise pressure control is therefore necessary to be able to drill such reservoirs. The lower line shows the static pressure, caused by the hydrostatic head pressure of the mud in the hole (MW). The upper line shows the additional term added by annulus friction pressure (AFP / ECD) caused by circulating mud. By sealing the well to create a pressure system and by use of a control valve, we get an additional adjustable pressure term (BP). This term can be used to change the well pressure. The variation in effective bottomhole pressure (EBHP) is given as (Hannegan 2006):

$$\text{EBHP} = \text{MW} + \Delta\text{AFP} + \Delta\text{BP} \tag{2.1}$$

It is now possible to adjust the pressure at the setpoint location without changing the mud density. This setpoint location is usually at the location with the smallest pressure margins.

2.1.3 Benefits of MPD

There are several motivating factors for using MPD (Kaasa 2007, Hannegan 2006-2007, van Riet, Reitsma & Vandecraen 2003). For instance:

- Reduced formation damage (this is a significant problem in the case of unstable formations and borehole stability problems).
- Improved Rate of Penetration (ROP).
- Reach "undrillable reserves" where pressure margins are too small for the well to be drilled without pressure control.
- Faster drilling operation.
- Reduced non-productivity time.

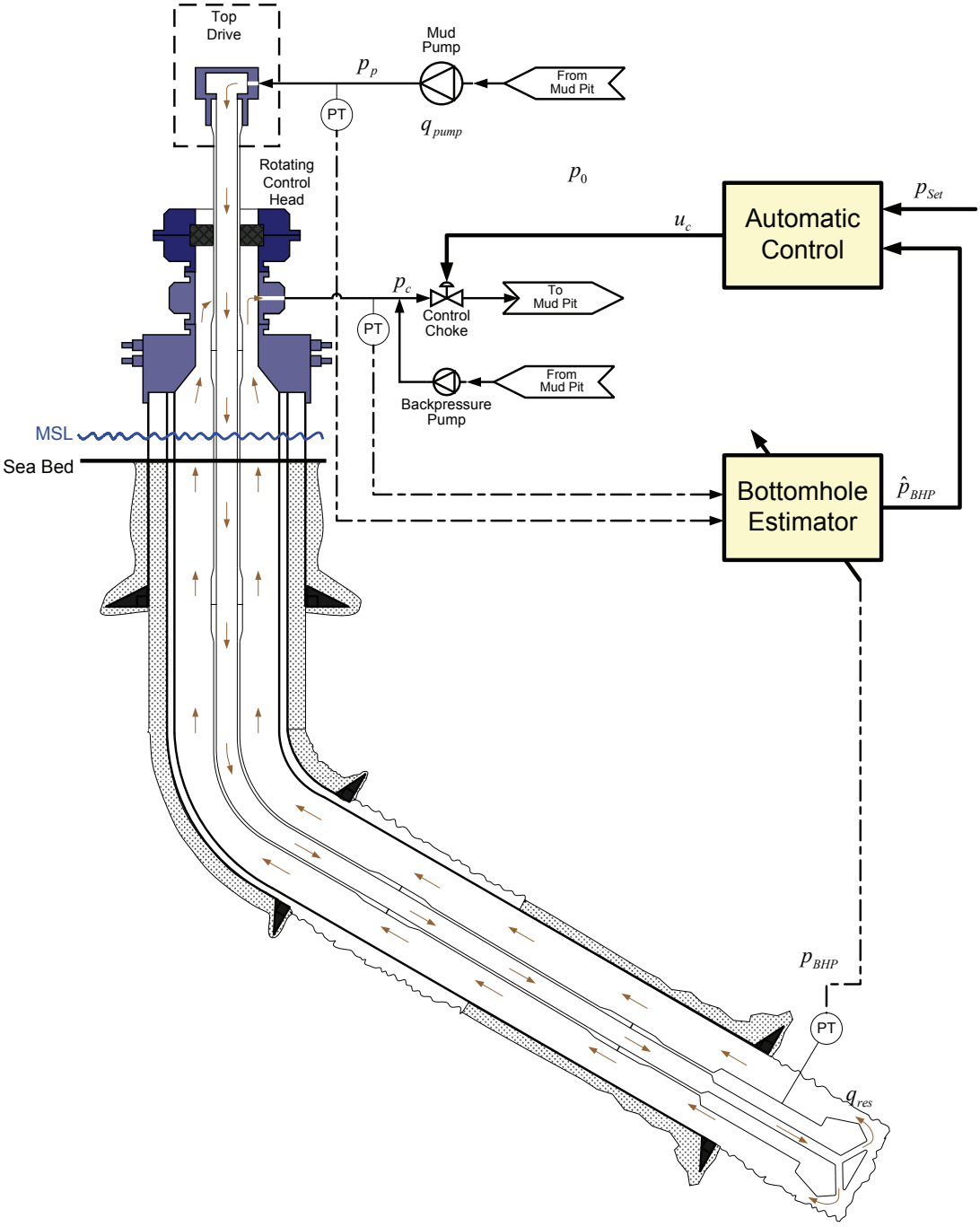

Figure 2.1: Managed Pressure Drilling illustrated (Kaasa 2008).

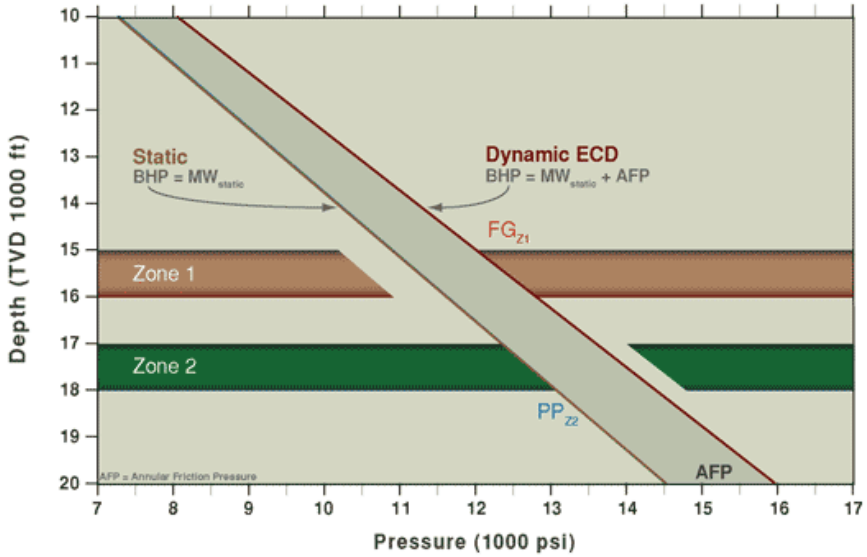

Figure 2.2: Well pressure limits (AtBalance 2008).

- Improved safety.
- Reduction of mud losses.
- Reduction of formation fluid influx.
- Automatic kick circulation.

In short: better economy, better safety margins, the possibility to drill previously "undrillable" wells and shorter time to production.

2.1.4 The Well

The well can be divided into two parts: the drill string and the annulus. This is illustrated in figure 2.3.

The drill string part consists of the topside assembly, sections of pipe, the Measurement While Drilling (MWD) unit and the bit. Drilling mud is pumped down the drill string and exits through the bit. There is a one-way valve at the bit, preventing flow into the drill string.

The MWD unit consists of a large section of measurement devices, which provides downhole measurements at a good sampling rate. However, the common way of sending data from the MWD unit to the topside installation is by Mud Pulse Telemetry (MPT), which works by creating rapid fluctuations in the pressure of a closed loop circulating system. The bit rate is very low, approximately 10-20 bps. This is not enough for real-time transmission of all the measured parameters. If the circulation is low, the pulsing is no longer possible, and we have no bottomhole measurements (Stamnes 2007).

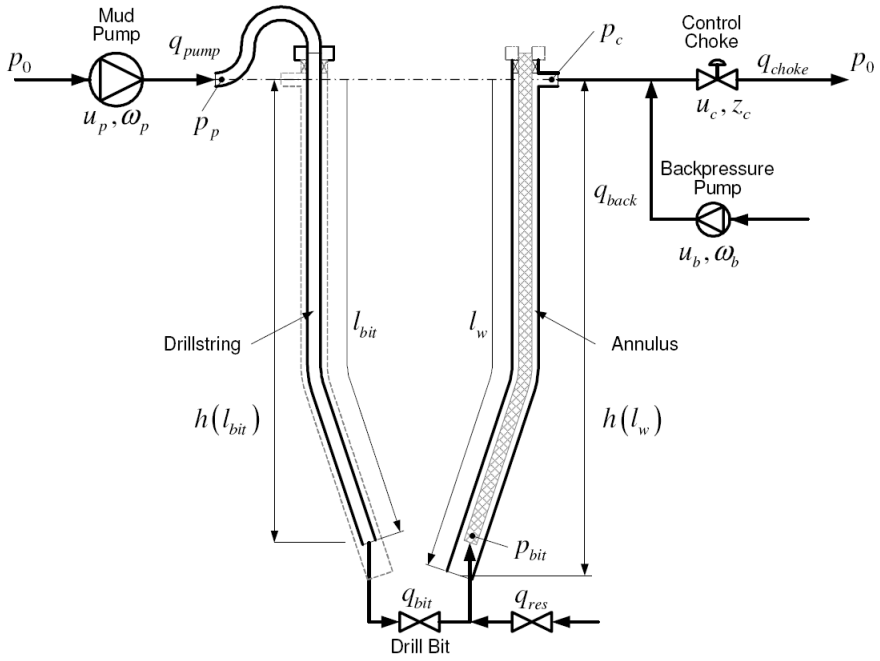

Figure 2.3: Simplified well schematic, from Kaasa (2007).

The annulus part consists of the well outside the drill string. At the bottom we find the open hole region (and possibly the reservoir), further up is the cased part of the well and the control choke.

The drilling mud has several functions; it removes cuttings, contains subsurface formation fluid pressures, provides hole stabilization and serves many minor tasks, such as cooling, lubrication and reducing the weight of the drill string (Azar & Samuel 2007).

2.1.5 Drilling Operations and Problems

There are several common drilling operations and severe problems which may occur during drilling. Here is a short presentation of some of the scenarios which we will look into in the simulation section.

Pipe connection

Pipe connection is the procedure of connecting a new stand, or adding a new length of pipe, to the drill string. A stand is approximately 27 meters long, and with a drill speed of 15 meters/hour this means one connection operation takes place every two hours. For the new stand to be connected, the main mud pump must be ramped down to zero flow, and excess fluid in the drill string is bled off through a valve and returned to the mud tanks to reduce the main pump pressure to atmospheric pressure. The procedure is completed in about ten minutes, and then the flow is ramped back up (Stamnes 2007).

Mud loss

Mud or fluid loss is defined as the loss of a mud filtrate into a permeable formation that is being drilled. Because of positive differential pressure between the well pressure and the formation pressure, fluid tends to flow into the formation. There is always some loss to form a filter cake against the wellbore walls and this is even positive, but high continuous loss is damaging and can lead to damages on the producing formation and lower rate of penetration (Azar & Samuel 2007).

Lost circulation

Lost circulation is the situation where one has a large loss of drilling mud into a formation, causing a decrease in the mud hydrostatic head. This may happen if we drill into zones which are highly permeable, cavernous, inherently fractured or fractured due to improper drilling, casing or tripping practices. The first three are unavoidable, but the last condition can be prevented (Azar & Samuel 2007). The consequences of lost circulation depend on the amount of mud lost and the location of the loss. If the loss is large and we are in an interval containing overpressure, we might get a sudden influx of formation fluid which could lead to a blowout or formation breakdown (Jahn, Cook & Graham 2008).

Power loss

Power loss is defined here to mean a complete loss of power to the main mud-pump. The choke power and backpressure pump are assumed to be operating at a separate and independent power supply.

Kick

During drilling operations, an intrusion of formation fluids into the wellbore is termed a kick, and the fluid is called kick fluid. If effective measures are not taken, there is a potential for blowout, an uncontrolled kick. Blowouts can happen during drilling, tripping, casing or workover operations. The occurrence of a blowout can endanger life, the monetary investments and the environment. The prevention of blowouts is therefore the most important task in any drilling venture (Azar & Samuel 2007).

In general, a kick will occur when the pressure of formation fluids becomes greater than the pressure induced from the drilling fluid and the backpressure system. This may happen if we drill into an unexpected high-pressure zone or by drops in the wellbore fluid pressure (Azar & Samuel 2007).

2.2 Mathematical Model of the Well

The mathematical model used to develop the controllers in this thesis is based on the Kaasa model (Kaasa 2007). The Kaasa model is a reduced order model that aims at capturing the dominant phenomena of the system. Fast dynamics are ignored, similar effects are lumped together and slowly varying parameters are treated as constants. The model gives us a set of ODEs for the pressure of the mud pump, the choke pressure and for the flow in the bit.

The equations are derived both in Kaasa (2007) and Stamnes (2007) and are only summarized here for the reader's benefit.

The mud pump equation is given by:

$$\frac{V_d}{\beta_d}\dot{p}_p = q_{pump} - q_{bit}, \tag{2.2}$$

where V_d is the volume of the drill string, β_d is the bulk modulus of the drill string, p_p the pressure of the mud pump, q_{pump} the mud pump flow and q_{bit} is the bit flow. The choke pressure equation is:

$$\frac{V_a}{\beta_a}\dot{p}_c = -\dot{V}_a + q_{bit} + q_{res} + q_{back} - q_c, \tag{2.3}$$

where V_a is the volume of the annulus, β_a is the bulk modulus of the annulus, $\dot{V}_a$ is the change in volume in the annulus, p_c the pressure of the choke, q_{res} the reservoir influx, q_{back} the backpressure pump flow and q_c is the choke flow. The bit flow equation is given by:

$$[M_a + M_d]\dot{q}_{bit} = p_p - p_c - F_d|q_{bit}|q_{bit} - F_a|q_{bit} + q_{res}|(q_{bit} + q_{res}) + (\bar{\rho}_d - \bar{\rho}_a)gh_{bit}, \tag{2.4}$$

where M_a is the mass coefficient of the annulus, M_d is the mass coefficient of the drill string, h_{bit} the vertical depth of the bit, $\bar{\rho}_d$ the average density in the drill string, $\bar{\rho}_a$ the average density in the annulus and g is gravity. We will also use that $M = M_d + M_a$.

The equation for the bit pressure is given by

$$p_{bit} = p_c + M_a\dot{q}_{bit} + F_a|q_{bit} + q_{res}|(q_{bit} + q_{res}) + \bar{\rho}_a g h_{bit}. \tag{2.5}$$

The equations are solved in Matlab using a fixed step ODE solver.

In Kaasa (2007) there are also equations prestented for friction and geometry. These and additional equations were used to create the simulator used for simulations in the later chapters. For more details see Pedersen (2008).

There are at least two ways to control the system: we can either control q_c or z_c, where z_c is the choke opening.

If we are to control q_c we need some inner control loop to set the correct choke opening. We can simulate this as an added choke flow dynamic for the system.

$$q_c = \frac{{\omega_c}^2}{s^2 + 2\zeta_c\omega_c s + \omega_c^2} q_{c0} \tag{2.6}$$

where q_{c0} is the desired flow rate, ζ_c a dampening coefficient and w_c the resonance frequency. This means we will get some delay on the input signals. We will look closer at the effects of this delay.

The choke equation for choke flow is given by:

$$q_c = K_{choke} z_c \sqrt{\frac{2}{\rho_0}(p_c - p_0)} \tag{2.7}$$

Where K_{choke} is the choke gain constant and p_0 is the atmospheric pressure.

2.3 Control Methods in MPD

There are several different control strategies available for pressure control in MPD, but they are usually placed in one of two groups (Hannegan 2006).

- Reactive MPD: We perform drilling in the classic fashion, but add some kind of MPD system on top to handle any surprises during drilling.
- Proactive MPD: The drilling plan is designed from the start with the goal of using all the advantages of MPD. Quite naturally this method offers the greatest benefits.

There are many variations of MPD and some of the more common are (Hannegan 2006):

- Constant Bottomhole Pressure (CBHP)
- Pressurized Mud Cap Drilling (PMCD)
- Dual Gradient (DG)
- Return Flow Control / HSE
- Reverse Circulation (RC)

We might also select different setpoints to control, and either control this setpoint directly or indirectly. In this thesis we discuss two control settings:

- Indirect topside control: The pressure is indirectly controlled by adjusting the topside annulus pressure (the choke pressure).
- Direct bottomhole control: The pressure is stabilized at the desired set point directly.

The two control settings considered offer different benefits and drawbacks. Indirect topside control offers high frequency and robust measurements. However, it also introduces a need for conversion between wanted bottomhole pressure and choke pressure. This leads to the requirement of some kind of reference trajectory generator. This reference trajectory can be created using simulations, or by the use of some kind of estimator to get the system parameters required to perform a conversion.

If we use bottomhole control we do not need to perform the pressure conversion, but we have the additional problem of very scarce and noisy measurements. Control using only bottomhole pressure readings every 30 seconds is clearly not sufficient. This leads to the need for developing observers for the bottomhole pressure. Such an observer can use the good top side measurements to create a fairly accurate pressure profile of the well. One possible choice is the observer developed in Stamnes (2007).

2.4 Adaptive Control

Adaptive control has received much attention from the control society, but it has also always been a controversial subject. Often you will hear statements like "adaptive control is complex", or "do not use adaptive control unless it is absolutely necessary". Unfortunately there is some truth to these statements, but many theoretical developments in the last decades has brought adaptive control much closer to practice. There are also many examples of successful industrial applications (Butler 1992).

So why use adaptive control? A fixed controller cannot provide acceptable system behavior in all situations, particularly if the process to be controlled has unknown or time-varying parameters (Butler 1992).

Adaptive control offers better performance when dealing with complex systems that have unpredictable parameter deviations and uncertainties, and can maintain consistent performance in the presence of uncertainty and variations in plant parameters. Robust control is an alternative to adaptive control and has some advantages when dealing with disturbances and quickly varying parameters, but adaptive control is superior in dealing with uncertainty in constant or slow-varying parameters. The best solution might thus be an adaptive augmentation of a robust baseline controller (Wise, Lavretsky & Hovakimyan 2008).

An interesting observation is that integral effect is adaptive control in its simplest form and that standard adaptive laws are essentially integrators with finite gain at all frequencies except zero (Tsakalis & Ioannou 1993).

2.5 Issues in Adaptive Control

There are several causes of instability in adaptive systems. Perhaps the most important according to Ioannou & Sun (1996) are:

- Parameter drift

- High-gain instability
- Instability resulting from fast adaptation
- High-frequency instability
- Effects of parameter variations

When the system is unable to differentiate between noise and good parameter information, the estimated parameters may drift slowly with time, and we can suddenly get large fluctuations in parameters and output. This phenomenon is known as bursting and may happen even in ideal simulations due to small numerical errors (Wise et al. 2008, Ioannou & Sun 1996).

Many methods have been developed to solve parameter drift issues and admissibility problems in adaptive control. Some of the primary methods are:

- Deadzone
- Excitation
- Parameter projection and / or leakage
- Model based supervision

The deadzone is implemented by switching off the estimator when the prediction error gets below a certain threshold. The parameters converge if the deadzone is large enough, but if it is too large, performance will suffer. If the threshold is too small, parameter drift is reintroduced (Dozal-Mejorada & Ydstie 2007).

Excitation methods present the estimator with informative data all the time. The parameter estimates will then remain close to the "true parameters". The problem with excitation is that we need strong excitation to overcome the noise, yet it must be subtle enough that performance does not suffer (Dozal-Mejorada & Ydstie 2007).

Parameter projection constrains the parameters so that they do not wander out of the admissible set. Projection solves the problem using hard constraints, while leakage uses soft constraints. Neither method solves the drift problem completely and we might get poor closed loop performance if the bounds / leakage parameters are not well chosen (Dozal-Mejorada & Ydstie 2007).

Model based supervision solves the problem of parameter drift and ensures admissibility by using a second adaptive controller to detect if an event really was informative before letting it into the data record. The second adaptive model estimates the disturbance and uses a switch to turn on adaptation only if the prediction error of the control design is larger than the estimate of the disturbance (Dozal-Mejorada & Ydstie 2007).

The adaptive control law can generate a high-gain feedback which excites unmodeled dynamics and leads to instability and unbounded solutions. This kind of instability is referred to as high-gain instability and can be avoided by keeping the controller gains small (small loop gain) (Ioannou & Sun 1996).

Large adaptation gains increase the speed of adaptation, which in turn excites the unmodeled dynamics and may thus lead to instability (Ioannou & Sun 1996). We will look

into how $\mathcal{L}_1$ adaptive control handles this challenge.

We can get high-frequency instabilities if the reference signal has high frequencies which excites unmodeled dynamics. This may cause low signal-to-noise ratio, and therefore lead to wrong adjustments of parameters over time and eventually lead to instability. It should be noted that this instability is caused by adaptation and by switching the adaptation off, the instability ceases (Ioannou & Sun 1996).

Time-varying parameters will lead to the appearance of parameter error disturbance terms. This makes concluding boundedness of signals much harder, and besides for special classes of plants, it is hard to conclude boundedness if these disturbance terms are not decaying to zero exponentially fast (Ioannou & Sun 1996).

2.6 Model-Reference Adaptive Control

The MRAC technique was first introduced by Whitacker in 1958. One of the most popular schemes is shown in figure 2.4 (Butler 1992). A reference model is chosen to generate a desired trajectory y_m, that the plant out y_p should follow. The tracking error $e_1 \triangleq y_p - y_m$ represents the deviation between the plant output and the desired performance. The system has an ordinary feedback loop composed of the process and a controller, and another feedback loop that changes the controller parameters. The parameters are changed on the basis of feedback from the tracking error. The mechanism for adjusting the parameters is obtained either by gradient method or by applying stability theory (Åström & Wittenmark 1995, Ioannou & Sun 1996).

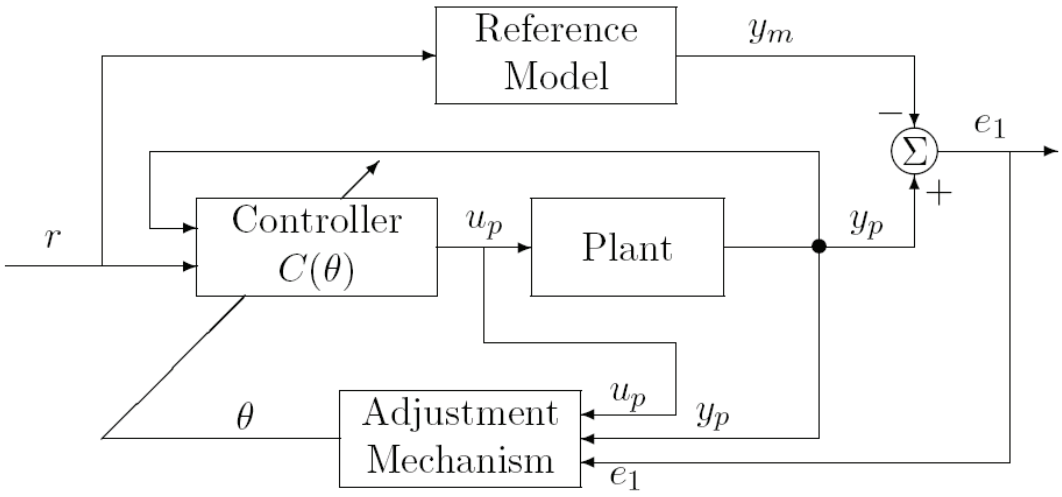

Figure 2.4: Illustration of the MRAC scheme (Ioannou & Sun 1996).

MRAC schemes can be either direct or indirect, and with normalized or unnormalized

adaptive laws. In direct MRAC the controller parameters are updated directly by an adjustment mechanism, while in indirect MRAC plant parameters are first estimated and then used to update the controller (Ioannou & Sun 1996).

There are many MRAC schemes which guarantee global asymptotic stability for linear continuous time minimum phase systems without unmodeled dynamics and disturbances. However, the very famous Rohrs example and the X-15 accident demonstrated that even small bounded disturbances and model mismatch might lead to instability.

When the input vectors to an MRAC system are rich enough, or persistently exciting of high enough order (the input is informative enough to allow the unique identification of system parameters), both simulations and analyses indicate that MRAC systems are robust with respect to non-parametric uncertainties. However, when the input is not rich enough, even small uncertainties may lead to severe problems (Wise et al. 2008).

2.7 $\mathcal{L}_1$ Adaptive Control

2.7.1 Introduction

In several papers, Chengyu Cao and Naira Hovakimyan have presented what they claim to be a novel adaptive control architecture. They name this control architecture $\mathcal{L}_1$ adaptive control (Cao & Hovakimyan 2006*a*, Cao & Hovakimyan 2006*b*).

So what is a $\mathcal{L}_1$ adaptive controller, and how does it work?

The starting point for the controller is a reparametrization of MRAC called Companion Model Adaptive Control (CMAC), which allows for the incorporation of a low-pass filter into the feedback loop. This structure along with a low-pass filter, will allow us to ensure a low-frequency control signal even in the presence of large adaptive gains.

This structure enables the possibility to enforce a desired transient performance, both for input and output signals, by increasing the adaptation gain . A problem is that we can no longer use the nice, clean reference system of MRAC. Unknown parameters are now part of the reference system, and we will need some other way of selecting the control specifications.

In this section we will take a closer look at how this works, what we need to select and what we gain from using an $\mathcal{L}_1$ adaptive controller. The section also includes a brief overview of some of the existing literature and what could be potential pitfalls of $\mathcal{L}_1$ adaptive control.

2.7.2 Existing Literature

Cao and Hovakimyan has produced many articles on $\mathcal{L}_1$ adaptive control, most are published in AIAA and ACC proceedings and journals, but quite a few are presented in large international control journals.

Evaluation on controller stability margins and proof of guaranteed transient performance for systems with bounded disturbances can be found in Cao & Hovakimyan (2008*a*), (2007*b*) and (2007*e*). The $\mathcal{L}_1$ adaptive controller is also developed for parametric strict feedback systems (Cao & Hovakimyan 2007*a*) and is shown to give good performance even with non-zero trajectory initialization error (Cao & Hovakimyan 2008*e*). The controller is also derived for the cases of unmodeled dynamics, unknown nonlinearities and unmatched disturbances (Cao & Hovakimyan 2008*d*, 2008*b*, 2008*c*).

The control architecture is extended to output feedback for time-varying unknown parameters, bounded disturbances and unknown dimension in Cao & Hovakimyan (2007*c*) and (2007*d*).

Articles showing possible uses include Patel, Cao, Hovakimyan, Wise & Lavretsky (2007), Cao, Hovakimyan, Kaminer, Patel & Dobrokhodov (2007) and Cao & Hovakimyan (2009).

2.7.3 Preliminaries

Most Cao and Hovakimyan papers begin with a short introduction of basic definitions and facts from linear systems theory that are needed for the derivation of the $\mathcal{L}_1$ adaptive controller, and I have chosen to do so as well.

$\mathcal{L}_\infty$ norms

For a signal ξ(t), $t \geq 0$, $\xi \in \mathbb{R}^n$, its truncated $\mathcal{L}_\infty$ norm and $\mathcal{L}_\infty$ norm are defined as

$$\|\xi_t\|_{\mathcal{L}_\infty} = \max_{i=1,..,n} \left(\sup_{0\leq\tau\leq t} |\xi_i(\tau)| \right), \tag{2.8}$$

$$\|\xi\|_{\mathcal{L}_\infty} = \max_{i=1,..,n} \left(\sup_{\tau\geq 0} |\xi_i(\tau)| \right), \tag{2.9}$$

where ξ_i is the i^{th} component of ξ.

$\mathcal{L}_2$ norm

The $\mathcal{L}_2$ norm for a transfer function is given by:

$$\|G(s)\|_{\mathcal{L}_2} = \left(\frac{1}{2\pi} \int_{-\infty}^{\infty} |G(j\omega)|^2 \, d\omega \right)^{1/2} \tag{2.10}$$

$\mathcal{L}_1$ gain

The $\mathcal{L}_1$ gain of a stable, proper SISO system $H(s)$ is defined to be

$$\|H(s)\|_{\mathcal{L}_1} = \int_0^{\infty} |h(t)| \, dt, \tag{2.11}$$

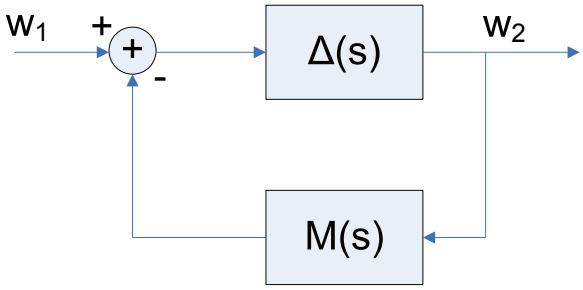

Figure 2.5: $\mathcal{L}_1$ gain: Interconnected system

where $h(t)$ is the impulse response of $H(s)$.

A continuous time LTI system (proper) with impulse response $h(t)$ is stable if and only if

$$\int_0^\infty |h(t)|\, dt < \infty \tag{2.12}$$

For a stable proper m input n output system $H(s)$ the $\mathcal{L}_1$ gain is defined as

$$\|H(s)\|_{\mathcal{L}_1} = \max_{i=1,..n} \left(\sum_{j=1}^{m} \|H_{ij}(s)\|_{\mathcal{L}_1} \right), \tag{2.13}$$

where $H_{ij}(s)$ is the *i*th row *j*th column element of element of $H(s)$.

For a stable proper MIMO system H(s) if the input $r(t) \in \mathbb{R}^m$ is bounded, then the output $x(t) \in \mathbb{R}^n$ is also bounded as $\|x_t\|_{\mathcal{L}_\infty} \leq \|H(s)\|_{\mathcal{L}_1} \|r\|_{\mathcal{L}_\infty}$, $\forall t \geq 0$.

$\mathcal{L}_1$ small gain theorem

The interconnected system in figure 2.5 with $w_2(s) = \Delta(s)(w_1(s) - M(s)w_2(s))$ with input $w_1(t)$ and output $w_2(t)$ is stable if

$$\|M(s)\|_{\mathcal{L}_1} \|\Delta(s)\|_{\mathcal{L}_1} < 1. \tag{2.14}$$

Projection operator

Consider a convex, compact set with a smooth boundary given by:

$\Omega_c \triangleq \{\theta \in \mathbb{R}^n \,|\, f(\theta) \leq c\},\ 0 \leq c \leq 1,$

where $f : \mathbb{R}^n \to \mathbb{R}$ is the following smooth convex function:

$$f(\theta) = \frac{\theta^\top \theta - \theta_{max}^2}{\epsilon_\theta \theta_{max}^2}, \tag{2.15}$$

where θ_{max} is the norm bound imposed on the parameter vector θ, and ϵ_θ denotes the convergence tolerance of our choice. Let the true value of the parameter θ, denoted by θ^*, belong to Ω_0, i.e. $\theta^* \in \Omega_0$.

The special structure of the function f should be interpreted as: if you solve $f(\theta) \leq 1$, which defines the boundaries of the outer set, then you get that $\theta^\top \theta \leq (1+\epsilon_\theta)\theta_{max}^2$. ϵ_θ specifies the maximum tolerance the adaptive parameter is allowed to exceed compared to its maximum conservative value.

The projection operator is defined as:

$$Proj(\theta, y) \triangleq \begin{cases} y & \text{if } f(\theta) < 0, \\ y & \text{if } f(\theta) \geq 0 \text{ and } \nabla f^T y \leq 0, \\ y - \frac{\nabla f}{\|\nabla f\|} \langle \frac{\nabla f^T}{\|\nabla f\|}, y \rangle f(\theta) & \text{if } f(\theta) \geq 0 \text{ and } \nabla f^T y > 0 \end{cases} \tag{2.16}$$

Time-delay margin

A measure of stability is the time-delay margin which is defined as the maximum delay τ^* for which the system is not losing its stability.

The relation to phase-margin is given by

$$\tau^* = \frac{\text{PM}}{\omega_c}$$

where PM is the phase-margin of the system and ω_c the crossover frequency (Skogestad & Postlethwaite 2007).

2.7.4 Problem Formulation

We are looking into a problem which can be thought of as a case of unknown high frequency gain with unknown time-varying parameters and disturbances. We can formulate this problem in the form of 2.17:

$$\dot{x}(t) = A_m x(t) + b\left(\omega u(t) + \theta^\top(t) x(t) + \sigma(t)\right),\ y(t) = c^\top x(t),\ x(0) = x_0, \tag{2.17}$$

where $x \in \mathbb{R}^n$ is the system state vector (measurable), $u \in \mathbb{R}$ is the control signal, $y \in \mathbb{R}$ is the regulated output, $b, c \in \mathbb{R}^n$ are known constant vectors, A_m is a known Hurwitz $n \times n$ matrix, $\omega \in \mathbb{R}$ is an unknown constant with known sign, $\theta(t) \in \mathbb{R}^n$ is a vector of time-varying unknown parameters, while $\sigma(t) \in \mathbb{R}$ is a time-varying disturbance.

We assume that

$$\omega \in \Omega_0 = [\omega_{l0}, \omega_{u0}],\ \theta(t) \in \Theta,\ |\sigma(t)| \leq \Delta_0,\ t \geq 0, \tag{2.18}$$

where $\omega_{l0} > \omega_{u0} > 0$ are known conservative upper and lower bounds, Θ is a known compact set and $\Delta_0 \in \mathbb{R}^+$ is a known conservative bound of $\sigma(t)$. It is further assumed that $\theta(t)$ and $\sigma(t)$ are continuously differentiable and that their derivatives are uniformly bounded such that

$$\|\dot{\theta}(t)\| \leq d_\theta < \infty, \ |\dot{\sigma}(t)| \leq d_\sigma < \infty, \ \forall t \geq 0, \tag{2.19}$$

where $\|\cdot\|$ is the 2-norm and the numbers d_θ, d_σ can be arbitrarily large.

2.7.5 Companion Model Adaptive Control

$\mathcal{L}_1$ adaptive control has many similarities with MRAC, but we replace the conventional MRAC reference system with a state-predictor based reparametrization. This is what Cao and Hovakimyan sometimes refer to as Companion Model Adaptive Control (CMAC[2]).

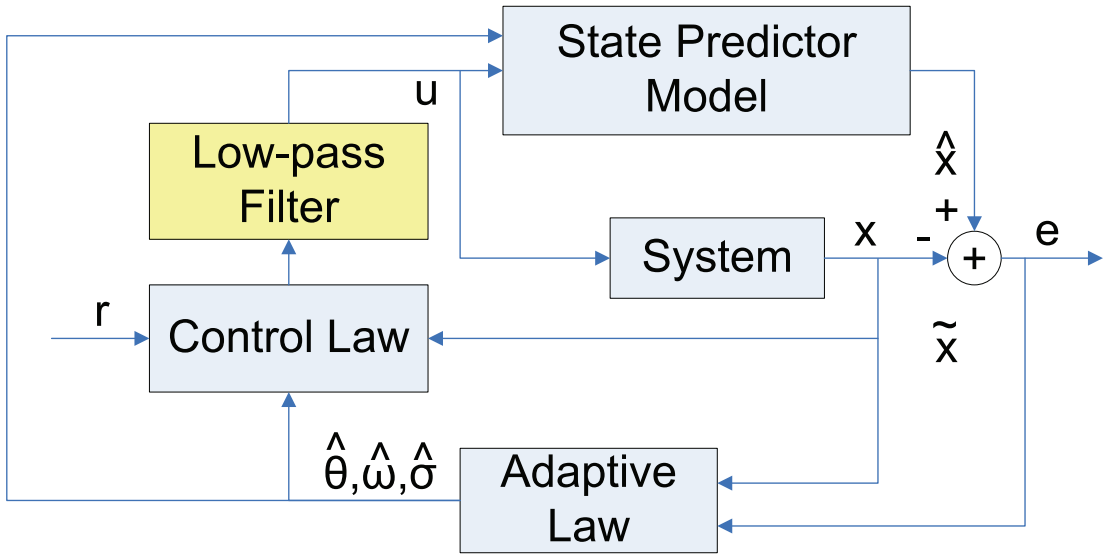

Figure 2.6: Illustration of the CMAC scheme

This reparametrization allows for the introduction of a low-pass filter into the control structure and is illustrated in figure 2.6. We can see that if we select the low-pass filter as $C(s) = 1$ the controller will degenerate back to an MRAC type.

2.7.6 The $\mathcal{L}_1$ Adaptive Controller

The $\mathcal{L}_1$ adaptive controller consists of three parts and one requirement.

[2]This is perhaps not the best name, and should not be confused with the Cerebellar Model Articulation Controller from neural networks theory

State predictor

The first part is the state predictor. The predictor is given as:

$$\dot{\hat{x}}(t) = A_m\hat{x}(t) + b\left(\hat{\omega}(t)u(t) + \hat{\theta}^\top(t)x(t) + \hat{\sigma}(t)\right),\ \hat{y}(t) = c^\top\hat{x}(t),\ \hat{x}(0) = x_0, \tag{2.20}$$

Adaptive laws

The second part is a set of adaptation laws.

$$\dot{\hat{\theta}}(t) = \Gamma_\theta\text{Proj}\left(\hat{\theta},\ -x(t)\tilde{x}^\top(t)Pb\right),\ \hat{\theta}(0) = \theta_0, \tag{2.21}$$

$$\dot{\hat{\sigma}}(t) = \Gamma_\sigma\text{Proj}\left(\hat{\sigma},\ -\tilde{x}^\top(t)Pb\right),\ \hat{\sigma}(0) = \sigma_0, \tag{2.22}$$

$$\dot{\hat{\omega}}(t) = \Gamma_\omega\text{Proj}\left(\hat{\omega},\ -\tilde{x}^\top(t)Pbu(t)\right),\ \hat{\omega}(0) = \omega_0, \tag{2.23}$$

where $\tilde{x}(t) = \hat{x}(t) - x(t)$, $\Gamma_\theta = \Gamma_c\mathbb{I}_{n\times n} \in \mathbb{R}^{n\times n}$, $\Gamma_\sigma = \Gamma_\omega = \Gamma_c > 0$ are the adaptation rates, and $P = P^\top > 0$ is the solution of the algebraic Lyapunov equation $A_m^\top P + PA_m = -Q$, $Q > 0$.

In the implementation of the projection operators the compact set Θ from 2.18 is used while Δ_0, Ω_0 is replaced by larger sets Δ and $\Omega = [\omega_l, \omega_u]$ such that

$$\Delta_0 < \Delta,\ 0 < \omega_l < \omega_{l0} < \omega_{u0} < \omega_u. \tag{2.24}$$

Control laws

The last part is the control signal, which is generated through gain feedback of the system:

$$\chi(s) = D(s)r_u(s), \tag{2.25}$$

$$u(s) = -k\chi(s), \tag{2.26}$$

where k is a feedback gain, $r_u(s)$ is the Laplace transformation of $r_u(t) = \hat{\omega}(t)u(t) + \bar{r}(t)$, $\bar{r}(t) = \hat{\theta}^\top(t)x(t) + \hat{\sigma}(t) - k_g r(t)$, $k_g = -1/(c^\top A_m^{-1}b)$, while $D(s)$ is any transfer function which leads to strictly proper stable

$$C(s) = \frac{\omega k D(s)}{1 + \omega k D(s)} \tag{2.27}$$

with low-pass gain $C(0) = 1$.

$\mathcal{L}_1$-gain stability requirement

The requirement is a $\mathcal{L}_1$-gain stability requirement placing an upper bound on the $\mathcal{L}_1$-norm. The bound is given by:

$$\lambda = \|G(s)\|_{\mathcal{L}_1} L < 1,\ G(s) = (s\mathbb{I} - A_m)^{-1} b(1 - C(s)), \tag{2.28}$$

where

$$L = \underset{\theta(t)\in\Theta}{max} \sum_{i=1}^{n} |\theta_i(t)|, \tag{2.29}$$

where $\theta_i(t)$ is the i^{th} element of $\theta(t)$.

2.7.7 Design Parameters - How to Achieve the Desired Specifications

In $\mathcal{L}_1$ adaptive control we cannot use the reference system to achieve the desired response. The state predictor depends on unknown parameters and can be thought of as a tool that generates an error signal for the adaptive laws. We have to introduce the specifications on the system in some other way.

To specify the desired performance Cao and Hovakimyan introduce some systems to help us, mainly a:

- Closed loop reference system.
- Design system.
- LTI system which will serve as an upper bound for the closed loop adaptive system.

Based on these systems they show that we get quantifiable bounds for performance, and that the control specifications reduce to the selection of some parameters (Cao & Hovakimyan 2006*b*):

- k - $\mathcal{L}_1$ gain constant that needs to be high enough to ensure stability, but a higher k will hurt the robustness of the system.
- $C(s)$ ($D(s)$) - Low-pass filter which influences both performance and robustness.
- Γ_c - Adaptation gain which will influence performance and CPU usage.

In addition we might need to select a K to stabilize $H_o(s)$, where $H_o(s) = (s\mathbb{I} - A_o)^{-1} b$, where $A_o = A_m - bK^\top$. This K may of course be selected as zero if the system is stable.

What do we sacrifice to get good tracking performance? The selections of $C(s)$ (or $D(s)$) define the trade-off between performance and robustness. A high bandwidth will lead to a smaller λ, but increasing the bandwidth of $C(s)$ will lead to reduced time-delay margin and hurt the robustness of the closed loop system. Usually the bandwidth of $C(s)$ needs to be larger than the bandwidth of $\sigma(t)$ and $r(t)$ to be able to give good

transient performance (Cao & Hovakimyan 2008*e*). It is possible to optimize the time-delay margin by design of the underlying filter (Li, Patel, Cao, Hovakimyan & Wise 2007).

Fast adaptation will also lead to close tracking, but increasing the adaption gains will lead to a reduction in the required step-size of integrations. This means that we need a very fast CPU to complete the operations required in time. In the writings of Cao and Hovakimyan little is said about the effects on sampling time. It is thus of great interest to check what happens if we only have sparse measurements. It is recommended to set the adaption gains as high as the CPU permits to get the best possible tracking performance, but as we will see the selection of $C(s)$ will also affect performance.

In the analysis chapter we will introduce a series of upper bounds on performance. The bounds are used to predict and analyze performance, and we will again see the effects of the choices we make on design parameters.

Selection of the low-pass filter

In Cao & Hovakimyan (2006*b*) and Hovakimyan (2008) we see that we need to determine $C(s)$ such that

$$i) \quad \lambda \text{ or } \|h_3\|_{\mathcal{L}_\infty} \text{ is sufficiently small,} \tag{2.30}$$

$$ii) \quad y_d(s) \approx D_d(s)r(s), \tag{2.31}$$

where $h_3(t)$ is the inverse Laplace transformation of

$$H_3(s) = (C(s) - 1)C(s)r(s)k_g H_o(s)\theta^\top H_o(s). \tag{2.32}$$

and where $D_d(s)$ is the desired LTI system. It is important to notice that the two objectives 2.30 and 2.31 are not in conflict with each other, and also that minimization of λ is consistent with the stability requirement of 2.28.

The two objectives can be met in two different ways. The first is to fix $C(s)$ and minimize $\|H_o(s)\|_{\mathcal{L}_1}$. The second is to fix $H_o(s)$ and minimize the $\mathcal{L}_1$-gain of one of the systems $\|H_o(s)(C(s) - 1)\|_{\mathcal{L}_1}$, $\|(C(s) - 1)r(s)\|_{\mathcal{L}_1}$ or $\|C(s)(C(s) - 1)\|_{\mathcal{L}_1}$ via the choice of $C(s)$ (Cao & Hovakimyan 2006*b*).

Design method 1

We can set $C(s) = D_d(s)$ and achieve minimization of $\|H_o(s)\|_{\mathcal{L}_1}$ with high feedback by choosing a sufficiently large K. This leads to large poles of $H_o(s)$ and the $\mathcal{L}_1$ adaptive controller degenerates into a high-gain robust controller. High K will also lead to reduced phase margin (Cao & Hovakimyan 2006*b*).

Design method 2

As we do in MRAC, we may assume that it is possible to select A_m such that we get $k_g c^\top (s\mathbb{I} - A_m)^{-1} b \approx D_d(s)$. We can then set $K = 0$, or one can alternatively choose K such that $k_g c^\top H_o \approx D_d(s)$ (Cao & Hovakimyan 2006*b*).

We start off by trying to minimize $\|H_o(s)(C(s)-1)\|_{\mathcal{L}_1}$. By selecting $C(s) = \frac{\omega}{s+\omega}$ we get the following lemma:

Lemma 1. *For any single-input n-output strictly proper stable system H(s) the following is true:*

$$\lim_{w\to\infty} \|(C(s)-1)H(s)\|_{\mathcal{L}_1} = 0.$$

The second way to minimize $\|H_o(s)(C(s)-1)\|_{\mathcal{L}_1}$ is to note that since $C(s)$ is a low pass filter, $1-C(s)$ is a high-pass filter. Since both $H_o(s)$ and $C(s)$ are strictly proper, cascading the two systems is equivalent to cascading a low-pass system with a high-pass system. If we choose the cut-off frequency of the high-pass filter larger than the bandwidth of $H_o(s)$, it ensures that $\|H_o(s)(C(s)-1)\|_{\mathcal{L}_1}$ is a "no-pass" system and we can render its $\mathcal{L}_1$ gain small (Cao & Hovakimyan 2006*b*).

The minimization of $\|h_3(s)\|_{\mathcal{L}_\infty}$ can be done in two ways:

$$i) \quad \|h_3(s)\|_{\mathcal{L}_\infty} \leq \|(C(s)-1)r(s)\|_{\mathcal{L}_1}\|h_4\|_{\mathcal{L}_\infty} \tag{2.33}$$

$$ii) \quad \|h_3(s)\|_{\mathcal{L}_\infty} \leq \|(C(s)-1)C(s)\|_{\mathcal{L}_1}\|h_5\|_{\mathcal{L}_\infty} \tag{2.34}$$

where $h_4(t)$ is the inverse Laplace transformation of $H_4(s) = r(s)k_gH_o(s)\theta^\top H_o(s)$ and $h_5(t)$ the inverse Laplace transformation of $H_5(s) = r(s)k_gH_o(s)\theta^\top H_o(s)$. $\|h_4(s)\|_{\mathcal{L}_\infty}$ and $\|h_5(s)\|_{\mathcal{L}_\infty}$ are finite so we can minimize $\|h_3(s)\|_{\mathcal{L}_\infty}$ by selecting $\|(C(s)-1)r(s)\|_{\mathcal{L}_1}$ or $\|(C(s)-1)C(s)\|_{\mathcal{L}_1}$. The first can be minimized by selecting the cut-off frequency of $(C(s)-1)$ higher than the bandwidth of $r(t)$. For the second choice we note that if $C(s)$ was an ideal low-pass filter the norm would be zero. This is of course not physically implementable, but we can still minimize the norm $\|(C(s)-1)C(s)\|_{\mathcal{L}_1}$ via the choice of the low-pass filter (Cao & Hovakimyan 2006*b*). The above approaches ensure that we have $C(s) \approx 1$ in the bandwidth of $r(s)$ and $H_o(s)$. Therefore it follows that $y_d(s) = C(s)k_gc^\top H_o(s)r(s) \approx k_gc^\top H_o(s)r(s)$, which implies $y_d(s) \approx D_d(s)r(s)$ (Cao & Hovakimyan 2006*b*).

Selection of higher order filters allows us to obtain the same performance with lower adaptation gains and can give improved time-delay margins. In Li et al. (2007) several filters are evaluated, and the low-pass Bessel filter and a general filter obtained by constrained optimization is shown to give better time-delay margins.

In figure 2.7 we illustrate the time-delay margin versus bandwidth to get a clearer picture of what happens as we increase k, which will increase the bandwidth. By selection of the appropriate higher order filter, it is possible to make this curve less steep. We also see the same illustration for λ. The selection of the filter will alter both the rate of decrease and the highest peak for the bound.

2.7.8 The Theory of Fast and Robust Adaptation

The theory about $\mathcal{L}_1$ adaptive control and the surrounding modifications are referred to, by Cao & Hovakimyan, as the theory of fast and robust adaptation and the advan-

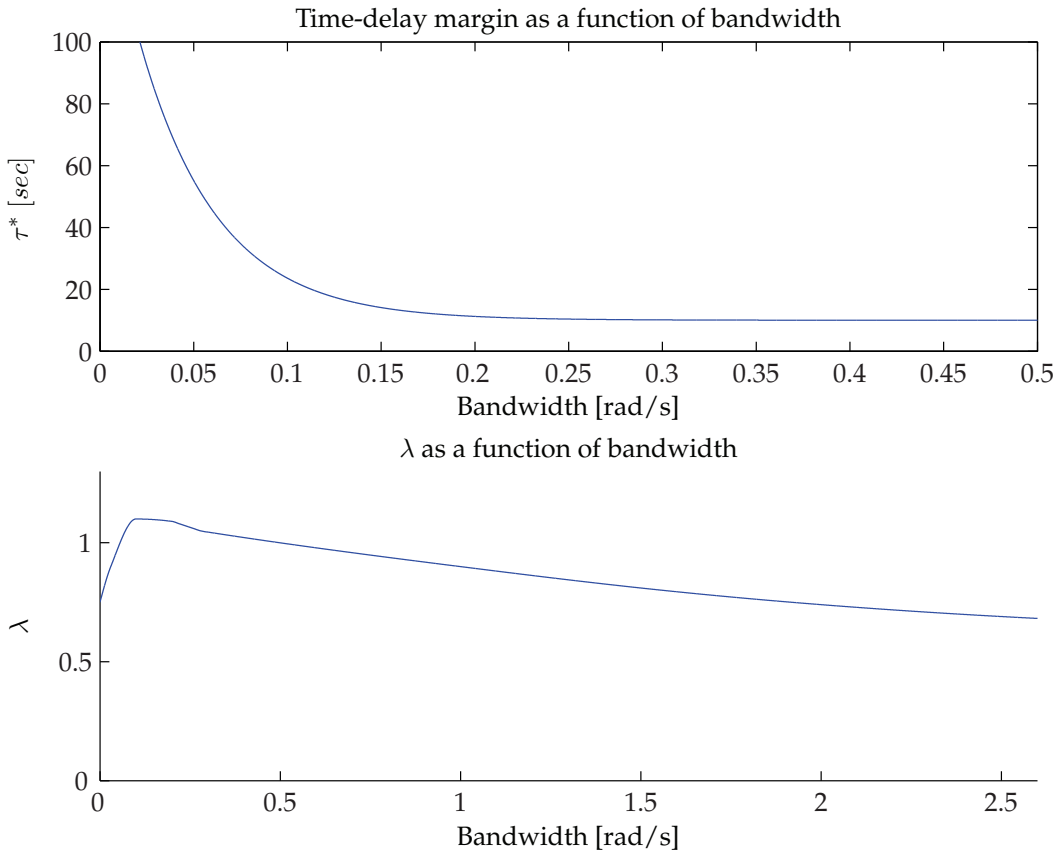

Figure 2.7: Time-delay margins and λ versus increased bandwidth

tages are supposedly many. In this section we look at the theoretical advantages and compare them especially to MRAC.

The main features of the theory of fast and robust adaptation are (Wise et al. 2008):

- Guaranteed fast adaptation.
- Guaranteed transient performance both for system input and output signal.
- Guaranteed time-delay margin.
- Uniformly scaled transient response dependent on changes in initial conditions, values of the unknown parameters and reference input.
- Suitable for the development of theoretically justified verification and validation tools for feedback systems.

The benefits of $\mathcal{L}_1$ versus MRAC are summarized in table 2.1 (Wise et al. 2008). We see that there are several improvements for the $\mathcal{L}_1$ adaptive scheme.

Table 2.1: Benefits of $\mathcal{L}_1$ versus MRAC

MRAC	$\mathcal{L}_1$ adaptive control
Ignores the explicit dependence on time	
Needs choice of basis functions	No selection of basis function
Needs significant tuning	Systematic tuning
Local results	Semiglobal results
Needs to tune transient	Guaranteed transient
Adaptation only on loop gain	Adaptation on loop gain and phase

2.7.9 Project Highlights

Reading quite a lot of $\mathcal{L}_1$ adaptive control papers, it is interesting to notice how some matters have been given much less attention than others. Applications are often very fast aircraft systems, where I suppose there are good measurements available.

Some of the more interesting topics to include in this study are:

- Are there any problems with slow sampling?
- What happens if the controller saturates?
- How fast do we need to set the adaptation gains to get good performance and how fast do the bounds imply?
- How good is the $\mathcal{L}_1$ controller compared to the PI controller?
- Does the selection of higher order $C(s)$ have any great impact ?
- How much tuning does the controller need?
- I have assumed that ω is constant, but this is not always true. What happens when we have slow or even fast variations in the system?

Chapter 3

Control Design

The background for this chapter is the Kaasa model presented in the previous chapter. The Kaasa model will serve as the basis for our design model both for topside and bottomhole control. More details follow in the next sections.

We start by presenting the benchmark controller: a standard PI-controller. We then move on to the more advanced structures: MRAC and $\mathcal{L}_1$ adaptive control.

3.1 Proportional plus Integral Controller

The reference controller employed is a standard PI controller. The controller is implemented with a simple anti windup scheme, using feedback from the control input. Bump less transfer is added by including a bias term, which is reset every time we have a change of controllers. An optional dead band region can be selected, to stop the control input if the error is sufficiently small.

Since we are mostly interested in comparing controllers which use as few measurement signals as possible we are considering a PI controller without feed forward from the pump disturbances. A feed forward controller would be expected to have better performance. This is however true for all the controllers considered. We also have some disturbances which cannot be measured.

The control equation is given by:

$$u = u_{bias} + K_c e(t) + \frac{K_c}{T_i} \int e(t)\, dt \tag{3.1}$$

where K_c and T_i are gain variables, and $e(t) = x_{ref} - x$ and u_{bias} are set from the previous control input when we have a change in controller type. The controller is the same for both topside and bottomhole control, though x, x_{ref} and the gains will vary.

The gains are selected using Skogestad SIMC tuning rules (see appendix B.3). The complete controller is summarized in table 3.1 and the gains are given in table 3.2.

Table 3.1: PI equations

Error equation:
$e(t) = x_{ref} - x$ (3.2) $x =$ p_c for choke control and $x = p_{bit}$ for bottomhole control (3.3)
Control Law:
$$u = u_{bias} + K_c \left(e(t) + \frac{1}{T_i} \int e(t)\, dt \right)$$ (3.4)
Design parameters:
Controller gains K_c and T_i.

Table 3.2: PI Gain Table

Gain	Topside control	Bottomhole control
K_c	$-2.05 \cdot 10^{-8}$	$-2.63 \cdot 10^{-8}$
T_i	3	8
x	p_c	p_{bit}

3.2 Model-Reference Adaptive Control

The structure for the MRAC controller for topside control was derived in Pedersen (2008), but is repeated here for reference.

3.2.1 System Model

If we use a topside scheme based on measurements from the choke, we can create a controller based on the choke equation 2.3:

$$\dot{p}_c(t) = \frac{\beta_a}{V_a}(-\dot{V}_a + q_{bit} + q_{res} + q_{back}) - \frac{\beta_a}{V_a}q_c, \tag{3.5}$$

$$\dot{p}_c(t) = \theta(\delta(t) - u(t)). \tag{3.6}$$

3.2.2 The Reference Model

The reference model specifies the desired process behavior. The perfect model-matching condition states that a controller parameter setting must exist for which the closed-loop behavior equals the reference model response. This places requirements on the relative degree of the reference model. The plant and the reference model must have the same (constant) relative degree (Tsakalis & Ioannou 1993). The reference model must be stable, controllable and minimum phase. It should be selected sensible in the sense that the process actually is able to follow the process. For example if the dynamic of the reference model is too fast, the control signal needs to be very large, which may lead to saturation and disturbances by high order unmodeled dynamics (Butler 1992).

Based on equation 2.3 a first order reference model is chosen. This reference model is chosen to be:

$$p_m = \frac{b_m}{s - A_m}r \tag{3.7}$$

By simulation (see Appendix B.2.1), we find that a fitting time parameter to meet the performance objectives is $A_m = -0.2$ which also gives $b_m = 0.2$

$$p_m = \frac{0.2}{s + 0.2}r \tag{3.8}$$

The model is realized in Matlab as a function which takes as input the reference, solves an ODE for the calculated pressure and returns the value to the system.

3.2.3 The Basic Controller

The control structure for the controller is selected as:

$$u = -k_0 r + k_1 p_c + k_2, \tag{3.9}$$

where k_0, k_1 and k_2 are the controller gains, r is the wanted choke pressure and p_c is the measured choke pressure. This gives both stabilization of the system and offset correction for a constant or slow-varying input disturbance.

3.2.4 The Update Laws

The normalized update laws were constructed in Pedersen (2008) and are given as

$$\dot{k_0} = -\gamma_0 e \frac{r}{r^2 + 1}, \tag{3.10}$$

$$\dot{k_1} = \gamma_1 e \frac{p_c}{p_c^2 + 1}, \tag{3.11}$$

$$\dot{k_2} = \gamma_2 e, \tag{3.12}$$

where γ_0, γ_1 and γ_2 are non-negative design parameters which will control the rate of adaptation of the control parameters.

3.2.5 Modifications for Improved Robustness

In addition to the control structures presented, there are some modifications on the actual implementation of the MRAC controller. I have added projection to the adaptation parameters to avoid unbounded growth. Normalization of the adaptation laws is done to make sure the rate of adaptation is not larger than intended, and that the adaptation rate will not increase with increased value of the plant output or reference. I have also added a deadzone to avoid parameter drift due to noise when there is low excitation of the system. Additional modifications should also be considered, such as the use of an orthogonal error signal to account for the presence of dead time (Butler 1992).

Simulations are performed using q_c as control input, but sometimes we need to use a choke controller. One simple choice is to invert the choke equation 2.7 to get equation 3.13:

$$z_c = \frac{q_{c0}}{K_{choke}\sqrt{\frac{2}{\rho_0}(p_{c0} - p_0)}} \tag{3.13}$$

A minimum fraction is set for $\Delta P = p_{c0} - p_0$ to avoid division by zero. However, this controller is not very good with unknown non-linearities or unknown K_{choke}. The MRAC equations are summed up in table 3.3.

Table 3.3: MRAC equations

Reference model and error equation:
$$\dot{p_m} = A_m p_m + b_m r \quad (3.14)$$ $$e = p_c - p_m \quad (3.15)$$
Control Laws:
$$q_{c0} = -k_0 r + k_1 p_c + k_2 \quad (3.16)$$ $$z_{c0} = \frac{q_{c0}}{K_{choke}\sqrt{\frac{2}{\rho_0}(p_{c0} - p_0)}} \quad (3.17)$$
Update Laws:
$$\dot{k_0} = -\gamma_0 e \frac{r}{r^2 + 1} \quad (3.18)$$ $$\dot{k_1} = \gamma_1 e \frac{p_c}{p_c^2 + 1} \quad (3.19)$$ $$\dot{k_2} = \gamma_2 e \quad (3.20)$$
Design parameters:
Adaptation gains: $\gamma_0, \gamma_1, \gamma_2 \geq 0$, initial values: $p_m(0)$, $k_0(0)$, $k_1(0)$ and $k_2(0)$ and reference model parameters A_m and b_m.

The design variables were, after considerations of parameters and tuning (see Appendix B.1), selected as given in table 3.4.

Table 3.4: MRAC - Design Parameters

$k_0(0)$ $8.1943 \cdot 10^{-9}$	$k_1(0)$ $8.1943 \cdot 10^{-9}$	$k_2(0)$ $q_c(0)$
γ_0 $1 \cdot 10^{-14}$	γ_1 $1 \cdot 10^{-14}$	γ_2 $5 \cdot 10^{-9}$
b_m 0.2	A_m -0.2	$p_m(0)$ $p_c(0)$

3.2.6 Bottomhole Control

The MRAC controller will not be derived for bottomhole control since the main focus is PI versus $\mathcal{L}_1$ adaptive control.

3.3 $\mathcal{L}_1$ Adaptive Controller

3.3.1 Topside Control

If we use a topside scheme based on measurements from the choke, we can, as we did in MRAC, create a controller based on the choke equation 2.3. We rearrange the equation, and add and subtract the design parameter A_m to get:

$$\dot{p_c}(t) = \frac{\beta_a}{V_a}(-\dot{V}_a + q_{bit} + q_{res} + q_{back}) - \frac{\beta_a}{V_a}q_c \tag{3.21}$$

$$\dot{x}(t) = \sigma(t) + \omega(t)u(t) \tag{3.22}$$

$$\dot{x}(t) = \sigma(t) + \omega(t)u(t) + A_m x(t) - A_m x(t) \tag{3.23}$$

$$\dot{x}(t) = A_m x(t) + \theta x(t) + \omega(t)u(t) + \sigma(t) \tag{3.24}$$

where $x(t) = p_c(t)$, $u(t) = q_c(t)$ and

$$\theta(t) = -A_m \tag{3.25}$$

$$\sigma(t) = \frac{\beta_a}{V_a}(-\dot{V}_a + q_{bit} + q_{res} + q_{back}) \tag{3.26}$$

$$\omega(t) = -\frac{\beta_a}{V_a} \tag{3.27}$$

We see that we need to estimate σ and ω, while there is no unknown θ in these equations. However, to allow for some unmodeled dynamics, I still give the equations for $\dot{\hat{\theta}}(t)$.

We construct the state predictor from equation 2.20:

$$\dot{\hat{x}}(t) = A_m\hat{x}(t) + \left(\hat{\omega}(t)u(t) + \hat{\theta}^\top(t)x(t) + \hat{\sigma}(t)\right),\ \hat{y}(t) = c^\top\hat{x}(t),\ \hat{x}(0) = x_0, \tag{3.28}$$

where $\hat{x}$ is an estimate of x. From equation 2.22-2.23, with $Q = -0.4$ and $A_m = -0.2$ we get

$$\dot{\hat{\theta}}(t) = \Gamma_\theta \text{Proj}\left(\hat{\theta},\ -x(t)\tilde{x}^\top(t)\right),\ \hat{\theta}(0) = \theta_0, \tag{3.29}$$

$$\dot{\hat{\sigma}}(t) = \Gamma_\sigma \text{Proj}\left(\hat{\sigma},\ -\tilde{x}^\top(t)\right),\ \hat{\sigma}(0) = \sigma_0, \tag{3.30}$$

$$\dot{\hat{\omega}}(t) = \Gamma_\omega \text{Proj}\left(\hat{\omega},\ -\tilde{x}^\top(t)u(t)\right),\ \hat{\omega}(0) = \omega_0, \tag{3.31}$$

where $\tilde{x} = \hat{x} - x$, and Γ_θ, Γ_σ and Γ_ω are adaptation gains.

We use the simple $D(s) = 1/s$ and get $k_g = 0.2$, and generate the control signal as:

$$\chi(s) = D(s)r_u(s), \tag{3.32}$$
$$u(s) = -k\chi(s) \tag{3.33}$$

where k is a gain constant and $r_u(s)$ the Laplace transformation of $r_u(t)$.

$$r_u(t) = \left(\hat{\omega}(t)u(t) + \hat{\theta}^\top(t)x(t) + \hat{\sigma}(t) + A_m r(t)\right) \tag{3.34}$$

Generating the feedback signal this way, introduced some windup issues during simulations. Therefore projection is added to the state $\chi(s)$ such that physical constraints on the controller will not lead to windup if the control input saturates.

$$\chi \in X,\ X = [\frac{u_{min}}{-k} = \chi_l, \chi_u = \frac{u_{max}}{-k}] \tag{3.35}$$

The author has not however evaluated the impact on the stability and performance proofs for the $\mathcal{L}_1$ adaptive controller, and this is something that should be looked into in future work.

The closed loop system is illustrated in figure 3.1.

By varying the different parameters in 3.26 and 3.27 we can get a conservative bound by selecting all parameters at their worst value, and also get a good initial estimate of the parameters. The values are given in table 3.5.

Table 3.5: $\mathcal{L}_1$ - Estimated bounds for choke control

Δ	Value	Ω	Value
$\hat{\sigma}_0$	$8.95 \cdot 10^5$	$\hat{\omega}_0$	$-2.44 \cdot 10^7$
$\hat{\sigma}_u$	$1.32 \cdot 10^7$	$\hat{\omega}_u$	$-1.0 \cdot 10^5$
$\hat{\sigma}_l$	$-4.5 \cdot 10^6$	$\hat{\omega}_l$	$-2.0 \cdot 10^8$

We also need conservative estimates of the maximum rate of change of θ and σ. These are set as $d_\theta = 0.1$ and $d_\sigma = 10000$.

The complete controller is summarized in table 3.6

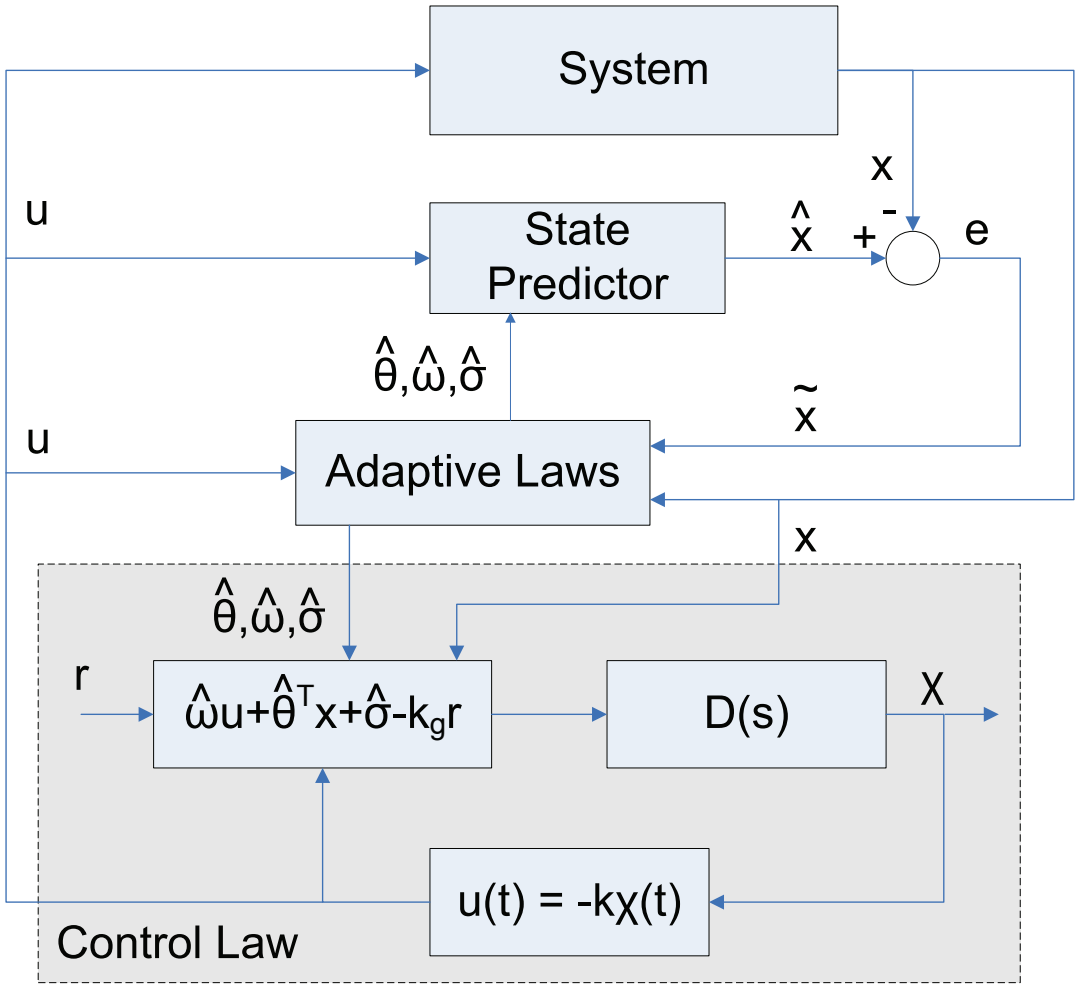

Figure 3.1: Closed loop with $\mathcal{L}_1$ adaptive controller

Table 3.6: $\mathcal{L}_1$ adaptive controller equations

State predictor model and error equation:

$$\begin{aligned}
\dot{\hat{x}}(t) &= A_m\hat{x}(t) + \left(\hat{\omega}(t)u(t) + \hat{\theta}^\top(t)x(t) + \hat{\sigma}(t)\right),\ \hat{y}(t) = c^\top\hat{x}(t),\ \hat{x}(0) = x_0,\\
\tilde{x} &= \hat{x} - x,\\
x &= p_c \text{ for choke control and } x = p_{bit} \text{ for bottomhole control}
\end{aligned}$$

Control Law:

$$\begin{aligned}
\chi(s) &= D(s)r_u(s),\\
u(s) &= -k\chi(s),\\
r_u(t) &= \hat{\omega}(t)u(t) + \hat{\theta}^\top(t)x(t) + \hat{\sigma}(t) + A_m r(t)
\end{aligned}$$

Update Laws:

$$\begin{aligned}
\dot{\hat{\theta}}(t) &= \Gamma_\theta \text{Proj}\left(\hat{\theta},\ -x(t)\tilde{x}^\top(t)\right),\ \hat{\theta}(0) = \theta_0,\\
\dot{\hat{\sigma}}(t) &= \Gamma_\sigma \text{Proj}\left(\hat{\sigma},\ -\tilde{x}^\top(t)\right),\ \hat{\sigma}(0) = \sigma_0,\\
\dot{\hat{\omega}}(t) &= \Gamma_\omega \text{Proj}\left(\hat{\omega},\ -\tilde{x}^\top(t)u(t)\right)\ \hat{\omega}(0) = \omega_0,
\end{aligned}$$

Stability requirement:

$$\begin{aligned}
\lambda &= \|G(s)\|_{\mathcal{L}_1} L < 1,\ G(s) = (s\mathbb{I} - A_m)^{-1}b(1 - C(s)),\\
L &= \max_{\theta(t)\in\Theta} \sum_{i=1}^{n} |\theta_i(t)|
\end{aligned}$$

Design parameters:

Adaptation gains: $\Gamma_\theta, \Gamma_\sigma, \Gamma_\omega \geq 0$ selected sufficiently high, initial values: $\hat{x}(0)$, $\hat{\theta}(0)$, $\hat{\sigma}(0)$ and $\hat{\omega}(0)$, feedback gain: k selected to meet the $\mathcal{L}_1$ stability requirement, $D(s)$ to create the strictly proper filter $C(s) = \omega k D(s)/(1 + \omega k D(s))$ with low-pass gain $C(0) = 1$, design parameter A_m and the selection of the sets Δ, Ω and Θ.

3.3.2 Bottomhole Control

If we assume p_{bit} is available for measurement either by wired drill pipe or from an estimator, we can create a controller based on equations 2.2-2.4 and 2.5.

We replace $\dot{q}_{bit}$ in 2.5 to get:

$$\begin{aligned} p_{bit} &= p_c + \frac{M_a}{M}(p_p - p_c - F_d|q_{bit}|q_{bit} - F_a|q_{bit} + q_{res}|(q_{bit}q_{res}) + (\bar{\rho}_d - \bar{\rho}_a)gh_{bit}) + \\ & F_a|q_{bit} + q_{res}|(q_{bit} + q_{res}) + \bar{\rho}_a g h_{bit}, \end{aligned} \tag{3.36}$$

and rearrange:

$$\begin{aligned} p_{bit} &= \Big(1 - \frac{M_a}{M})p_c + \frac{M_a}{M}p_p - \frac{M_a F_d}{M}|q_{bit}|q_{bit} + (F_a - \frac{M_a F_a}{M})|q_{bit} + q_{res}|(q_{bit} + q_{res}) + \\ & \frac{M_a}{M}(\bar{\rho}_d - (1 - \frac{M}{M_a})\bar{\rho}_a)gh_{bit}\Big). \end{aligned} \tag{3.37}$$

We then separate out $\frac{1}{M}$ and insert for $M = M_a + M_d$:

$$\begin{aligned} p_{bit} &= \frac{1}{M}(M_d p_c + M_a p_p - M_a F_d|q_{bit}|q_{bit} + M_d F_a|q_{bit} + q_{res}|(q_{bit} + q_{res}) + \\ & (M_a\bar{\rho}_d + M_d\bar{\rho}_a)gh_{bit}). \end{aligned} \tag{3.38}$$

The p_{bit} dynamics can then be taken as:

$$\dot{p}_{bit} = \frac{1}{M}\left(M_d\dot{p}_c + M_a\dot{p}_p - 2M_a F_d\dot{q}_{bit}q_{bit} + 2M_d F_a\dot{q}_{bit}(q_{bit} + q_{res})\right). \tag{3.39}$$

Inserting for $\dot{p}_c$, $\dot{p}_p$ and $\dot{q}_{bit}$ gives us:

$$\begin{aligned} \dot{p}_{bit} &= \frac{1}{M}\Big(M_d\frac{\beta_a}{V_a}(-\dot{V}_a + q_{bit} + q_{res} + q_{back} - q_c) + M_a\frac{\beta_d}{V_d}(q_{pump} - q_{bit}) \\ & -2M_a F_d(\frac{1}{M}(p_p - p_c - F_d|q_{bit}|q_{bit} - F_a|q_{bit} + q_{res}|(q_{bit} + q_{res}) \\ & +(\bar{\rho}_d - \bar{\rho}_a)gh_{bit})(q_{bit}) + 2M_d F_a(\frac{1}{M}(p_p - p_c - F_d|q_{bit}|q_{bit} \\ & -F_a|q_{bit} + q_{res}|(q_{bit} + q_{res}) + (\bar{\rho}_d - \bar{\rho}_a)gh_{bit})(q_{bit} + q_{res})\Big) \end{aligned} \tag{3.40}$$

which we might put in the form of 2.17, with $A_m = -0.2$ and get:

$$\dot{x}(t) = A_m x(t) + \Big(\omega(t)u(t) + \theta^\top(t)x(t) + \sigma(t)\Big) \tag{3.41}$$

where now $x(t) = p_{bit}(t)$ and:

$$\theta(t) = -A_m \tag{3.42}$$

$$\begin{aligned}\sigma(t) = \frac{1}{M}\Big(& M_d\frac{\beta_a}{V_a}(-\dot{V}_a + q_{bit} + q_{res} + q_{back}) + M_a\frac{\beta_d}{V_d}(q_{pump} - q_{bit}) \\ & -2M_aF_d(\frac{1}{M}(p_p - p_c - F_d|q_{bit}|q_{bit} - F_a|q_{bit} + q_{res}|(q_{bit} + q_{res}) \\ & +(\bar{\rho}_d - \bar{\rho}_a)gh_{bit})(q_{bit}) + 2M_dF_a(\frac{1}{M}(p_p - p_c - F_d|q_{bit}|q_{bit} \\ & -F_a|q_{bit} + q_{res}|(q_{bit} + q_{res}) + (\bar{\rho}_d - \bar{\rho}_a)gh_{bit})(q_{bit} + q_{res})\Big)\end{aligned} \tag{3.43}$$

$$\omega(t) = -\frac{M_d\beta_a}{MV_a} \tag{3.44}$$

Estimated bounds and initial conditions are given in table 3.7.

Table 3.7: $\mathcal{L}_1$ - Estimated bounds for bottomhole control

Δ	Value	Ω	Value
$\hat{\sigma}_0$	$5.76 \cdot 10^5$	$\hat{\omega}_0$	$-1.82 \cdot 10^7$
$\hat{\sigma}_u$	$1.45 \cdot 10^{10}$	$\hat{\omega}_u$	$-1.50 \cdot 10^9$
$\hat{\sigma}_l$	$-8.80 \cdot 10^9$	$\hat{\omega}_l$	-2500

The estimates of the maximum rate of change of θ and σ are set as $d_\theta = 0.1$ and $d_\sigma = 20000$.

We get the same control structure as in the topside case, but now with different adaptation gain k, initial conditions and different bounds.

3.4 Bottomhole Control - Determining an Observer

If we assume that we have wired drill pipe or some other means of ensuring good bottomhole measurements, we might get by without an observer, and this is of course the simplest solution. However, an observer might come in handy even though we have fast measurements, for example during the connection operation or if we lose measurement signals.

There are several possibilities for choice of an observer ranging from complex UKF to simpler observers based on system models. The one employed here is the observer derived in Stamnes (2007).

The equations[1] for the observer are given in table 3.8. For further details, consult the original thesis.

We have some problems with the observer, namely some strict assumptions and no convergence of parameters. The assumption $q_{res} = 0$ is not true, and the estimated friction and density might not (and probably will not) converge to their true values. The goal of this thesis is however not to evaluate observer designs and some error in the estimated values is an additional challenge for the control system.

In the implementation of the observer we must ensure that

$$\dot{\hat{q}}_{bit} = \frac{1}{M}(p_p - p_c) - \hat{\theta}_1|\hat{q}_{bit}|\hat{q}_{bit} + \hat{\theta}_2 h_{bit} \tag{3.45}$$

is larger or equal to zero if q_{bit} is zero. This a consequence of the assumption of $q_{bit} \geq 0$ (one-way valve).

3.5 Topside Control - Determining a Path Generator

Because we know the bottomhole pressure equation of the simulator, we can, by inverting this equation, generate the exact path for $p_{c,ref}$ to get the correct $p_{bit,ref}$

$$p_{c,ref} = p_{bit,ref} - M_a\dot{q}_{bit} - F_a|q_{bit} + q_{res}|(q_{bit}q_{res}) - \bar{\rho}_a g h_{bit}. \tag{3.57}$$

However, this assumes knowledge of some very uncertain parameters. Other possibilities include estimation of the parameters in the equation by the use of an estimator or generating the path by simulations in a high-fidelity flow model based on gathered seismic and drilling data.

The observer employed in the previous section can be used to estimate the unknown parameters in 3.57 and this is what I have done. We get the same problems with the assumptions and convergence as in the previous section.

[1] Some of the notation from the original thesis has been changed to avoid confusion between this thesis and Stamnes' thesis, and to avoid introducing too many new parameters.

Table 3.8: Summary of the Stamnes observer

Observer equations:

$$\begin{aligned}
\hat{p}_{bit} &= p_c + M_a\left(\frac{1}{M}(p_p - p_c) - \hat{\theta}_1|\hat{q}_{bit}|\hat{q}_{bit} + \hat{\theta}_2 h_{bit}\right) \\
&\quad +(M\hat{\theta}_1 - F_d)|\hat{q}_{bit}|\hat{q}_{bit} + (\rho_d g - M\hat{\theta}_2)h_{bit} && (3.46)\\
\hat{q}_{bit} &= \hat{\xi}_1 - l_1 p_p && (3.47)\\
\dot{\hat{\xi}}_1 &= l_1\frac{\beta_d}{V_d}(q_p - \hat{q}_{bit}) - \hat{\theta}_1|\hat{q}_{bit}|\hat{q}_{bit} + \hat{\theta}_2 h_{bit} + \frac{1}{M}(p_p - p_c) && (3.48)\\
\hat{\xi}_1(0) &= \hat{q}_{bit}(0) + l_1 p_p(0) && (3.49)
\end{aligned}$$

Adaptive laws:

$$\begin{aligned}
\hat{\theta} &= \hat{\zeta} - \eta(\hat{q}_{bit}, h_{bit}) && (3.50)\\
\dot{\hat{\zeta}} &= -l_1\frac{\partial\eta}{\partial\hat{q}_{bit}}\frac{\beta_d}{V_d}(q_p - \hat{q}_{bit}) + \frac{\partial\eta}{\partial\hat{q}_{bit}}\dot{\hat{\xi}} + \frac{\partial\eta}{\partial h_{bit}}\dot{h}_{bit} && (3.51)\\
\hat{\zeta}(0) &= \hat{\theta}(0) + \eta\left(\hat{q}_{bit}(0), h_{bit}(0)\right) && (3.52)\\
\eta(\hat{q}_{bit}, h_{bit}) &= \Gamma\begin{bmatrix}\frac{|\hat{q}_{bit}|^3 V_d}{3l_1\beta_d}\\ \frac{-h_{bit}\hat{q}_{bit}V_d}{l_1\beta_d}\end{bmatrix} && (3.53)\\
\frac{\partial\eta}{\partial\hat{q}_{bit}} &= \Gamma\begin{bmatrix}\frac{|\hat{q}_{bit}|\hat{q}_{bit}V_d}{l_1\beta_d}\\ \frac{-h_{bit}V_d}{l_1\beta_d}\end{bmatrix},\ \frac{\partial\eta}{\partial h_{bit}} = \Gamma\begin{bmatrix}0\\ \frac{-\hat{q}_{bit}V_d}{l_1\beta_d}\end{bmatrix} && (3.54)
\end{aligned}$$

Design parameters:

Observer gain $l_1 > 0$, Adaptation gain: $\Gamma = \Gamma^\top > 0$,
Initial conditions: $\hat{q}_{bit}(0)$ and $\hat{\theta}(0)$.

Estimated variables:

$$\begin{aligned}
\theta_1 &= \frac{F_d + F_a}{M} > 0 \Rightarrow F_a = M\theta_1 - F_d && (3.55)\\
\theta_2 &= \frac{(\bar{\rho}_d - \bar{\rho}_a)g}{M} \Rightarrow \bar{\rho}_a = \bar{\rho}_d - \frac{M}{g}\theta_2 && (3.56)
\end{aligned}$$

Assumptions made:

It is assumed that p_p, p_c, q_p, h_{bit} and $\dot{h}_{bit}$ are measured or known, β_d, M_a, M_d and F_d are known, and that p_p, p_c, q_{bit}, q_p and h_{bit} are bounded, and $q_{res} = 0$ and $q_{bit} \geq 0$.

Chapter 4

Analysis

In this chapter we look at stability, performance and time-delay margins for the different controllers. The main focus is on the upper bounds presented for $\mathcal{L}_1$ adaptive control, and we again return to how our selections of design parameters influence the $\mathcal{L}_1$ adaptive controller.

4.1 Model-Reference Adaptive Control

4.1.1 Stability

In Pedersen (2008) I showed that we have three parameters which need to be estimated. They are included with the tracking error to form a Lyapunov function candidate. We get:

$$V = A_m^2 e^2 + \frac{1}{\gamma_0'}(\theta k_0 - b_m)^2 + \frac{1}{\gamma_1'}(-\theta k_1 - A_m)^2 + \frac{1}{\gamma_2'}(\theta\delta - \theta k_2)^2. \tag{4.1}$$

By differentiating V with respect to k_0, k_1 and k_2 we get that:

$$\dot{V} = 2A_m^2 e\dot{e} + \frac{2\theta}{\gamma_0'}\dot{k_0}(\theta k_0 - b_m) - \frac{2\theta}{\gamma_1'}\dot{k_1}(-\theta k_1 - A_m) - \frac{2\theta}{\gamma_2'}\theta\dot{k_2}(\theta\delta - \theta k_2) \tag{4.2}$$

$$\dot{V} = 2A_m^3 e^2 + 2A_m^2 e(\theta k_0 - b_m)r + 2A_m^2 e(-\theta k_1 - A_m)p_c + 2A_m^2 e(\theta\delta - \theta k_2) + \frac{2\theta}{\gamma_0'}\dot{k_0}(\theta k_0 - b_m) - \frac{2\theta}{\gamma_1'}\dot{k_1}(-\theta k_1 - A_m) - \frac{2\theta}{\gamma_2'}\dot{k_2}(\theta\delta - \theta k_2). \tag{4.3}$$

We set the last terms to be zero to get the update laws for the parameters

$$2A_m^2 e(\theta k_0 - b_m)r + \frac{2\theta}{\gamma_0'}\dot{k_0}(\theta k_0 - b_m) = 0 \tag{4.4}$$

$$2A_m^2 e(-\theta k_1 - A_m)p_c - \frac{2\theta}{\gamma_1'}\dot{k_1}(-\theta k_1 - A_m) = 0 \tag{4.5}$$

$$2A_m^2 e(\theta\delta - \theta k_2) - \frac{2\theta}{\gamma_2'}\dot{k_2}(\theta\delta - \theta k_2) = 0 \tag{4.6}$$

which gives:

$$\dot{k_0} = -\frac{\gamma_0'}{\theta}A_m^2 er \tag{4.7}$$

$$\dot{k_1} = \frac{\gamma_1'}{\theta}A_m^2 ep_c \tag{4.8}$$

$$\dot{k_2} = \frac{\gamma_2'}{\theta}A_m^2 e \tag{4.9}$$

which can be written as:

$$\dot{k_0} = -\gamma_0 er \tag{4.10}$$

$$\dot{k_1} = \gamma_1 ep_c \tag{4.11}$$

$$\dot{k_2} = \gamma_2 e \tag{4.12}$$

We can then set the terms including the the parameters to zero and get:

$$\dot{V} = 2A_m^3 e^2 \tag{4.13}$$

We have that $A_m > 0$ which means the derivative of V with respect to time is thus negative semidefinite, but not negative definite. This implies that $V(t) \leq V(0)$ and thus that e, k_0, k_1 and k_2 must be bounded. This implies that $p_c = e + p_m$ also is bounded. We see that:

$$\ddot{V} = 4A_m^3 e\dot{e} = 4A_m^3 e\left(A_m e + (\theta k_0 - b_m)r + (-\theta k_1 - A_m)p_c + \theta(\delta - k_2)\right). \tag{4.14}$$

Since r, e, p_c and δ are bounded, it follows that $\ddot{V}$ is bounded. Hence V is uniformly continuous. From theorem 2 it then follows that the error e will go to zero. It does not however show that the parameter values will converge to their true values, only that they are bounded. To have parameter convergence it is necessary to impose conditions on the excitation of the system, but we do not need to have parameter convergence to get a working controller.

4.2 $\mathcal{L}_1$ Adaptive Controller

Rigorous derivations and proofs of the stability margins of the $\mathcal{L}_1$-adaptive controller for systems of the form 2.17 can be found in Cao & Hovakimyan (2007*e*) and Cao & Hovakimyan (2007*b*).

Consider the following closed-loop reference system with its control signal and system response defined as (Cao & Hovakimyan 2007*b*):

$$\dot{x}_{ref}(t) = A_m x_{ref}(t) + b\left(\omega u_{ref}(t) + \theta^\top(t) x_{ref}(t) + \sigma(t)\right), \tag{4.15}$$

$$u_{ref}(s) = \frac{C(s)}{\omega}\bar{r}_{ref}(s),\ x_{ref}(0) = x_0, \tag{4.16}$$

$$y_{ref}(t) = c^\top x_{ref}(t), \tag{4.17}$$

where $\bar{r}_{ref}(s)$ is the Laplace transformation of the signal

$$\bar{r}_{ref}(t) = -\theta^\top(t) x_{ref}(t) - \sigma(t) + k_g r(t). \tag{4.18}$$

We have that the reference system is stable if (Cao & Hovakimyan 2007*b*):

Lemma 2. *If D(s) verifies the condition in 2.28, the closed-loop reference system of 4.15-4.17 is stable.*

4.2.1 Stability

This gives us a stability requirement on the selection of the $\mathcal{L}_1$ gain feedback constant k. We need to select the constant high enough that we fulfill 2.28.

The calculation of the $\mathcal{L}_1$ gain requirement, where we have that the highest value of the $\mathcal{L}_1$ gain comes from the lowest value of ω, was performed based on the values from table 3.5 and 3.7. We calculate the $\mathcal{L}_1$ gain, and find that for topside control we need to select k such that

$k > -1 \cdot 10^{-6}$ or $k\omega > 0.1$ and $k\omega \neq -A_m$.

I therefore select $k = -5 \cdot 10^{-6}$, remembering that a higher k will lead to reduced robustness. This gives us table 4.1 for the lowest, initial and highest value for ω. We see here that if we have large uncertainty in ω we will be forced to select a higher k, and thus risk a less robust controller than if the uncertainty is small.

For bottomhole control the stability analysis shows that we need

$k > -4 \cdot 10^{-5}$ or that $k\omega > 0.1$ and that $k\omega \neq -A_m$,

The value for k is selected as $1.2 \cdot 10^{-4}$, which gives the $\mathcal{L}_1$ gains in table 4.2.

Table 4.1: Topside: $\mathcal{L}_1$ Gain

Topside Control	λ
ω_l	0.4343
ω_0	$3.25 \cdot 10^{-3}$
ω_u	$4.00 \cdot 10^{-4}$

Table 4.2: Bottomhole: $\mathcal{L}_1$ Gain

Topside Control	λ
ω_l	0.593
ω_0	$1.83 \cdot 10^{-4}$
ω_u	$2.22 \cdot 10^{-6}$

4.2.2 Performance

To prove uniform tracking and steady state tracking between the closed-loop adaptive systems with the $\mathcal{L}_1$ adaptive controller and the reference system, a bound on the prediction error is presented in Cao & Hovakimyan (2007*b*):

Lemma 3. *For the system in 2.17 and the $\mathcal{L}_1$-adaptive controller in 2.20, 2.21-2.23 and 2.25, the prediction error is bounded by:*

$$\|\tilde{x}\|_{\mathcal{L}_\infty} \leq \gamma_0 = \sqrt{\frac{\theta_m}{\lambda_{min}(P)\Gamma_c}} \tag{4.19}$$

where

$$\theta_m \triangleq \max_{\theta \in \Theta} \sum_{i=1}^{n} 4\theta_i^2 + 4\Delta^2 + 4(\omega_u - \omega_l)^2 + 4\frac{\lambda_{max}(P)}{\lambda_{min}(Q)}(\max_{\theta \in \Theta}\|\theta\| d_\theta + d_\sigma \Delta). \tag{4.20}$$

We see from equation 4.20 that if we have large parametric uncertainties or large disturbances we will get a very large value for θ_m. From equation 4.19 we find that we can reduce the bound on the estimation error by increasing the adaptation gains. This term is included as $\sqrt{\Gamma_c}$. It is thus possible to render the prediction error arbitrarily small by increasing the adaptation gains. However, it is more efficient, if possible, to reduce the uncertainties or disturbances.

In Cao & Hovakimyan (2008*e*) bounds are presented on the performance and deviations from the wanted x_{ref} and u_{ref}:

Theorem 1. *For the closed-loop system in 2.17 and the $\mathcal{L}_1$ adaptive controller defined via 2.20, 2.21-2.23 and 2.25 subject to 2.28, we have:*

$$\|x - x_{ref}\|_{\mathcal{L}_\infty} \leq \gamma_1, \tag{4.21}$$

$$\|u - u_{ref}\|_{\mathcal{L}_\infty} \leq \gamma_2, \tag{4.22}$$

where

$$\gamma_1 = \frac{\|C(s)\|_{\mathcal{L}_1}}{1 - \|H(s)(1 - C(s))\|_{\mathcal{L}_1} L} \sqrt{\frac{\theta_m}{\lambda_{min}(P)\Gamma_c}},$$

$$\gamma_2 = \left\| \frac{C(s)}{\omega} \right\|_{\mathcal{L}_1} L\gamma_1 + \left\| \frac{C(s)}{\omega} \frac{1}{c_0^\top H(s)} c_0^\top \right\|_{\mathcal{L}_1} \sqrt{\frac{\theta_m}{\lambda_{min}(P)\Gamma_c}}.$$

and c_0 is selected such that

$$c_0^\top H(s) = \frac{N_n(s)}{N_d(s)},$$

where the degree of $N_d - N_n = 1$ and both $N_n(s)$ and $N_d(s)$ are stable polynomials.

Corollary 1. *For the closed-loop system in 2.17 and the $\mathcal{L}_1$ adaptive controller defined via 2.20, 2.21-2.23 and 2.25 subject to 2.28, we have for all $t \geq 0$ that:*

$$\lim_{\Gamma_c \to \infty} (x(t) - x_{ref}(t)) = 0, \tag{4.23}$$

$$\lim_{\Gamma_c \to \infty} (u(t) - u_{ref}(t)) = 0. \tag{4.24}$$

The tracking errors are thus uniformly bounded by a constant, which is inversely proportional to the adaptation rate Γ_c. We can during the transient phase achieve arbitrarily close tracking performance by increasing Γ_c (Cao & Hovakimyan 2008*e*).

We calculate the actual bounds for the topside controller for different values of Γ_c to see how it affects the tracking performance and how big the gains will need to be if we have large uncertainties or large disturbances.

Table 4.3: $\mathcal{L}_1$ - Topside: Estimated performance bounds

bound / Γ_c	$5 \cdot 10^5$	$5 \cdot 10^{10}$	$5 \cdot 10^{15}$
γ_0	$5.67\ [bar]$	$0.1793\ [bar]$	$5.67 \cdot 10^{-5}\ [bar]$
γ_1	$5.69\ [bar]$	$0.1799\ [bar]$	$5.69 \cdot 10^{-5}\ [bar]$
γ_2	345	1.09	0.0035

We see from table 4.3 that the adaptive gain will need to be very large to be able to guarantee good performance in the presence of large disturbances. This is all quite theoretical and is based on many conservative estimates, and the chance of actually reaching the bound is very low. I do not think the value of the actual bounds is very large, but it shows how both increased adaptive gain, reduced uncertainty and reduced disturbances influence performance bounds.

Another interesting observation is that in the case of $C(s) = 1$, the magnitude of $\left\| \frac{C(s)}{\omega} \frac{1}{c_0^\top H(s)} c_0^\top \right\|_{\mathcal{L}_1}$ cannot be finite. Thus it is not possible in MRAC to reduce γ_2 by increasing the adaptation gain.

The same calculations were performed for the bottomhole structure and are summarized in table 4.4.

Table 4.4: $\mathcal{L}_1$ - Bottomhole: Estimated performance bounds

bound / Γ_c	$5 \cdot 10^5$	$5 \cdot 10^{10}$	$5 \cdot 10^{15}$
γ_0	600 $[bar]$	1.9 $[bar]$	$6.03 \cdot 10^{-3}$ $[bar]$
γ_1	600 $[bar]$	1.91 $[bar]$	$6.04 \cdot 10^{-3}$ $[bar]$
γ_2	$1.58 \cdot 10^7$	50048	158

4.3 Stability margins

The time-delay and gain margins for the three different controllers are computed using numerical simulations. We introduce a time-delay at the plant input and a time-delay at the output. The delays are increased until the system loses stability. The method is illustrated in figure 4.1.

The time-delay margin is found for both the $\mathcal{L}_1$ adaptive and PI controller for the topside and the bottomhole control scheme. For MRAC we only find it for the topside case. All time-delays are found for the regular values of the plant. If we get changes in plant parameters, the time-delay margins will change for the controllers. We will however see in the next sessions that the $\mathcal{L}_1$ adaptive controller offers a guaranteed lower bound, given that we are within the estimated bounds.

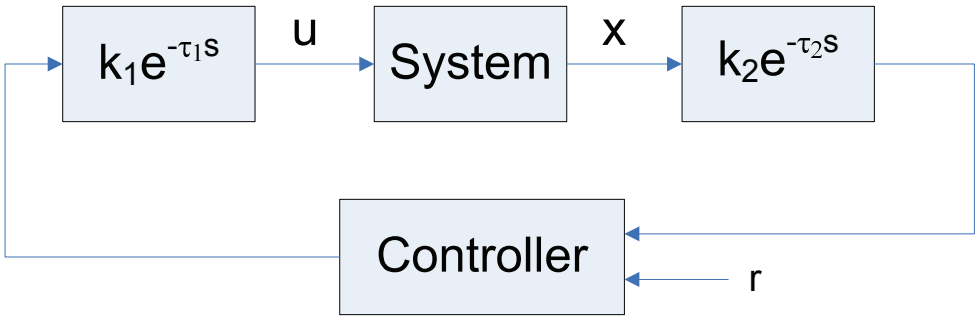

Figure 4.1: Finding time-delay and gain margins

For the PI controller we find the time-delay margins as given in table 4.5. We also find the time-delay margins for the more aggressive tuning parameters calculated in the tuning chapter.

Table 4.5: PI: Time-delay margins

Parameter	Topside q_l	Topside q_h	Bottomhole q_l	Bottomhole q_h
τ	2.40	2.47	2.68	2.34
Aggressive	0.63	0.63	0.66	0.61

MRAC time-delay margins are calculated for the topside case. They are listed in table

4.6 along with time-delay margins using slower adaptive gains, where $\gamma_0 = \gamma_1 = 1 \cdot 10^{-15}$ and $\gamma_2 = 5 \cdot 10^{-10}$.

Table 4.6: MRAC: Time-delay margins

Parameter	Topside q_l	Topside q_h
τ	1.61	1.63
Low gain	6.0	6.5

Finally, for the $\mathcal{L}_1$ adaptive controller we get the time-delays given in table 4.7. We see that we get very small margins for the standard values of k. A lower $k = 5 \cdot 10^{-8}$ is also evaluated and we see a large increase in time-delay margins, but we have no guarantee for stability. If ω falls too low, we might break the $\mathcal{L}_1$ gain stability criteria. We see that it might prove difficult to select one k to cover the entire range of ω if this gain parameter has a large range of variation. We know that a higher order filter might give better time-delay margins.

Another possibility is to reduce the uncertainty of the parameters by using known information and signals. One could add feedforward compensation to compensate for known pump disturbances. Since this is possible, the lower value for k will be used in simulations because of the extremely low robustness margins for the calculated k for guaranteed stability.

Table 4.7: $\mathcal{L}_1$: Time-delay margins

Parameter	Topside q_l	Topside q_h	Bottomhole q_l	Bottomhole q_h
τ	0.01	0.01	$4.5 \cdot 10^{-4}$	$4.5 \cdot 10^{-4}$
Low k	1.13	1.13	1.45	1.45

4.4 $\mathcal{L}_1$ Time Delay and Gain Margin Analysis

For the $\mathcal{L}_1$ adaptive control scheme it is possible to derive a conservative, but guaranteed bound for the time-delay margin analytically. This is done by introducing an equivalent LTI system, which can be related to the closed loop adaptive system. This is done for the case of an unknown, but constant θ in Cao & Hovakimyan (2007*b*) and Hovakimyan (2008). All listed values are given in seconds.

The time-delay margin is given as:

$$\mathcal{T}(H_o(s)) = \text{PM}(H_o(s))/\omega_c \tag{4.25}$$

where $\text{PM}(H_o(s))$ is the phase-margin of

$$H_o(s) = \frac{C(s)}{1 - C(s)}(1 + \theta^\top \bar{H}(s)), \tag{4.26}$$

where $\bar{H}(s) = (sI - A_m - b\theta^\top)^{-1}b$.

To establish the equivalence between the LTI system and the closed loop adaptive systems we get some additional requirements on the set of Δ and the lowest gain Γ_c (Hovakimyan 2008).

The calculated lower bounds for the time-delay margins are listed in table 4.8, and are in accordance with the expected values based on the numerical simulations.

Table 4.8: $\mathcal{L}_1$: Analytic time-delay margins

Setting	$\tau\ [sec]$	PM $[degrees]$	$\omega_c\ [Hz]$
Top	0.0099	89.99	1000
Top Low k	0.9742	88.85	10
BH	$5.4831 \cdot 10^{-5}$	90.00	18000
BH Low k	0.1314	89.85	75

Introducing a gain module $\omega_g = \omega g$ into the control loop implies the need to increase the set ω_0, and we get the larger set Ω which was introduced in the theory chapter. The gain margin is determined by

$$\mathcal{G}_m = [\omega_l/\omega_{l0},\ \omega_u/\omega_{u0}] \tag{4.27}$$

and if $g \in \mathcal{G}_m$, then the closed loop system satisfies the $\mathcal{L}_1$ gain theorem and the system is stable. This implies that the arbitrary gain margin might be obtained through appropriate selection of Ω (Cao & Hovakimyan 2007*e*). Note however that increasing the set will lead to stricter demands on selection of k, which again might hurt the time-delay margin.

Chapter 5

Simulation

In this chapter a simulation study of the different controllers and control structures is performed. We start off by looking at some common drilling scenarios, and then evaluate some common control issues. We move on to how changing system parameters affects robustness and performance, and finally we compare topside to bottomhole control.

Simulations are performed using the topside control scheme, unless stated otherwise. It is also of importance to notice that the control system measurements are saved only so often, so some of the high-frequency oscillations in the $\mathcal{L}_1$ state predictor are hidden. We also select a much lower $\mathcal{L}_1$ adaptive gain ($\Gamma_c = 5 \cdot 10^5$) than the estimates from the last chapters indicate we should select as the standard simulation value, but we will see that as long as the adaptive gain is high enough we will still have good performance. However we can select a much higher time-step. The positive effects of these two choices are less required memory, less required storage and faster run-time.

5.1 Simulation Tools

Simulations are performed by the use of the simulation structure developed in Pedersen (2008). Some testing, tuning and evaluation has also been performed on Simulink models based on the Kaasa equations. The simulation structure has been extensively reworked to facilitate the introduction of the $\mathcal{L}_1$ adaptive controller.

The models used are in no way optimized for best run-time performance; they are constructed to be robust and easy to modify. Any results on simulation length are thus not comparable to a field implemented control system, but are only meant to illustrate the impact of different settings.

5.2 Simulation of Scenarios

In the introduction and background chapter we introduced several common drilling operations and issues. In this section we will take a closer look at some selected scenarios and how they are implemented in the simulator. In appendix C.1 I give a complete list of all the simulations performed. All the simulation data are available on the compact disk (Approximately 300 MB), but only a small subsection of the most interesting observations are included in this thesis. Our nominal case, used to evaluate performance, is the connection scenario. The connection scenario is selected because it is a very common drilling operation, and because it can be used to illustrate the effects of both pump disturbances and changing reference trajectory at different operating points.

A typical drilling window is $5\ [bar]$, this means the pressure is allowed to vary $\pm 2.5\ [bar]$ around the set point (Godhavn 2009). This means that we will allow for a maximum overshoot when changing setpoint and no poorer disturbance rejection than $\pm 2.5\ [bar]$.

5.2.1 A Connection

The connection scenario (from chapter 2.1.5) is implemented in the simulator as a simple ramp down, wait and further ramp up of the main mud pump.

The ramp down is initialized after two minutes; we go from $2000\ [l/min]$ to $0\ [l/min]$ in two minutes. When the mud pump input flow falls below $200\ [l/min]$ the backpressure pump automatically kicks in and goes from $200\ [l/min]$ to $400\ [l/min]$.

The connection is assumed to take an additional 11 minutes, before we get a symmetric ramp up. During the connection we induce a change in the pressure setpoint. For the topside scenario we go from $10\ [bar]$ to $5\ [bar]$, and back up. The same step is performed after the mud pump is back at full output. The corresponding values for bottomhole control is $260\ [bar]$ to $250\ [bar]$.

It should be mentioned that this is a simplification of the real procedure. Many more effects could be added; for example would it also be interesting to consider the tripping and heave forces experienced while removing and adding drill string from the well, but this is not done here.

We see from figure 5.1 and 5.2 that all controllers are well within the drilling window. The deviations between controllers are influenced by differences in tuning. More about the tuning performed and the consequences of tuning choices follows in the discussion chapter and is available in appendix B.

We see that the $\mathcal{L}_1$ adaptive controller gives somewhat better performance than the two other controllers. Most interesting is perhaps the observation that the PI controller needs quite hard tuning to be able to give good disturbance rejection. One could think the tuning parameters for the PI controller could perhaps have been selected to give some more deviations during the pump change and give less overshoot, but the next scenario will show that this is not possible.

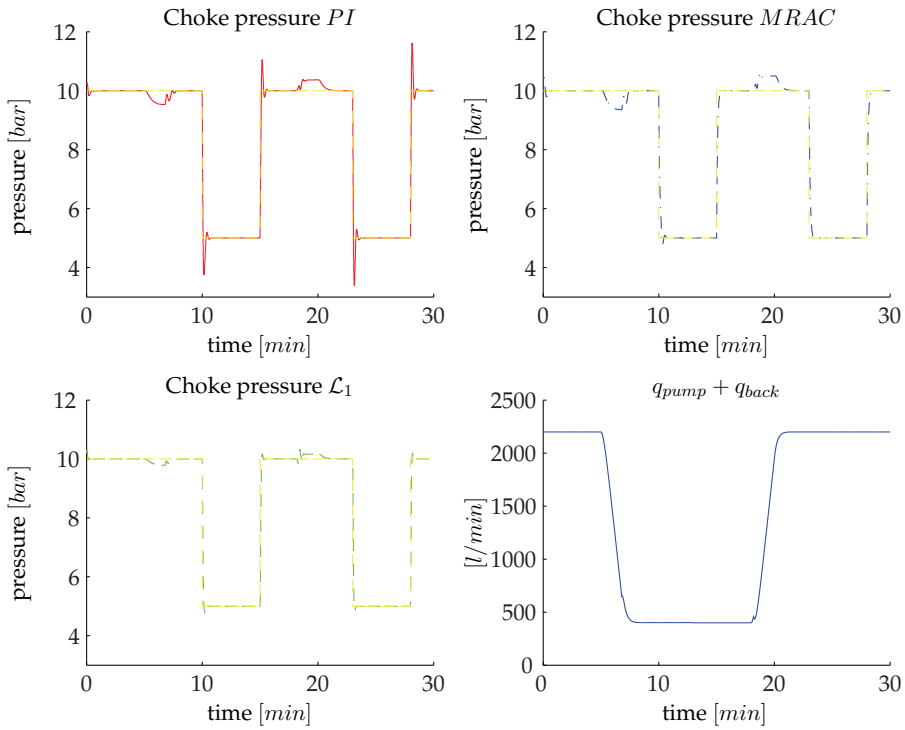

Figure 5.1: Connection scenario: Tracking performance

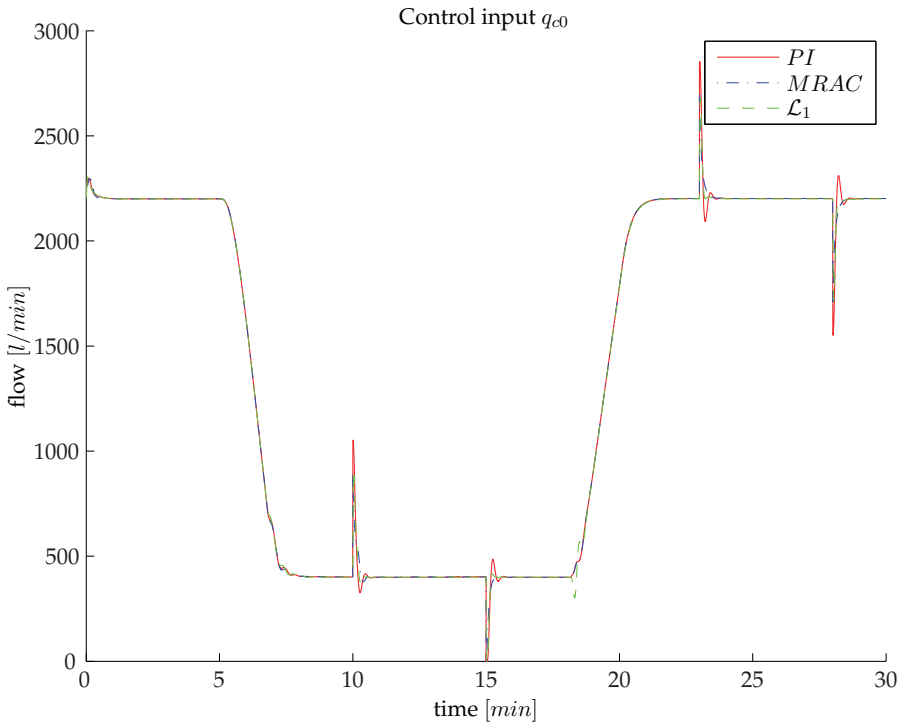

Figure 5.2: Connection scenario: Control input

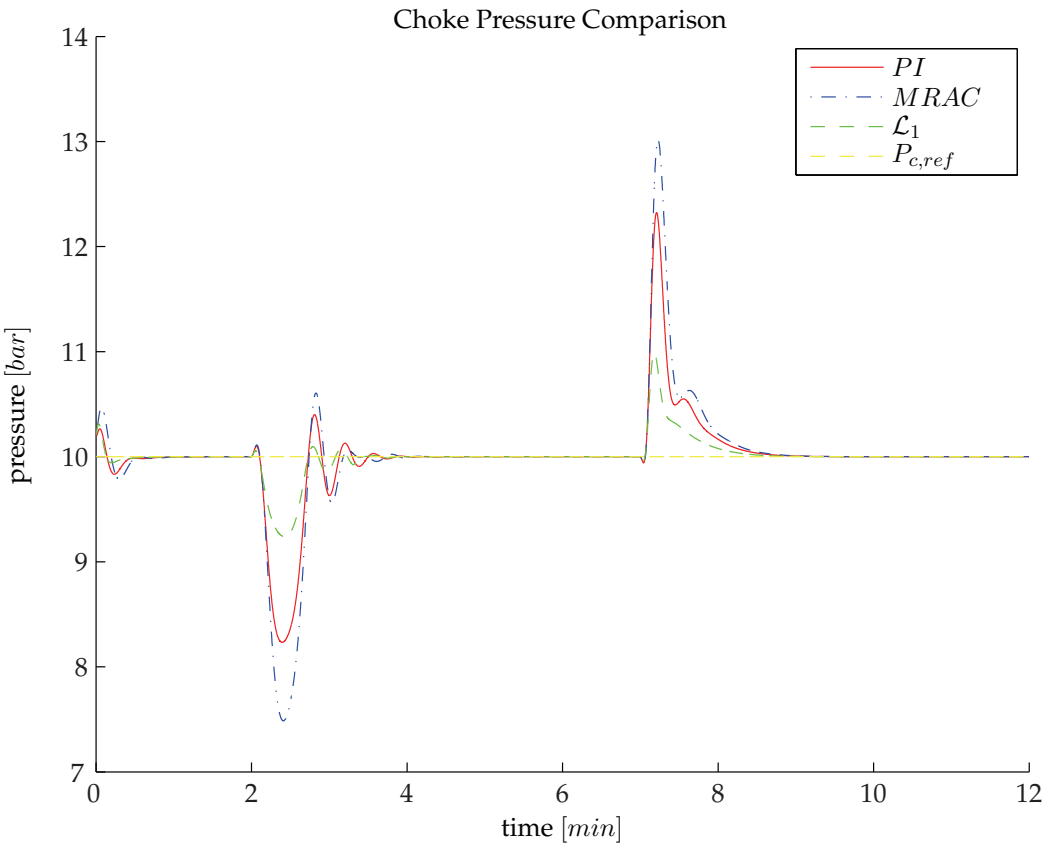

Figure 5.3: Power loss scenario: Tracking performance

5.2.2 Power-loss

Power-loss is simulated as an abrupt step change, from full input to zero, in the mud pump input. We get a fall in pump flow as fast as the pump dynamic permit. The power-loss is initiated after two minutes, and lasts for five minutes. This scenario gives one of the fastest input disturbances and we see from figure 5.3 that the integral effect needs to be high to provide good disturbance rejection for the PI controller. The same is true for the adaptive gains for MRAC. In fact, the PI controller is just inside the maximum peak deviation while the MRAC does not give entire satisfactory rejection in this scenario, with the peak error just above 3 $[bar]$. The $\mathcal{L}_1$ controller, with its high adaptive gains, showed good performance for this scenario.

5.2.3 Reservoir Fluid Loss and Influx

The difference from the the other input disturbances is that the loss and influx from the reservoir are not measured. If we are to design a good compensator, we thus need some kind of estimator for the additional fluid leaving or entering the system. It might also bring the system to new operating points not considered in the design.

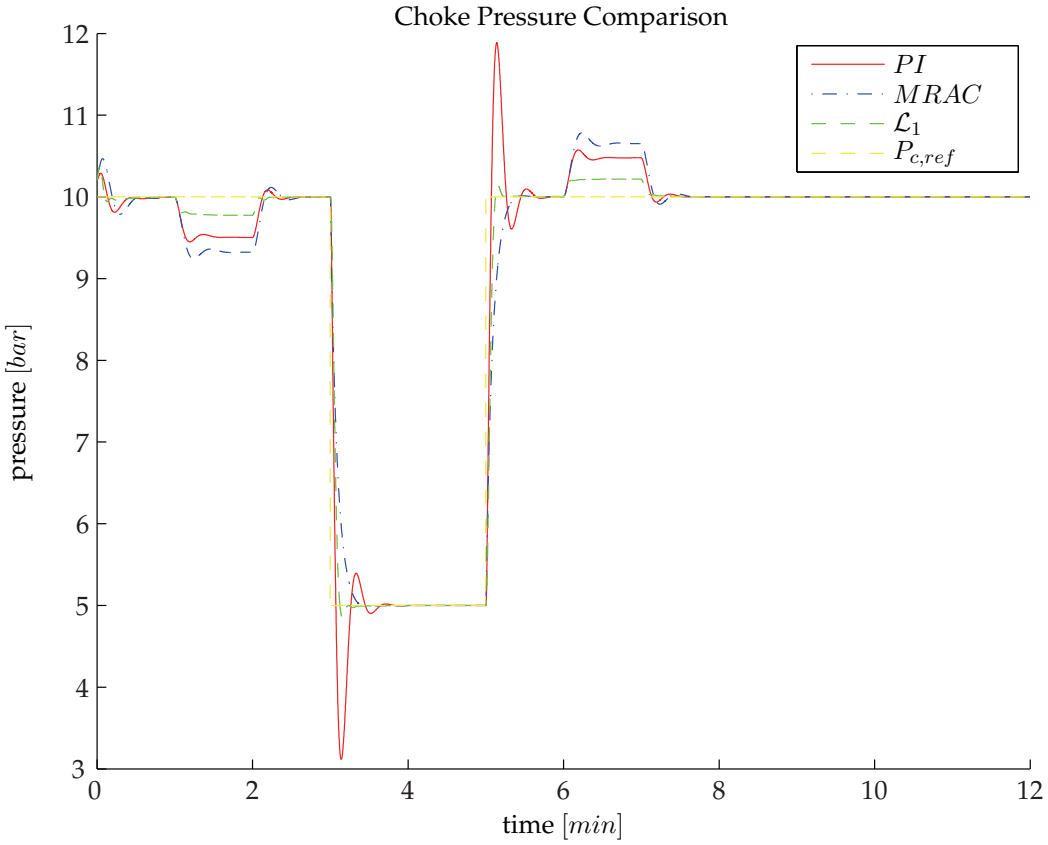

Figure 5.4: Loss scenario - High flow: Tracking performance

The mud-loss scenario simulates the loss of mud to the reservoir. The modeling of loss is very simple and it is implemented only as a sudden loss, going from $q_{res} = 0$ $[l/min]$ to -1200 $[l/min]$ in one minute. The influx is stable for 4 minutes before we get a symmetric ramp up. The scenario is tested both for full mud pump flow and for zero mud pump flow. In the former we perform a reference step, while the last one naturally leads to saturation. We will come back to saturation in a few sections.

We see from figure 5.4 that in the first loss scenario all the controllers are within the specified limits. The performance is similar to the connection scenario with the $\mathcal{L}_1$ controller providing the best performance. For the second scenario (fig: 5.5) the best action the controller can perform is to quickly close the choke. The $\mathcal{L}_1$ adaptive controller does this fastest followed by the MRAC controller. However, the overall differences are small.

The small kick scenario simulates an influx of fluid from the reservoir. The modeling of the influx is the inverse of the loss scenario and it is implemented as a sudden influx, going from $q_{res} = 0$ $[l/min]$ to 1200 $[l/min]$ in one minute. The influx is stable for 4 minutes before we get a symmetric ramp down.

Figure 5.6 indicates that the performance for the controllers during the kick scenario is approximately the same as for both the connection and the first loss scenario.

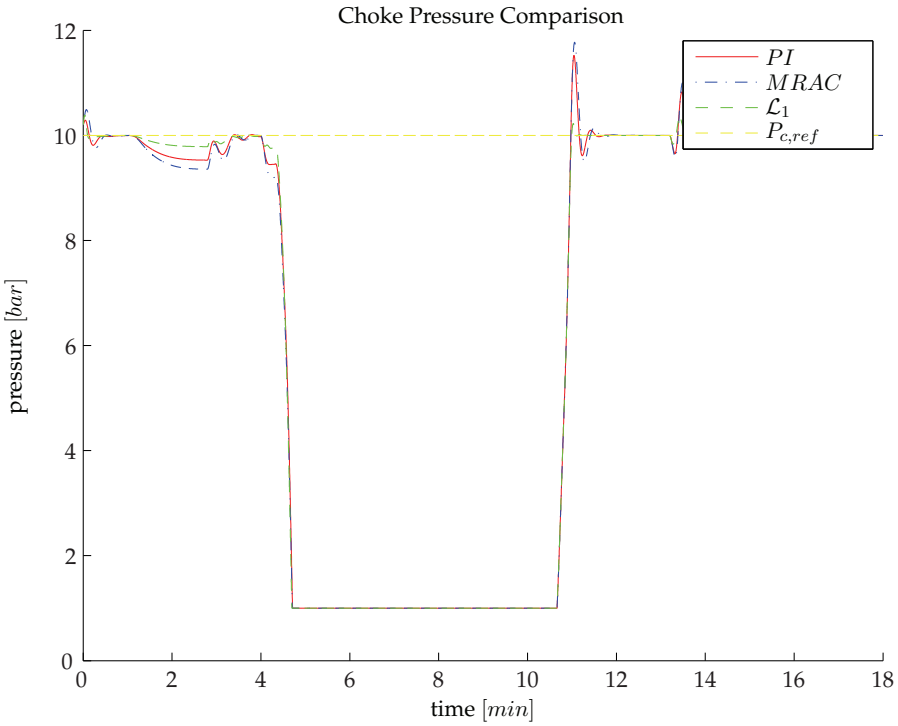

Figure 5.5: Loss scenario - Low flow: Tracking performance

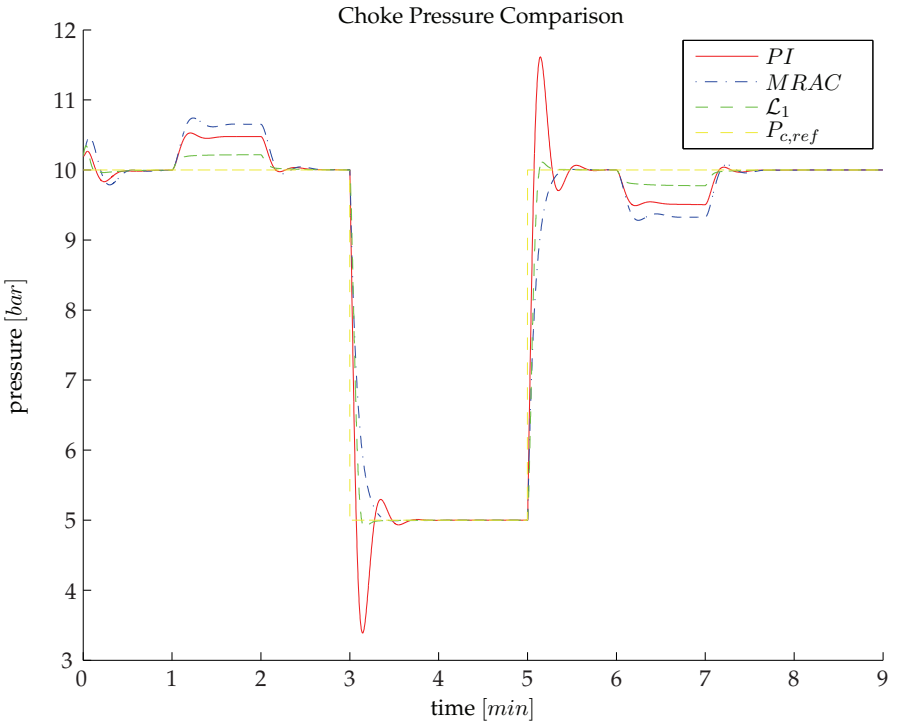

Figure 5.6: Kick scenario: Tracking performance

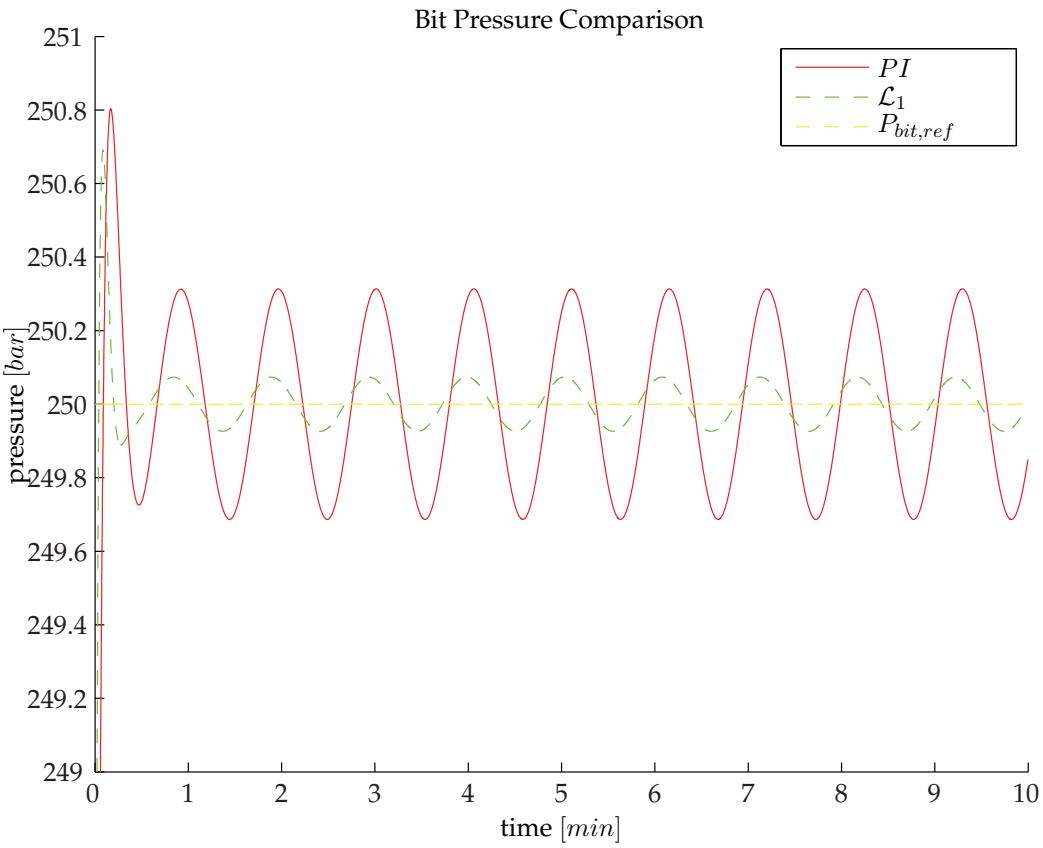

Figure 5.7: Fast ΔP term: Tracking performance

5.2.4 Fast Changing Pressure Term

In this scenario we simulate a rapidly changing pressure term. We have a variation of vertical depth h_{bit} of twenty meters over a period of one minute. Left unchecked, this would result in pressure deviations at the bit of approximately ± 0.89 $[bar]$. This scenario is performed using the bottomhole structure, and only the PI and $\mathcal{L}_1$ adaptive controllers are evaluated.

We see from figure 5.7 that the PI controller is not able to suppress much of the disturbances, and we still have changes of ± 0.313 $[bar]$. The $\mathcal{L}_1$ controller does much better and reduces the perturbations to ± 0.074 $[bar]$. The observed oscillations are thus 35.17 percent and 8.31 percent of the original disturbance.

5.2.5 Inner Flow Dynamics and Gas in the Choke

Until now we have ignored the inner flow dynamics and assumed that we can set q_c directly. We will now include the extra dynamics equation from chapter 2.2. We will also see what happens if we get gas in the choke leading to slower control dynamics with more oscillations, and increased time-delay. The scenario is implemented by changing

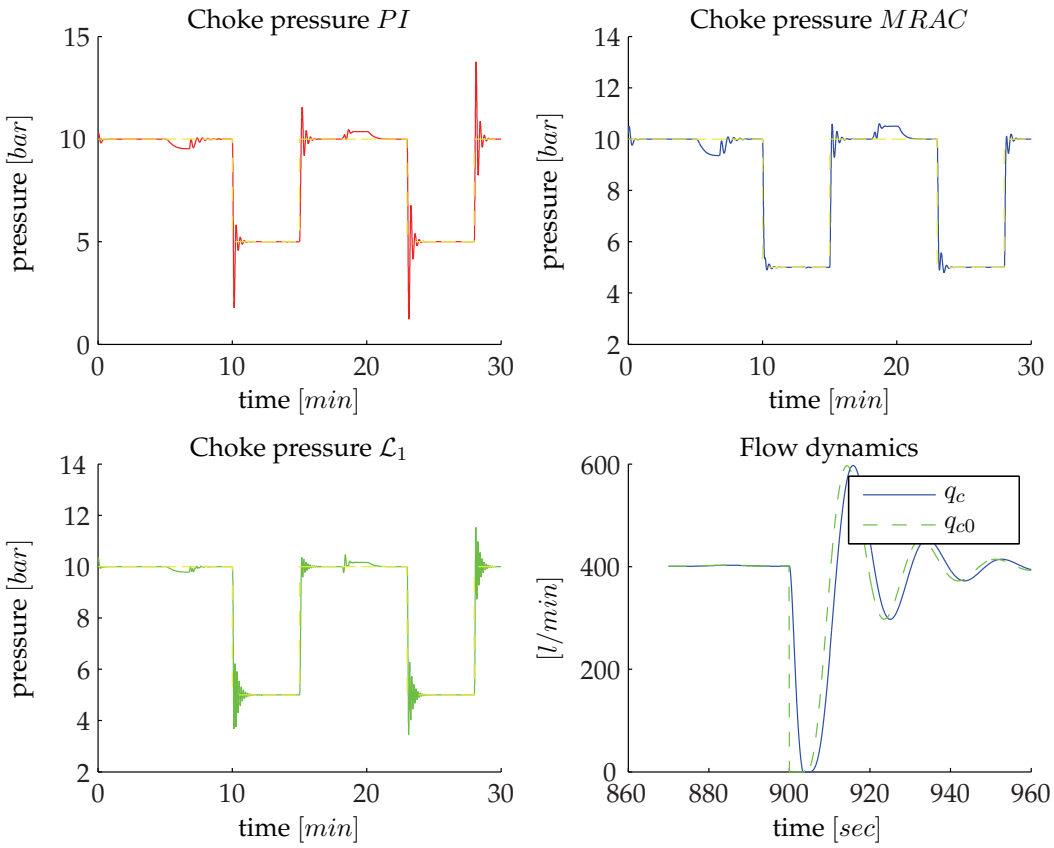

Figure 5.8: Slow inner flow dynamics: Tracking performance

the flow dynamics parameters as given in table 5.1. We try three different inner flow dynamics (normal, slow and slower) and see how they affect tracking performance for the connection scenario.

Table 5.1: Inner dynamics

Scenario	w_c	ζ_c
$Normal$	4	0.7
$Slow$	1	0.7
$Slower$	0.5	0.7

For the slow scenario the amount of delay in the control signal is already quite evident and we see from figure 5.8 that we have degradation in control performance for all the controllers. Though the $\mathcal{L}_1$ adaptive controller still has numerically low deviations for the controlled variable, we have fast oscillations. We know that the amount of time-delay we can permit is not very high, and we are close to the limit. The PI controller no longer gives sufficient performance, with peak values outside the drilling window, and we need to retune the controller. The MRAC gives the best performance for this scenario, but we know the disturbance rejection is a bit low.

5.3 Controller Issues

5.3.1 Measurement Noise

We introduce measurement noise on all signals available for the control systems, and see if we get any issues with control input usage or adaptation. The noise is calculated as normally distributed noise with a mean of zero percent and standard deviation of one percent. This is multiplied with the measurements, giving a percentual deviation from the real signal.

A Connection with Noise

We return to our test case, the connection scenario. We see from figure 5.9 that simulations performed showed no real degradation of control performance, and all the controllers are well within the drilling window. We do not see much drift in parameter estimates; however this case has quite good excitation of signals, even though we get even more high frequencies in the estimated parameters for the $\mathcal{L}_1$ adaptive controller, and thus also in the state predictor. Simulations also showed more erratic use of control input and we should add a filter on the measured signals.

Drift Issues

Since the connection scenario has such good excitation, we introduce a simple case where we simply want to follow a constant reference with no change of pump inputs. The parameter estimation is thus dominated by the noise induced changes. This scenario is of course only interesting for the adaptive controllers.

The $\mathcal{L}_1$ adaptive controller parameter estimates drift to the projection limits, but the controller still shows good performance. The MRAC parameters also shows some drift, but this drift is very slow because of the low adaptive gains. The drift might however become a problem over very long time, but can be stopped by for example a dead zone addition.

5.3.2 Control Input Saturation

In this section we take a closer look at what happens if the control input saturates. The scenario is implemented using the inner flow dynamics. We get a very high step, from $10\ [bar]$ to $100\ [bar]$, after two minutes. The high step leads to saturation of the control input, the flow goes to zero and it is not possible to get negative choke flow (we do not include the backpressure pump as a control input). After three minutes the setpoint is set to $40\ [bar]$.

Simulations show that all controllers have saturation issues if not properly implemented. However, available countermeasures were easy to implement. For the PI controller a

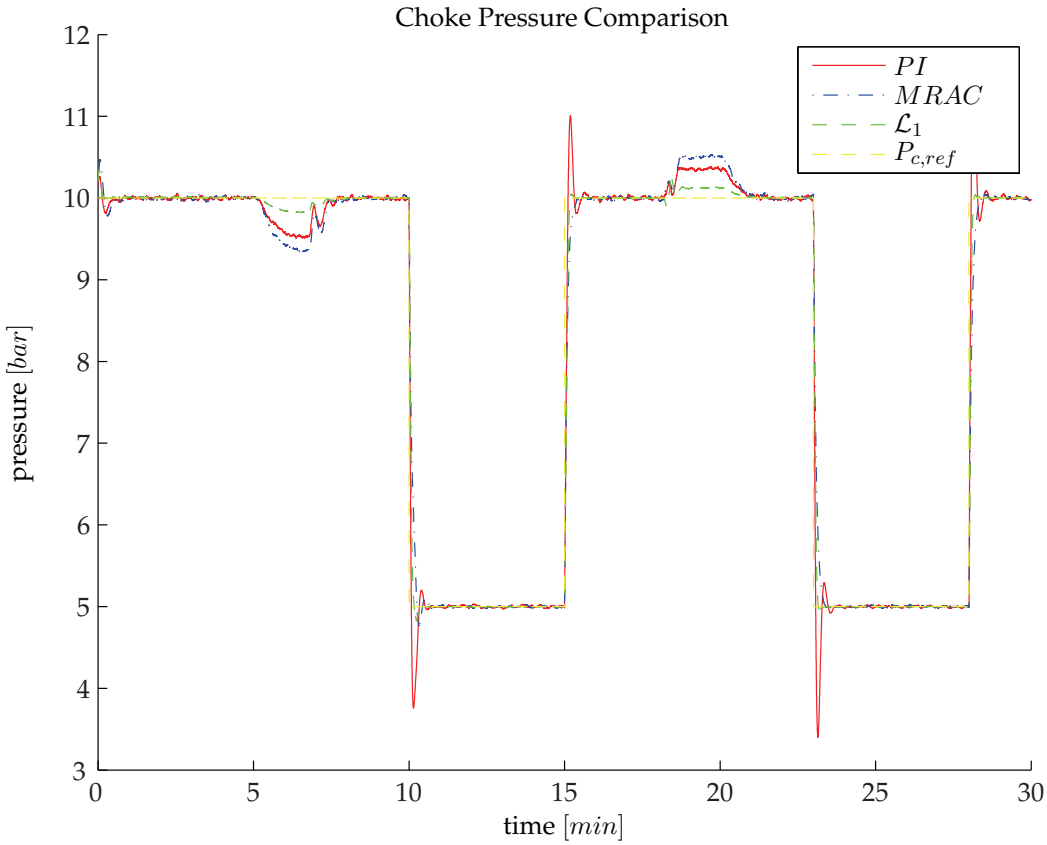

Figure 5.9: Noise: $\mathcal{L}_1$ adaptive controller. Measurement noise added to all signals

simple anti-windup mechanism was introduced to stop the integral error from increasing / decreasing if the control input has saturated. For the MRAC controller it was necessary to stop the adaptation at the saturation limit, while for the $\mathcal{L}_1$ adaptive controller we added projection on the state χ. The projection has not been theoretically justified.

5.3.3 Sampling and Numerical Effects

In this section we look at how the sample time and the numerical time-steps affect the controllers. For $\mathcal{L}_1$ adaptive control we know that a fast low-pass filter needs a small time-step. How does this affect stability and what happens if we select a too large time-step, and what happens if we do not have fast measurements?

Time-step

We start by setting the same $\mathcal{L}_1$ gain constant and adaptive gains for the $\mathcal{L}_1$ adaptive controller, and then we try three different time-step sizes h for the adaptive controller. We see from figure 5.10 that if we set the time-steps too high we may cause instability. Only for the lowest time-step do we have a good transient performance at all times.

Note here that the adaptive gains selected are set low, but the results will be similar for any gain.

The effect of slow sampling

The controllers run at different numerical step-lengths due to the stability issues with the $\mathcal{L}_1$ controller. While the MRAC and PI controller are updated every 0.1 $[sec]$, the loop time for the $\mathcal{L}_1$ adaptive controller is set to 0.001 $[sec]$. Does this mean that we need very fast measurements for the $\mathcal{L}_1$ adaptive controller? We will see that is not so. The control system is tried for four different update speeds for the measurements from the simulator plant: $0.1,\ 0.5,\ 1.0$, and 2.0 $[sec]$. Finally the system is simulated with both dynamics and a sampling rate of 1.0 $[sec]$

From figure 5.11 and 5.12 we see that for the 1.0 $[sec]$ sampling rate, all the controllers provide good performance, while for the two second sampling all controllers are still stable, but the PI controller is at its performance limit. The controllers show some better stability margins than predicted, but note that this is for output delays.

We also see that we do not have to implement the control input to the plant as often as the control system time-step, something that would quickly destroy the control choke. We simulate with inner flow dynamics, a new measurement and a change in the control input every 0.5 $[sec]$. We see from figure 5.13 that we still have acceptable performance for all controllers.

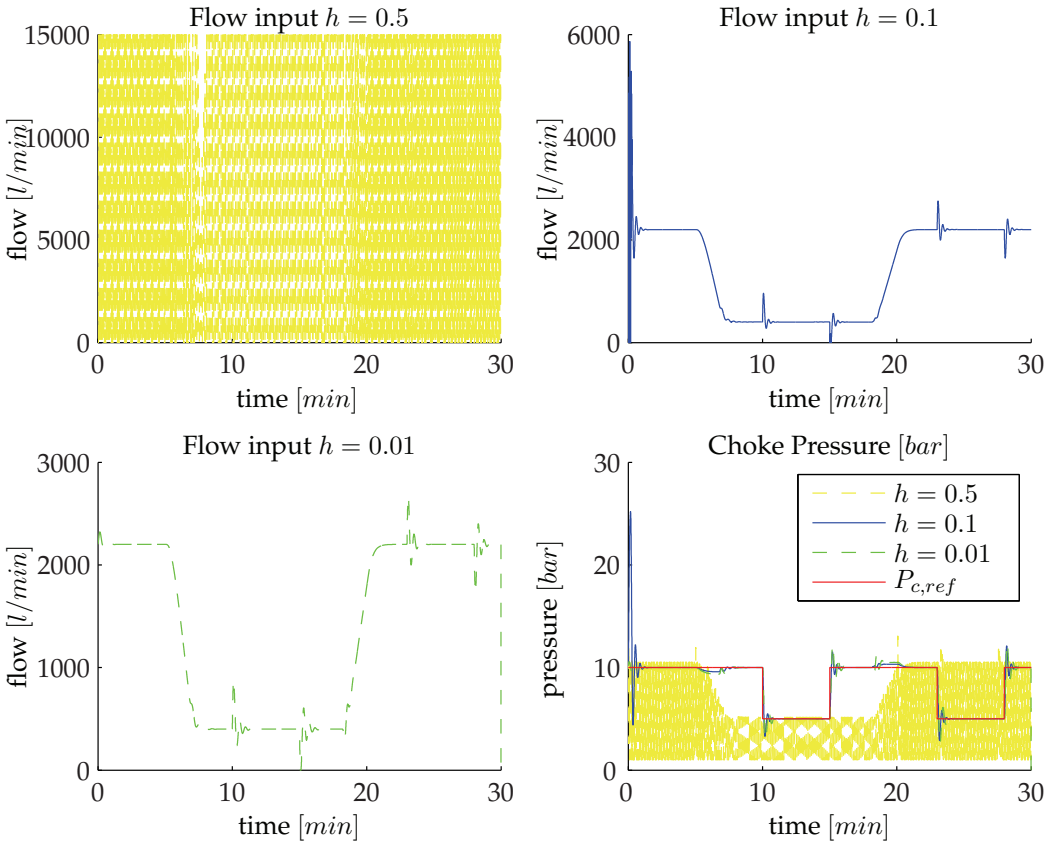

Figure 5.10: $\mathcal{L}_1$ adaptive controller. Simulation with the same $\mathcal{L}_1$ gain constant and adaptive gains for three different step-sizes.

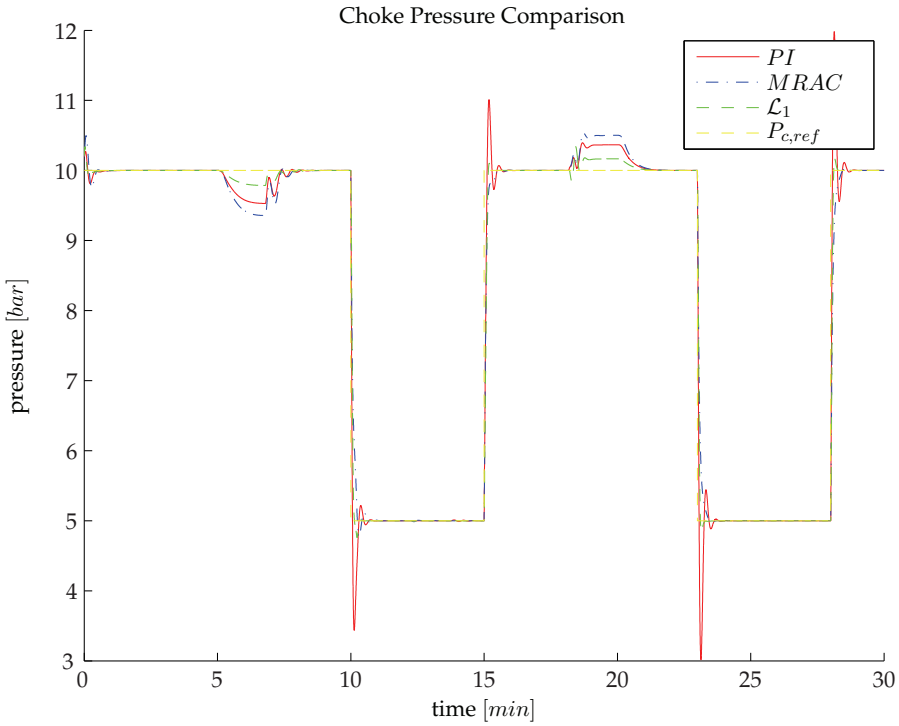

Figure 5.11: Sampling 1 $[sec]$: Tracking performance

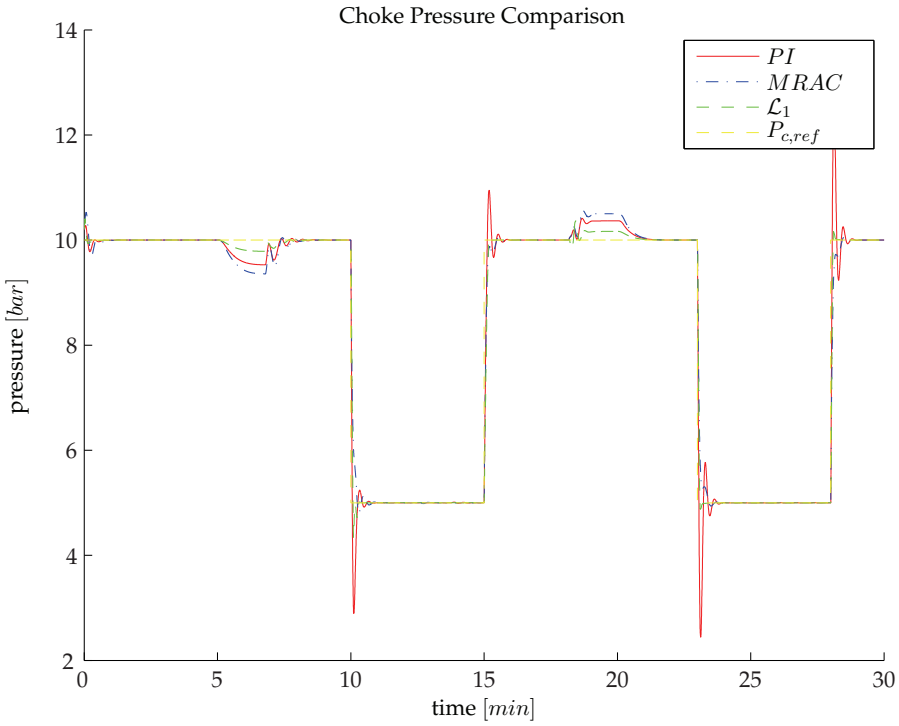

Figure 5.12: Sampling 2 $[sec]$: Tracking performance

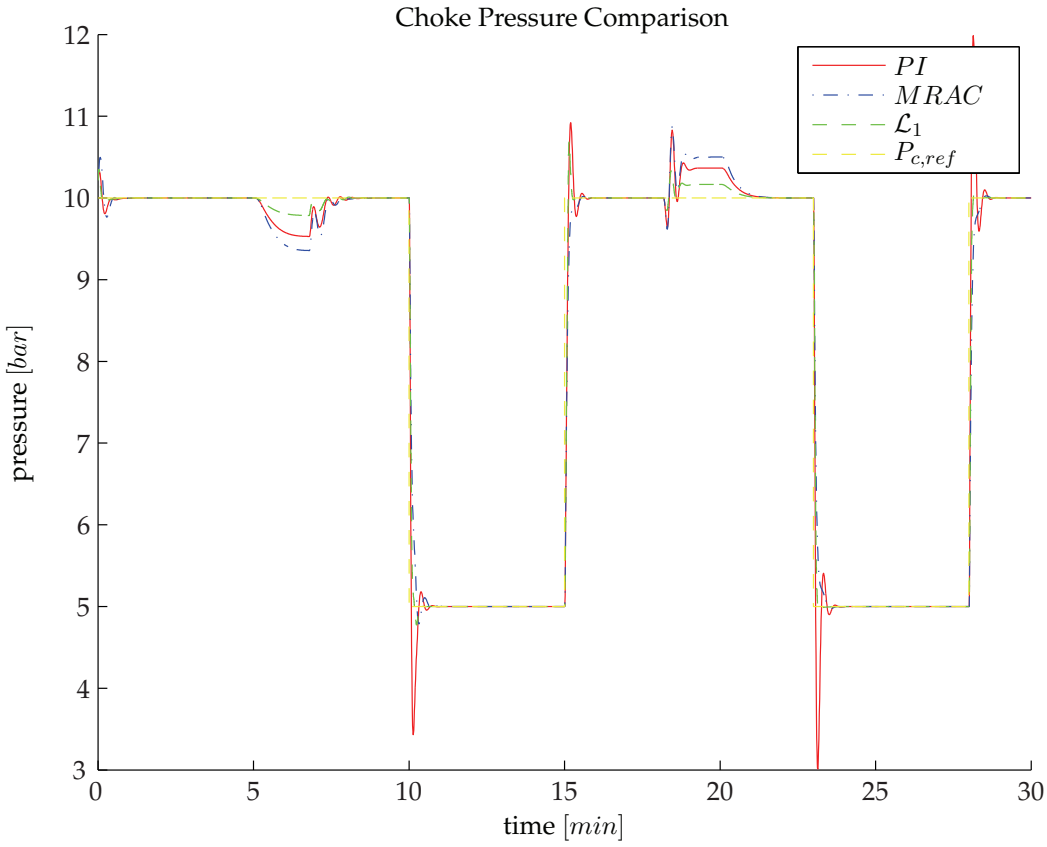

Figure 5.13: Tracking performance for connection with sampling and new control input every 0.5 $[sec]$ and included inner dynamics

However, the control system itself will need to operate at quite high speeds. This means that the computational needs of $\mathcal{L}_1$ adaptive control, especially for large adaptive gains, might be larger than a standard control solution will provide.

Simulation run-time

We have seen that the performance of the $\mathcal{L}_1$ adaptive controller depends on the adaptive gains. High adaptive gains require small time-steps. Small time-steps require fast CPU. So how low do we need to set the time-step for perfect tracking? Based on fixed-step simulation in Simulink, using ODE4 and a inner sample time of 0.1 $[sec]$ for the system, we find the numbers in table 5.2. Note that the exact time-step was not tried found, but the numbers indicate the area in which they lie.

Table 5.2: $\mathcal{L}_1$: Gain versus time-step

Γ_c	Time-step h
$1 \cdot 10^2$	$1 \cdot 10^{-1}$
$1 \cdot 10^3$	$1 \cdot 10^{-2}$
$1 \cdot 10^4$	$1 \cdot 10^{-2}$
$1 \cdot 10^5$	$1 \cdot 10^{-3}$
$1 \cdot 10^6$	$1 \cdot 10^{-3}$
$1 \cdot 10^7$	$1 \cdot 10^{-4}$
$1 \cdot 10^8$	$1 \cdot 10^{-4}$
$1 \cdot 10^9$	$1 \cdot 10^{-5}$
$1 \cdot 10^{10}$	$1 \cdot 10^{-5}$

We see that these numbers get very low after $1 \cdot 10^6$. This means we will need a very fast control system.

The actual run-time for the simulator for a connection scenario with slow dynamics was by comparison: $h = 1 \cdot 10^{-2}$ lasted 25.4 minutes; $h = 1 \cdot 10^{-3}$ lasted for 260.5 minutes; and $h = 1 \cdot 10^{-4}$ lasted 2292,2 minutes.

5.4 Changing Well Parameters

In this section we will look at robustness and performance when changing some important system parameters. The perhaps most interesting parameters to change are the mud weight, bulk modulus of the annulus β_a and the friction in the annulus F_a.

5.4.1 Changing Mud Weight

This scenario simulates changing the mud density during drilling. This is a slow process where all the mud is changed with a heavier / lighter oil. This is simulated by

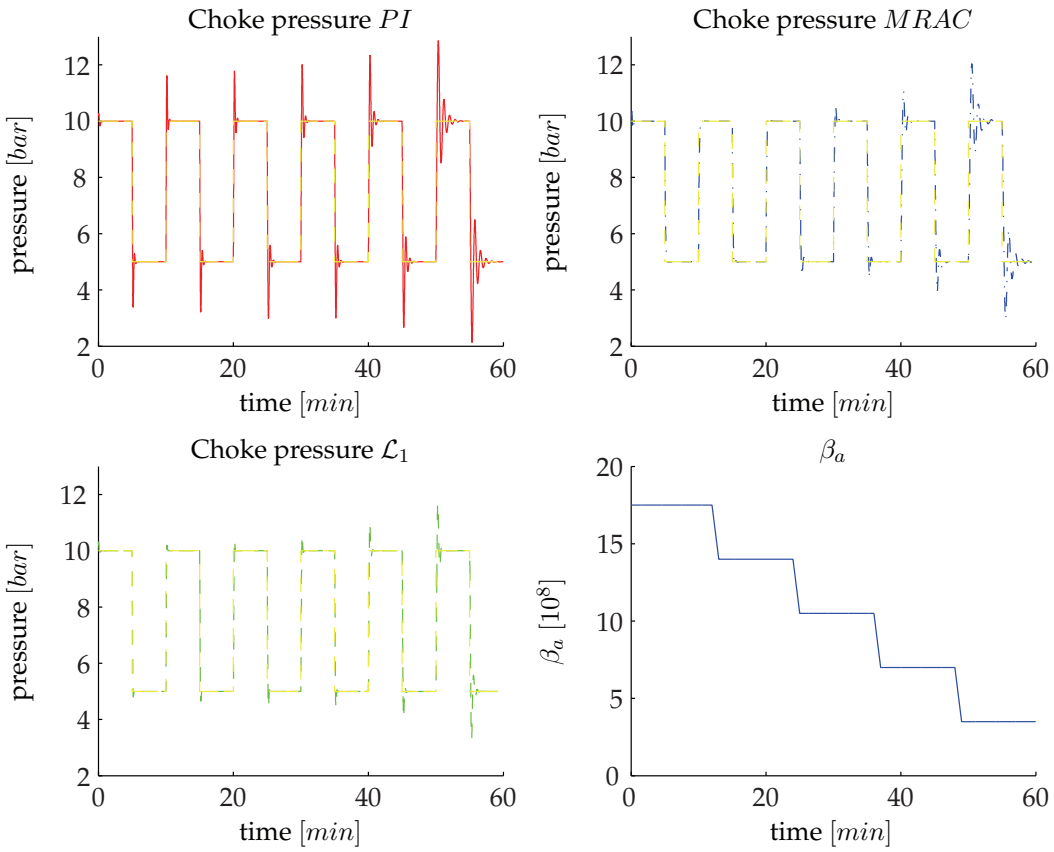

Figure 5.14: Changing bulk modulus β_a: Control performance in tracking

slowly changing the mud density ρ_d in the drill string by a linear ramp. This is assumed to take 30 minutes. The total change is $\Delta\rho = -100$. We get the same ramp in the annulus for ρ_a, but with a time delay of 20 minutes. To check if we get any large changes in performance we are constantly running a change in reference pressure. The scenario was performed using bottomhole control and only the PI and $\mathcal{L}_1$ adaptive controller were tested.

Simulation results showed that none of the controllers faced any real degradation in performance.

5.4.2 Changing Bulk Modulus

Change in bulk modulus is most interesting in the annulus where small amounts of gas in the drilling mud might lead to a lower bulk modulus β_a. This is simulated by lowering the bulk modulus every twelve minutes and running the same step reference changes over one hour.

We see from the simulations results from figure 5.14 and 5.15 that the best results are from the adaptive controllers, and especially the $\mathcal{L}_1$ adaptive controller. However wee

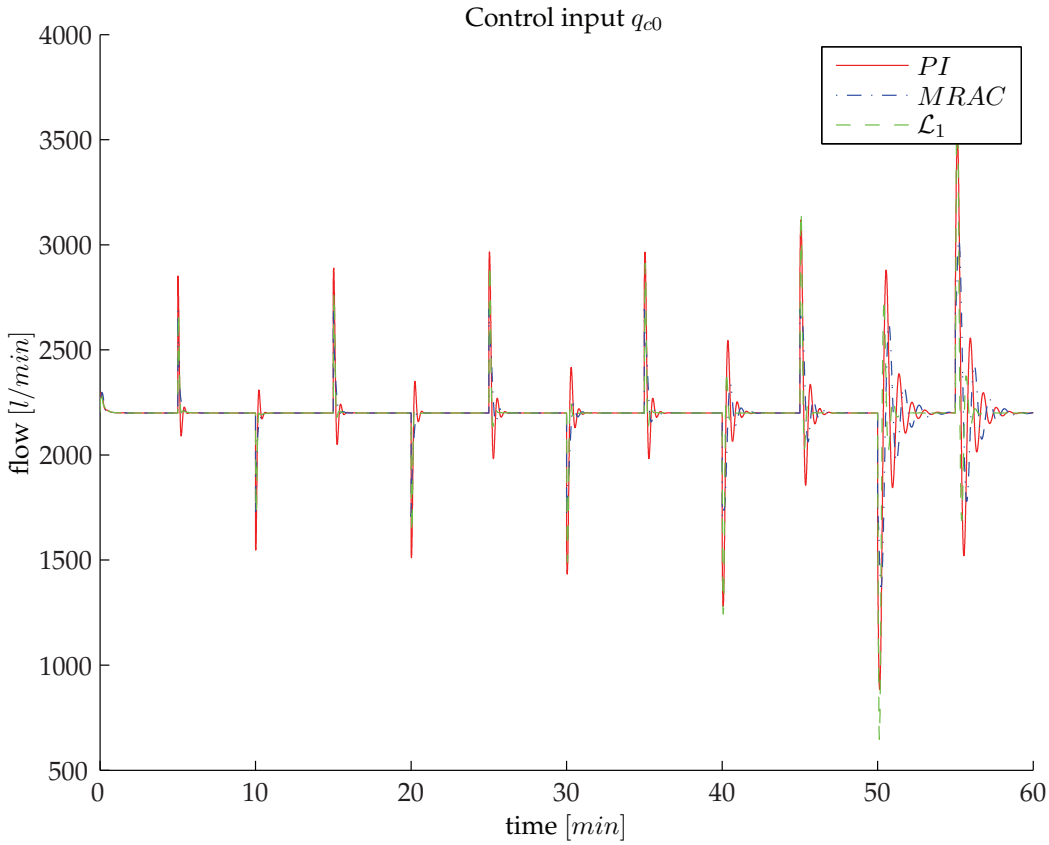

Figure 5.15: Changing bulk modulus β_a: Control performance in tracking

see that even for the adaptive controller we get a decrease in performance. We note however that the controller initially assumes a constant high-frequency gain and that with decreasing gain we get an increase in λ which implies worse performance.

5.4.3 Changing Friction Parameters

Changing friction parameters might occur if we drill into new types of rock, have changes to well topology or because we change equipment. This is simulated as a change in the friction parameters for the annulus.

We change the friction in steps as we did for the bulk modulus scenario; the changes are sudden and result in a total increase of F_a of approximately 50 percent. The scenario is performed for the bottomhole settings and thus only for the PI and $\mathcal{L}_1$ adaptive controller.

Comparison of the two controllers show small differences for this scenario, with good control performance for both controllers.

5.5 Control Structure

Finally we take a look at the control structures and evaluate topside versus bottomhole control. What are the strengths of the two different systems? The comparison is done for both the PI controller and the $\mathcal{L}_1$ adaptive controller. As mentioned before we will consider both the use of ideal values and the use of an observer.

5.5.1 Topside Control

Generating a control trajectory

In the ideal case, inversion of the bit pressure equation from 3.5, will produce the correct control path. However, this requires knowledge of all parameters. Another way to generate this path would be by the use of high-fidelity simulations. We may also use the Stamnes observer to estimate the unknowns in the bit pressure equation, and combine with measurements and known parameters to generate the path. The first and the last method are used to generate a control path comparable to direct bottomhole control.

5.5.2 Bottomhole Control

Getting good measurements

Direct control of the bottomhole pressure requires fast measurements, or at least good estimates of the bottomhole pressures. We consider two cases; in the first, good mea-

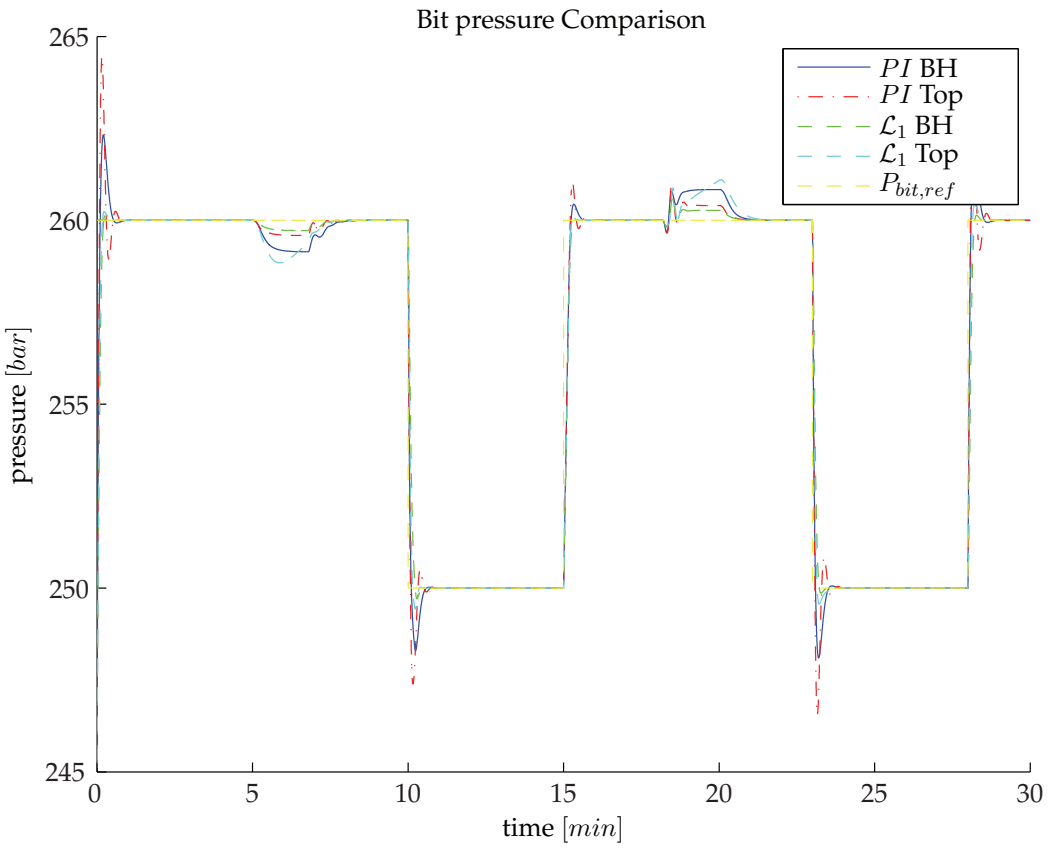

Figure 5.16: Ideal conversion: Direct bottomhole measurements are considered versus the ideal conversion scheme

surements are available through wired drill pipe, and in the second we use the Stamnes observer to estimate the bottomhole pressure.

5.5.3 Comparison of Control Structures

We start by comparing the two ideal cases. As we expect, we see from figure 5.16 that the differences are small, and most likely due to tuning differences.

For the observer case we note from figure 5.17 that the bottomhole values produce the best results. Conversion based on the estimated parameters give somewhat bad performance when we have disturbances. The large spike in the $\mathcal{L}_1$ adaptive controller is actually there because of saturation of the control input, without taking any measures to handle this saturation.

A consideration we have to make, is that it will be hard to include non-predicted events into pre-generated simulations, while adaptive observer based simulation might be able to handle these events.

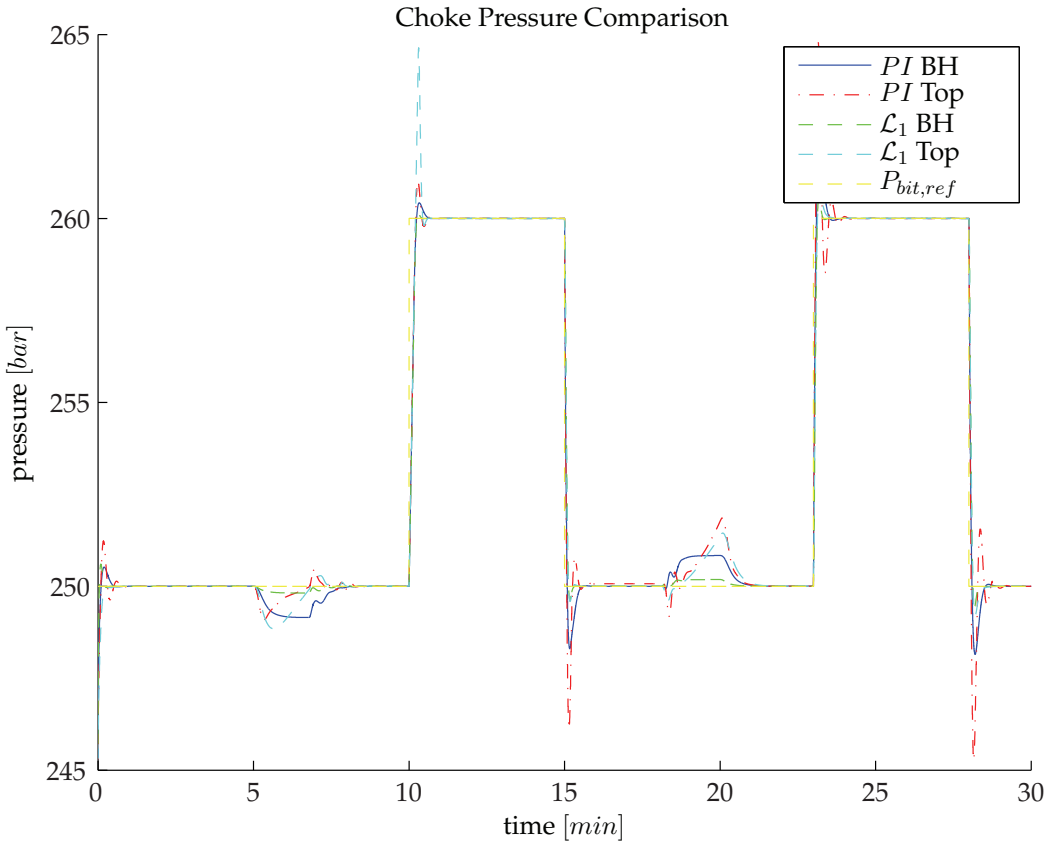

Figure 5.17: Bottomhole control based on estimated bit pressure is compared to a reference trajectory generated by an observer

Chapter 6

Discussion

In this chapter we look back at the results from chapter four and five. We look into controller complexity and implementation, robustness and performance, tuning requirements and common controller issues. How did the different control structures behave and what are their strengths and weaknesses? Finally I give some additional recommendations for future work on the area.

6.1 Controller Complexity

We know that the controller complexity might be a large obstacle for introduction into real industrial applications. Complex systems are harder to understand and maintain. How much additional complexity does the adaptive controllers introduce and how large is the impact on computational speed?

6.1.1 The PI Controller

The PI-controller is well-known, relatively easy to implement and has proved its value in millions of control systems. The controller complexity is low and there are many options for tuning. There is however need for some ad-hock solutions to handle some common problems with PI-controllers. The most important of these is perhaps the anti-windup implementation. It is vital to stop the integral error from increasing when the controller has already saturated and can provide no more or no less input. The overall complexity is still low and there is much knowledge on how to tune and implement the controller.

6.1.2 The MRAC Controller

The MRAC is widely used in some control environments and has many examples of use in the industry, but one cannot expect that drilling engineers have the same familiarity

to MRAC as they have to PI control. The controller adds additional complexity and new problems.

We introduce several new components, including the reference system and the adaptive laws. Most of the challenges are connected to the adaptive laws. One needs to consider new parameters, more gains and more initial conditions. There are few good analytic tools available to evaluate performance and much has to be done on an experimental basis.

6.1.3 The $\mathcal{L}_1$ Adaptive Controller

The $\mathcal{L}_1$-adaptive controller has recently been introduced and has seen few applications in the industry, in fact is has not even seen many evaluations. Here one can certainly not expect drilling engineers to know the controller, when most control experts do not even know of its existence. The controller is however in some environments getting a lot of attention, especially in the aeronautics community.

The control structure itself is not much more complex than MRAC, but we introduce a more difficult setup and performance selection. The complexity is thus quite high.

Selection of higher order filters is also an issue, and we may need to solve an optimization problem to get good time-delay margins.

In defense of the $\mathcal{L}_1$-adaptive controller, the additional complexity during creation might lead to less tuning and changes during actual operation.

6.1.4 Sampling and Numerical Issues

Sampling and numerical issues are quite important for the $\mathcal{L}_1$-adaptive controller. The wrong choice of numerical solver or time-steps can lead to instability or reduced performance. Though this is true for any controller, it is the author's opinion, that making the wrong choices is easier with this control method.

The run-time differences of the controllers were quite large. The fastest simulations were naturally for the PI controller, with a typical runtime of 5.88 minutes to simulate 30 minutes. The MRAC was not much worse with 9.36 minutes, while the the $\mathcal{L}_1$ adaptive controller used approximately 260 minutes, or 44 times the PI run-time. These numbers are influenced by computer load, subsystems loaded more often for $\mathcal{L}_1$ adaptive controller and many more parameters. However, typically the ODE solvers for the $\mathcal{L}_1$ adaptive controller represented 75 percent of the total simulation time. The $\mathcal{L}_1$ adaptive controller has very high observed computational needs.

6.2 Tuning Aspects

One of the reasons for evaluating adaptive control in MPD was to hopefully reduce the need for tuning. Does a larger operating area without any tuning justify introducing

several new tuning parameters and initial conditions? In this section we discuss the tuning needs of the three different controllers.

6.2.1 The PI Controller

There are many ways to tune PI-controllers, ranging from simple analytical tuning rules to self adjusting mechanisms. If the PI-controller always has to have good performance, we need to retune for changing dynamics and for large changes in parameters. This leads to a need for manual or automatic retuning for drilling operations. One solution is to create a wide array of tuning settings and use some kind of feedback mechanism to select the appropriate gain. Another possibility is to use a self-adjusting mechanism, but this leads to additional complexity, and it might not be possible or it might be very costly to make the changes of control input needed to identify all the parameters needed.

Tuning of the PI-controller in this thesis was done using the simple SIMC tuning methods from Skogestad (2003). The tuning is simple, with few tuning parameters.

The system did not need large changes to system parameters or dynamics to deteriorate control performance below the acceptable limits. The need for continuous re-tuning are thus high.

6.2.2 The MRAC

The tuning of the MRAC controller introduces a set of new tuning parameters. We need to select initial conditions for estimated variables, adaptation gains and the reference system.

Though we see better performance over varying parameters and disturbances, it was found that there is still a quite large need for tuning. It is hard to set good adaptation gains to offer both robustness and fast disturbance rejection, and we need to change these gains if we have large changes in parameters.

It is also of great importance to have good estimates of the parameters, as non-zero initialization errors might lead to poor performance during transients.

The reference system must also be selected to meet control specifications and to meet any matching conditions.

The tuning come with a greater startup cost and requires good estimates. However during operation the controller requires less tuning.

6.2.3 The $\mathcal{L}_1$ Adaptive Controller

The $\mathcal{L}_1$ adaptive controller has many tuning parameters and we have to make many choices of parameters and sets. We have however seen that only a few of the choices we make are critical to performance. There is a somewhat large difference between

the theoretically calculated values and the observed needed values, but then again the calculations have many strict requirements and conservative estimates.

The adaptive gains need to be selected sufficiently high. An easy rule is to set them as high as hardware permits. This may of course lead to a requirement of new hardware if the adaptive gain need to be selected very high.

The $\mathcal{L}_1$ adaptive controller also showed good performance for all disturbances, operating points and even with changing parameters. The needs for retuning are thus low, but we know that we might not have stability for very low ω, so some tuning with changing system gain might be needed.

6.3 Controller Performance and Robustness

From the previous chapter we can make some conclusions on controller performance.

While the PI controller performs well enough when correctly tuned, it needs very high integral effect to be able to counter fast disturbances like the power failure scenario. The high integral effect means we need quite aggressive tuning and it does not allow much change in parameters or dynamics before the observed performance is no longer sufficient. The time-delay margin for stability of the controller is good, but we have seen that stability does not equal good performance.

The MRAC controller in this thesis was perhaps tuned to allow for too much offset by disturbances. The performance during steps was tuned to have little overshoot and met the control demands in a very good fashion. The controller allows more changes to parameters and dynamics while still meeting the performance objectives. The time-delay margins are less than for the PI controller, but still quite good.

The $\mathcal{L}_1$ adaptive controller provides the best disturbance rejection, overall good tracking and has the largest operating area. The controller also has the lowest time-delay margins, which means that the time-delay of the overall control loop cannot be very high. Combined with the high computational needs this requires a high-end control system.

None of the controllers showed much performance degradation under the influence of noise, but drift limiting modifications were already in the design for both MRAC and the $\mathcal{L}_1$ adaptive controller. All controllers have potential windup if the control input saturates, and this must be handled.

6.4 Evaluation of Control Structures

The different control structures have somewhat different benefits and problems. We have seen that we have good measurements for the topside case, while the bottomhole case needs an observer to function.

Adjusting the bottomhole pressure via the choke pressure will give poor results if the estimated control trajectory is not accurate. We might need to combine observer data with simulations to change the control trajectory while drilling to be able to account for changes in the system.

For the bottomhole control method we will get poor performance if the estimates for the bottomhole pressure are not accurate.

The evaluation of the performance of the two control strategies is thus complicated, since the performance is more or less decided by the performance of the trajectory generator or the observer. The lesson learned might be that a good observer is a requirement no matter the control structure for MPD operations.

6.5 $\mathcal{L}_1$ Highlights

In the theory and background chapter I introduced some $\mathcal{L}_1$ adaptive control potential issues, which needed further investigation. Based on observations from the design, analysis and simulation chapter, we have seen that most of the issues were negligible.

We have seen that fast sampling of the control system is not a requirement, besides the need to keep the added contribution to time-delay below the stability limits. This may introduce the need for faster control systems and database operations might need to be kept outside the control loop.

Saturation needs to be handled, and an easy countermeasure is provided, but has not been theoretically justified.

The estimated values for adaptive gains based on the bounds provided showed not to be of great practical value. They however show us how we can increase performance.

The overall performance of the controller is good and it has showed great disturbance rejection. The $\mathcal{L}_1$ adaptive controller has shown both better performance and better ability to keep this performance during changes in the system than the PI controller.

The tuning requirements are somewhat complex, with many tuning parameters, but there are guidelines for selecting the most important tuning parameters. Once correctly initialized the controller needed little retuning even with changes in system parameters, but we might need to retune with a large drop in ω.

Changing ω did not lead to any stability issues, but to somewhat reduced performance.

Time did not permit the evaluation of higher order $C(s)$.

6.6 Conclusions

We have seen that the MRAC and $\mathcal{L}_1$ adaptive control provide better performance at the cost of a more complex control system, more complex setup and higher requirements on the available equipment. The employment of adaptive control is thus an issue of

added initial costs for hopefully lower long-time operating costs. $\mathcal{L}_1$ adaptive control provides the best results as long as we can keep the time-delay of the control loop below the stability margins, and if we can meet the computational requirements.

The comparison between the controllers is summed up in table 6.1.

Table 6.1: Comparison of the evaluated controllers

Evaluation	PI	MRAC	$\mathcal{L}_1$ adaptive control
Complexity	Low	Medium	High
Tuning parameters	Few	Some	Many
Tuning difficulty	Low	Medium	Medium
Tuning need	High	Medium	Low
Operating area	Small	Medium	Large
Overall performance	Poor	Medium	Good
Disturbance rejection	Medium	Medium	Good
Time-delay margins	Good	Medium	Poor
Computational needs	Low	Low	High

The control performance of the different control structures is decided by the performance of the trajectory generator or the observer. A good observer is a requirement no matter which control solution we select.

6.7 Contributions

One of the main contributions of this thesis is, to the author's knowledge, the first independent review of $\mathcal{L}_1$ adaptive control. $\mathcal{L}_1$ adaptive control is a very new control method and I believe the thesis offers a valuable evaluation of the control solution.

The other main contribution is the evaluation of two adaptive control methods versus the benchmark PI controller for MPD . As stated in the introduction chapter, the existing control solutions do not always satisfy the needs of all drilling operations. I have showed that adaptive control can help on some of the issues faced by conventional control, but not without costs.

6.8 Future work

There are several topics which need further development and analysis. The performance of the $\mathcal{L}_1$ adaptive controller needs to be further evaluated against other robust and adaptive control schemes.

I have also made some assumptions and modifications which need theoretical justification. Most notably the addition of projection on the state χ and allowing ω to be a time-varying gain. I suspect that it will be difficult to obtain hard results in the last case.

Finally one should try to use known parameters and signals to reduce the estimated bounds. Reducing the bounds will make a good choice of k easier and will give better performance.

The largest problems of the $\mathcal{L}_1$ adaptive control was the small time-delay margins and the high CPU cost. We know that higher-order filter design might provide the solution to both problems. It should be of high priority to look into good design choices for $C(s)$.

Appendix A

Preliminaries

This chapter holds theorems and some basic definitions used in the derivations of this thesis.

A.1 Theorems

Theorem 2. *Let $D = \{x \in R^n \mid \|x\| < r\}$ and suppose that $f(x,t)$ is locally Lipschitz on $D \times [0,\infty)$. Let V be a continuously differentiable function such that*

$$\alpha_1(\|x\|) \leq V(x,t) \leq \alpha_2(\|x\|)$$

and

$$\frac{dV}{dt} = \frac{\delta V}{\delta t} + \frac{\delta V}{\delta x} f(x,t) \leq -W(x) \leq 0$$

$\forall t \leq 0$, $\forall x \in D$, where α_1 and α_2 are class K functions defined on $[0,r)$ and $W(x)$ is continuous on D. Further, it is assumed that dV/dt is uniformly continuous in t.

Then all solutions to $\frac{dx}{dt} = f(x,t)$ with $\|x(t_0)\| < {\alpha_2}^{-1}(\alpha_1(r))$ are bounded and satisfy

$$W(x(t)) \to 0 \text{ as } t \to \infty$$

Moreover, if all assumptions hold globally and α_1 belongs to class K_∞, the statement is true for all $x(t_0) \in R^n$.

Appendix B

Tuning

This chapter holds closer information and plots from the tuning of the different controllers.

B.1 $\mathcal{L}_1$ Tuning

B.1.1 Different gain settings for the update laws for the $\mathcal{L}_1$ adaptive controller

Different values for the adaptation gains (see table B.1) are here used to illustrate how the gain affects tracking performance. The need to tune the adaptive gains in $\mathcal{L}_1$ adaptive control is limited, as one selects the gains as high as hardware permits. The gain must be selected sufficiently high, while increasing the gain much above this limit will have diminishing effect.

We see from figure B.1 that if the adaptive gains are set too low, we cannot provide acceptable performance, while gains set higher than necessary give only small improvements in performance. The control input is showed in figure B.2 and has no apparent issues. The estimated parameters are shown in figure B.3 and B.4; we see that the low gain has problems giving good estimates. In figure B.5 the high gain state estimate is plotted against the low gain estimate and the actual states. It can be observed that the estimate for the low gain is very poor.

Table B.1: $\mathcal{L}_1$ - Adaptation gain table

Gain setting	Γ_σ	Γ_ω
Low	0.01	0.01
Medium	1	1
High	100	100

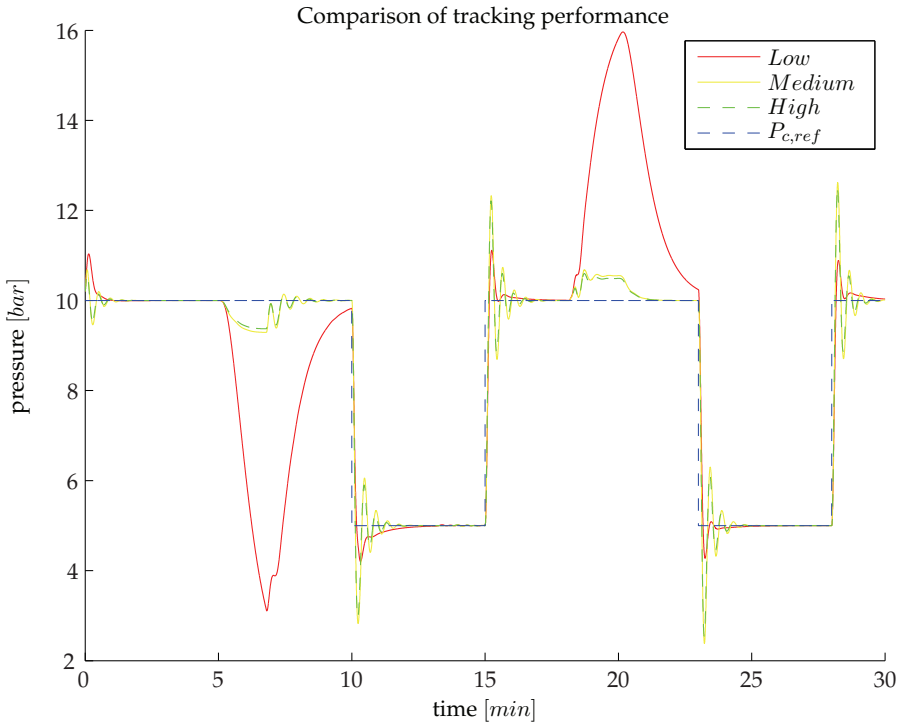

Figure B.1: Tuning of L1: Adaptive gains - Tracking performance.

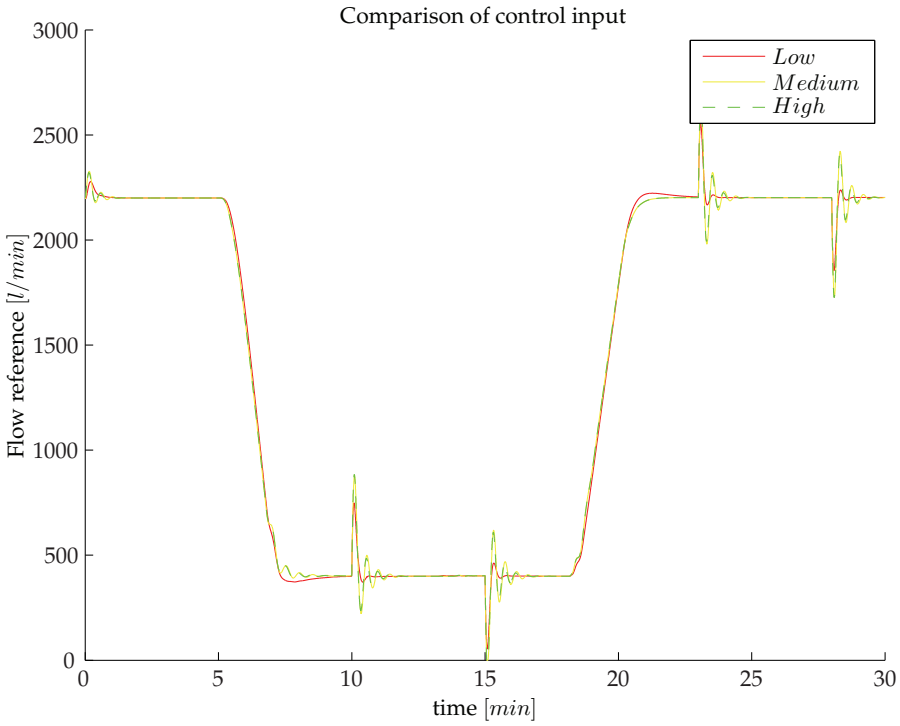

Figure B.2: Tuning of L1: Adaptive gains - Control input usage.

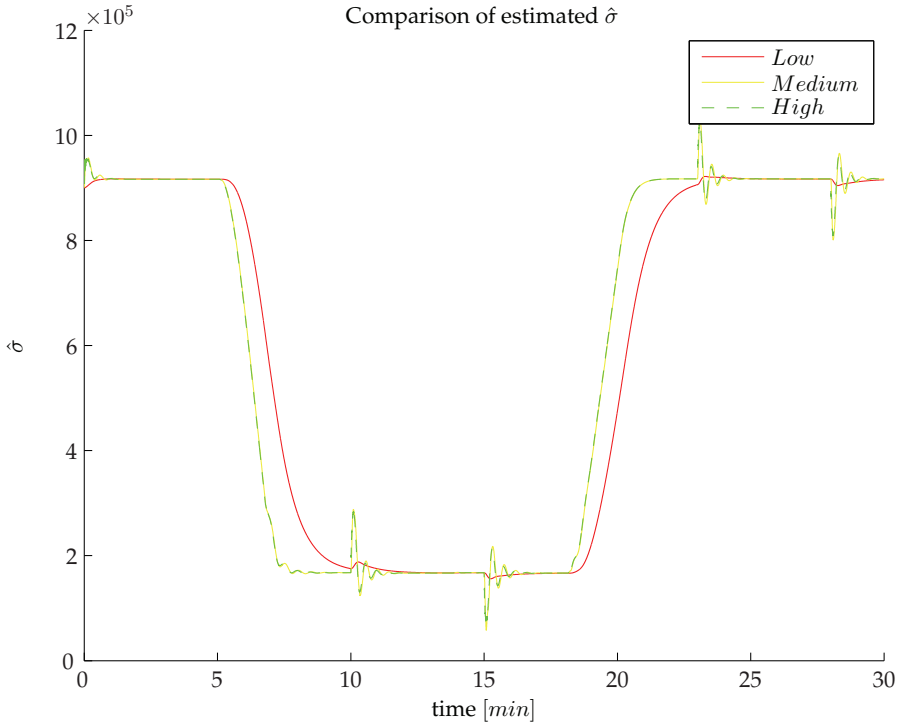

Figure B.3: Tuning of L1: Adaptive gains - parameter σ.

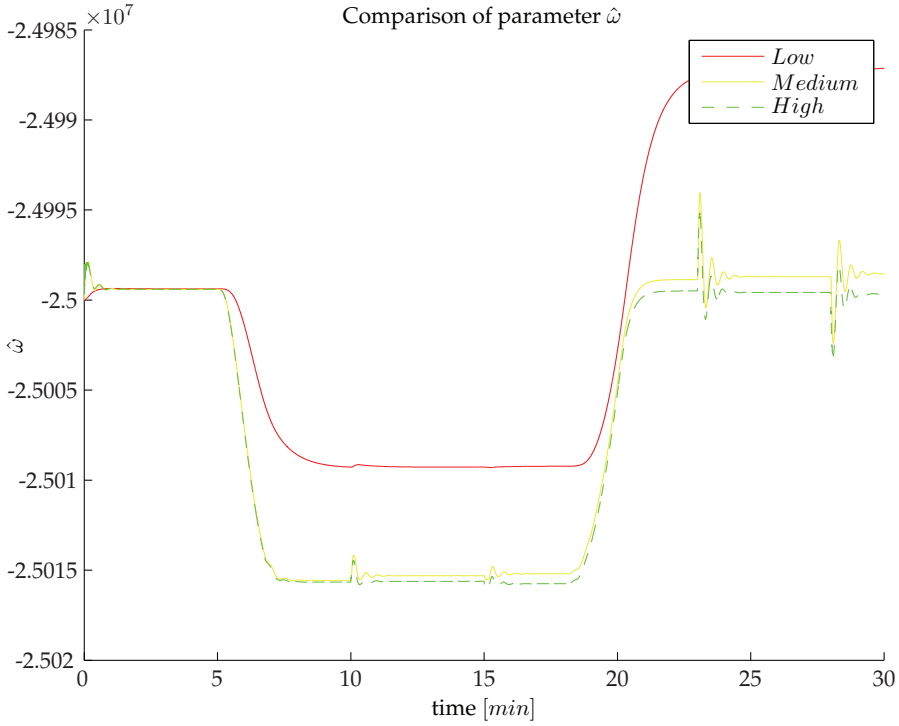

Figure B.4: Tuning of L1: Adaptive gains - parameter ω.

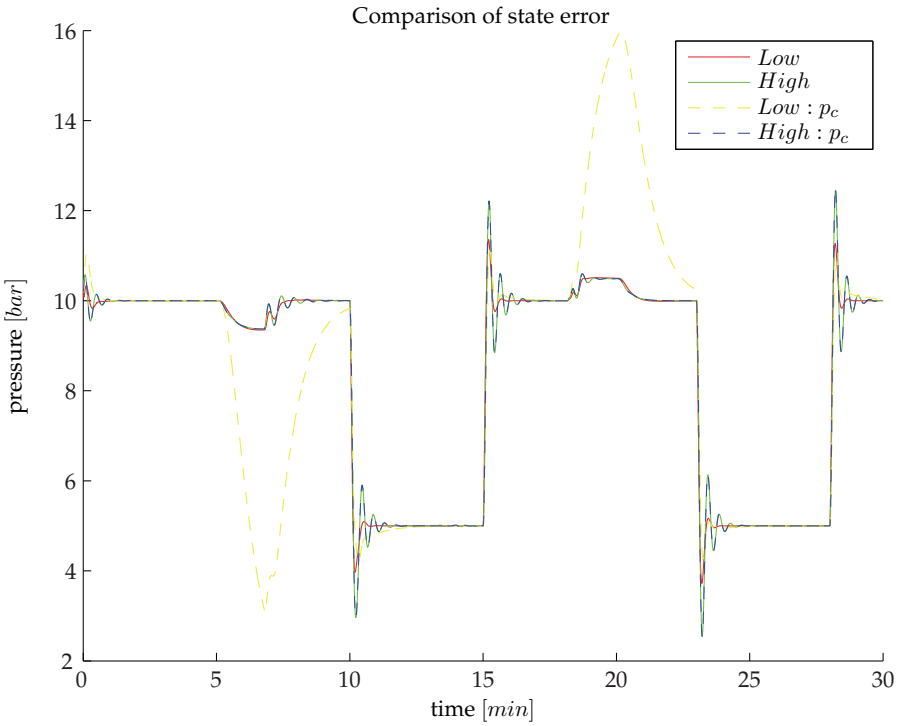

Figure B.5: Tuning of L1: Adaptive gains - State estimate.

B.1.2 Selection of Initial Values

How important is the selection of initial conditions for the estimated parameters in $\mathcal{L}_1$ adaptive control? We know for MRAC that non-zero trajectory initialization can lead to large transient tracking errors, but in Cao & Hovakimyan (2008*e*) it is shown that for the $\mathcal{L}_1$ adaptive controller this will only lead to exponential decaying errors in the transient phase. We simulate this by employing the estimated values $k^* = [\hat{\sigma}_0, \hat{\omega}_0]$, and $0.2 \cdot k^*$ and $5 \cdot k^*$.

Simulations showed that we get a short period where the parameters adjust, however, we see no change in performance at all. The need for very good estimates is thus low.

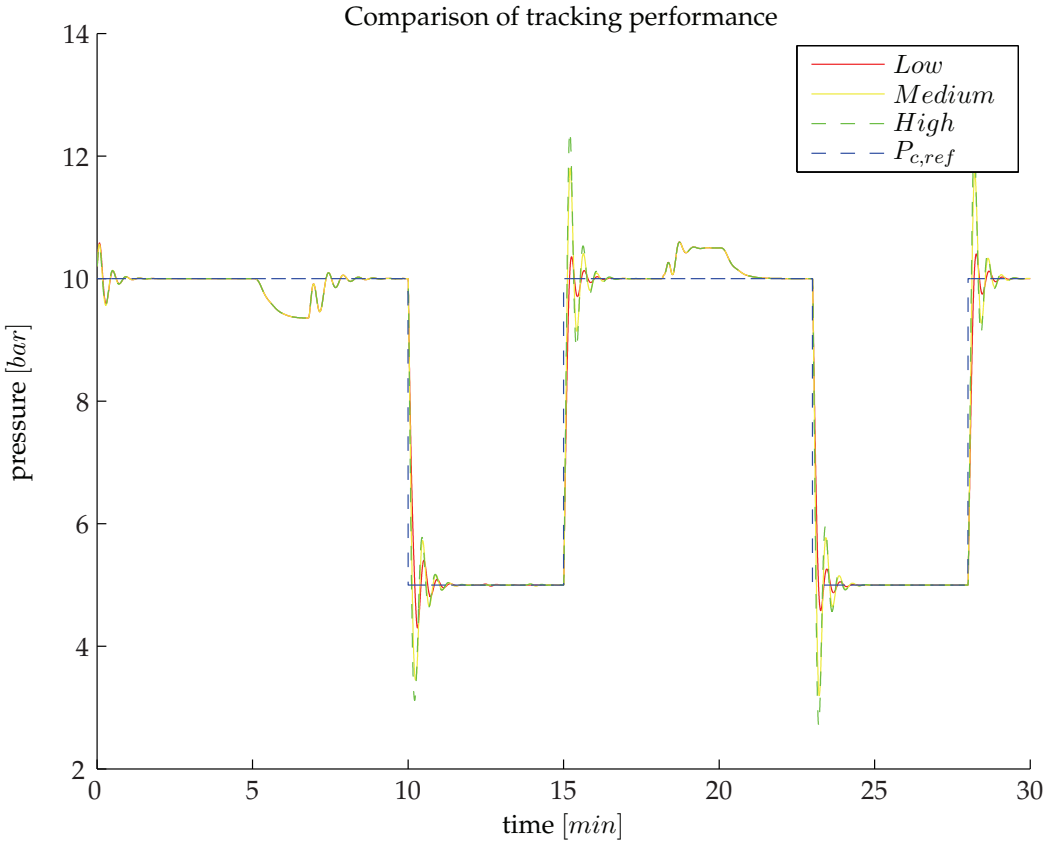

Figure B.6: Tuning of MRAC: Reference systems - Tracking performance.

B.2 MRAC Tuning

B.2.1 Different Reference Model Settings for the MRAC

We compare different reference models to show how they specify control performance of the MRAC. A first order reference model of the form of equation 3.7 is selected, and the different settings for A_m is used in simulation of the connection scenario. However, the medium value is also acceptable.

Table B.2: MRAC - Reference Model settings

Gain setting	A_m	b_m
Low	-0.2	0.2
Medium	-0.5	0.5
High	-1	1

We see from figure B.6 and B.7 that the low value for the reference systems gives the smoothest tracking performance and has the best gain usage.

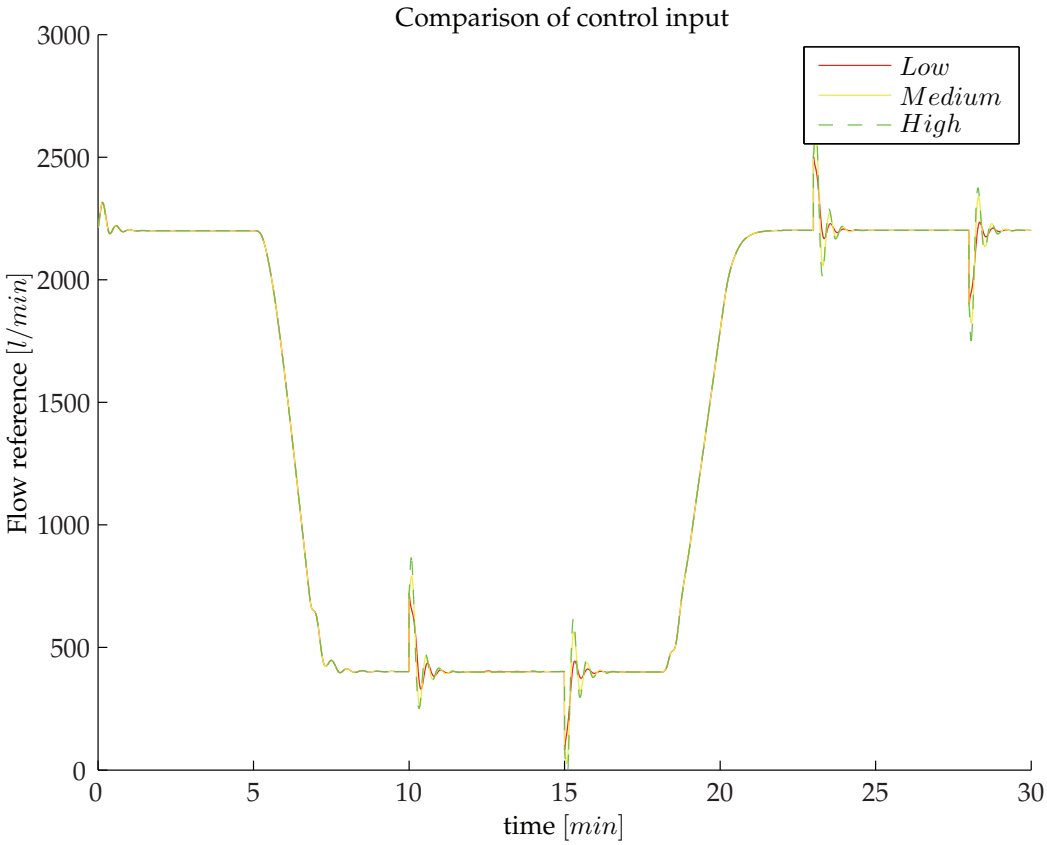

Figure B.7: Tuning of MRAC: Reference systems - Control Input.

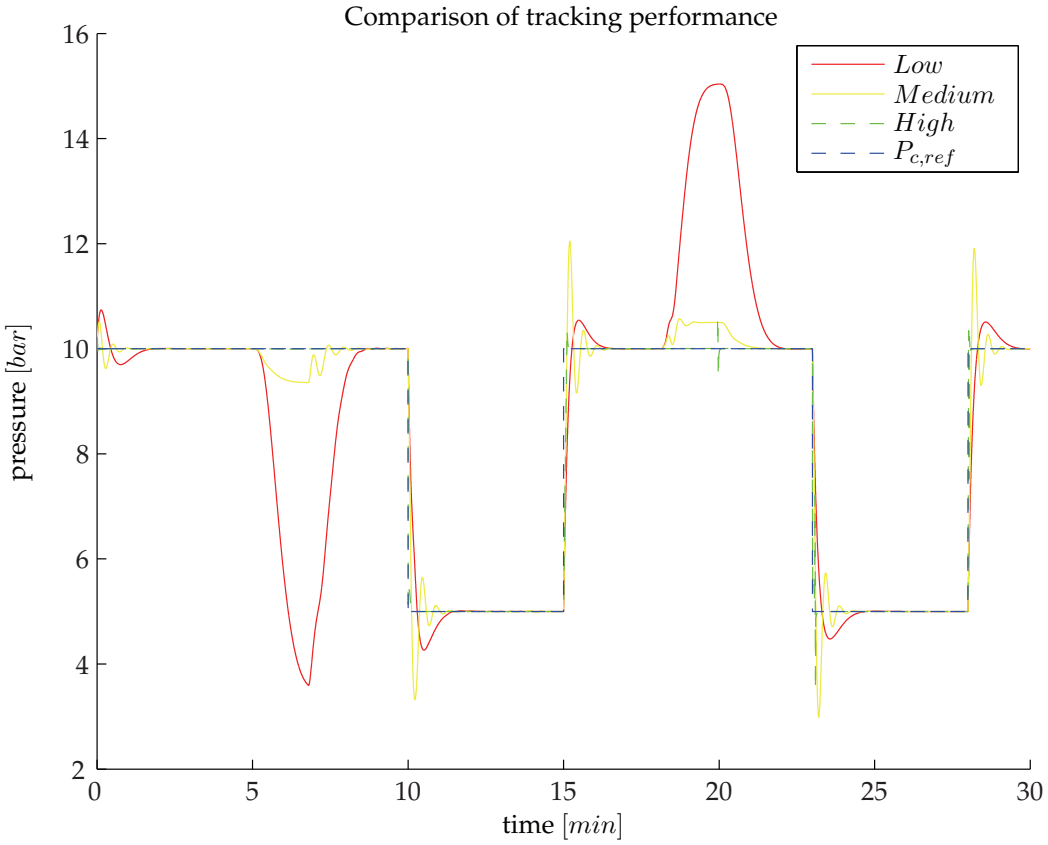

Figure B.8: Tuning of MRAC: Adaptive gains - Tracking performance.

B.2.2 Selection of Adaptive Gains

We want to select the adaptive gains as high as possible to get good performance in the presence of changes and disturbances. However, we know that selecting high gains will hurt the time-delay margin. Selection of the adaptive gains is thus a compromise between tracking performance and robustness and it can be hard to find good gains.

Table B.3: MRAC - Adaptive gains settings

Gain setting	γ_0	γ_1	γ_2
Low	$1 \cdot 10^{-11}$	$1 \cdot 10^{-11}$	$5 \cdot 10^{-11}$
Medium	$1 \cdot 10^{-10}$	$1 \cdot 10^{-10}$	$5 \cdot 10^{-9}$
High	$1 \cdot 10^{-5}$	$1 \cdot 10^{-5}$	$1 \cdot 10^{-7}$

In figure B.8 we see the difference between three different adaptive gains and the influence on tracking performance. We select the medium values, but set them somewhat lower ($\gamma_0 = \gamma_1 = 1 \cdot 10^{-14}$) to improve robustness.

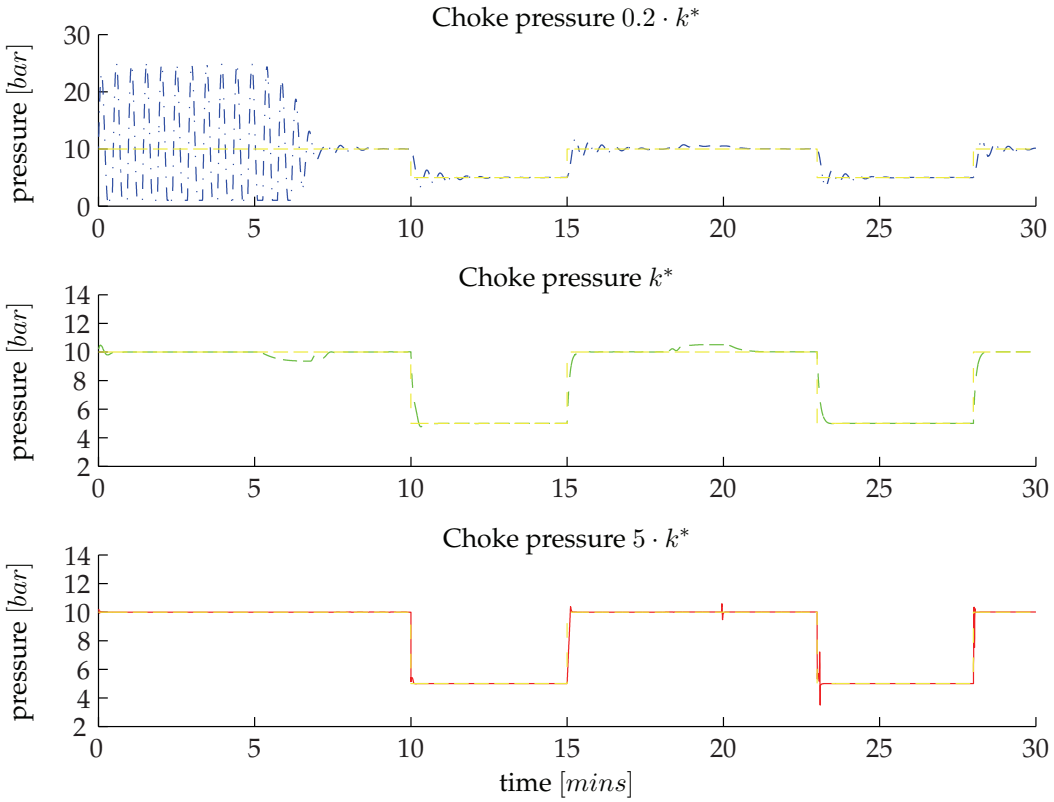

Figure B.9: Tuning of MRAC: Initial values - Tracking performance.

B.2.3 Selection of Initial Values

We have good estimates for the initial conditions of k_0, k_1 and k_2, but what happens if the estimates are bad? We try evaluating different initial conditions for the MRAC. We call the good guess for k^*. The bad guesses are set as $0.2 \cdot k^*$ and $5 \cdot k^*$.

From figure B.9 and B.10 we see that the bad guesses for initial values give very poor performance during the initial phase. Especially the low initial guess gives an unacceptable transient phase for the controlled variable, but also the high initial estimate gives high spikes in the control input.

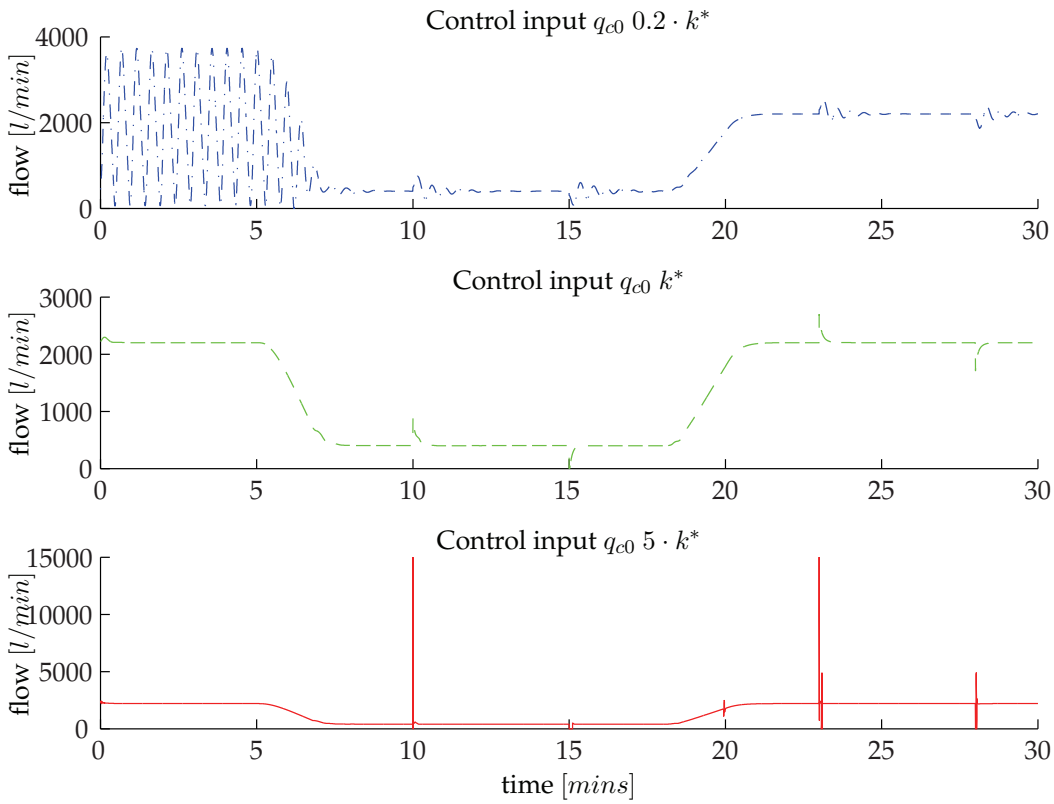

Figure B.10: Tuning of MRAC: Initial values - Control Input.

B.3 PI Tuning

B.3.1 Different Tuning Settings for the PI-Controller

The PI-Controller was tuned using SIMC (Skogestad/Simple IMC) tuning rules for integrating processes. The basis for this method is to approximate the process with a first-order plus time delay model (Skogestad 2003, Skogestad & Postlethwaite 2007),

$$G(s) = \frac{k}{\tau s + 1} e^{-\theta s} \tag{B.1}$$

or for integrating processes

$$\frac{k}{\tau s + 1} \approx \frac{k}{\tau s} = \frac{k'}{s} \tag{B.2}$$

For a PI controller Skogestad suggest the following settings

$$K_c = \frac{1}{k} \frac{\tau}{\tau_c + \theta} = \frac{1}{k'} \frac{1}{\tau_c + \theta}, \tag{B.3}$$

$$\tau_I = \min\left(\tau,\ 4(\tau_c + \theta)\right). \tag{B.4}$$

where τ_c is a tuning parameter where $-\theta < \tau_c < \infty$ and $k' = k/\tau$. The selection of τ_c is a trade-off between

1. Fast speed of response and good disturbance rejection, and
2. Stability, robustness and small input usage

The first is favored by a small value of τ_c and the second by a large value for τ_c (Skogestad 2003).

From a bump test of the well, using a Simulink model, we get the parameters for the topside control scheme for the first-order plus time delay model. We list them in table B.4 and the corresponding gains, in B.5.

Table B.4: Skogestad Tuning - Topside: First order plus time delay model

Operating point	τ	θ	Δy	Δu	k
$q_{c,h} = 2200$ [l/min]	3	0	2.39 [bar]	200 [l/min]	$-7.16 \cdot 10^7$
$q_{c,l} = 400$ [l/min]	6	0	4.88 [bar]	200 [l/min]	$-1.46 \cdot 10^8$

Is there really no deadtime in the system? The bump test was carried out on the much simpler Simulink models, and from simulations of the complete simulation model we see that there is deadtime in the system. The slower inner dynamics, the longer deadtime. The deadtime is however small, but one could consider increasing T_i.

Table B.5: Skogestad Tuning - Topside: Gain Table

τ_c	0.5	2	10
$K_{c,h}$	$-8.38 \cdot 10^{-8}$	$-2.09 \cdot 10^{-8}$	$-4.19 \cdot 10^{-9}$
$T_{i,h}$	2	3	3
$K_{c,l}$	$-8.20 \cdot 10^{-8}$	$-2.05 \cdot 10^{-8}$	$-4.10 \cdot 10^{-9}$
$T_{i,l}$	2	6	6

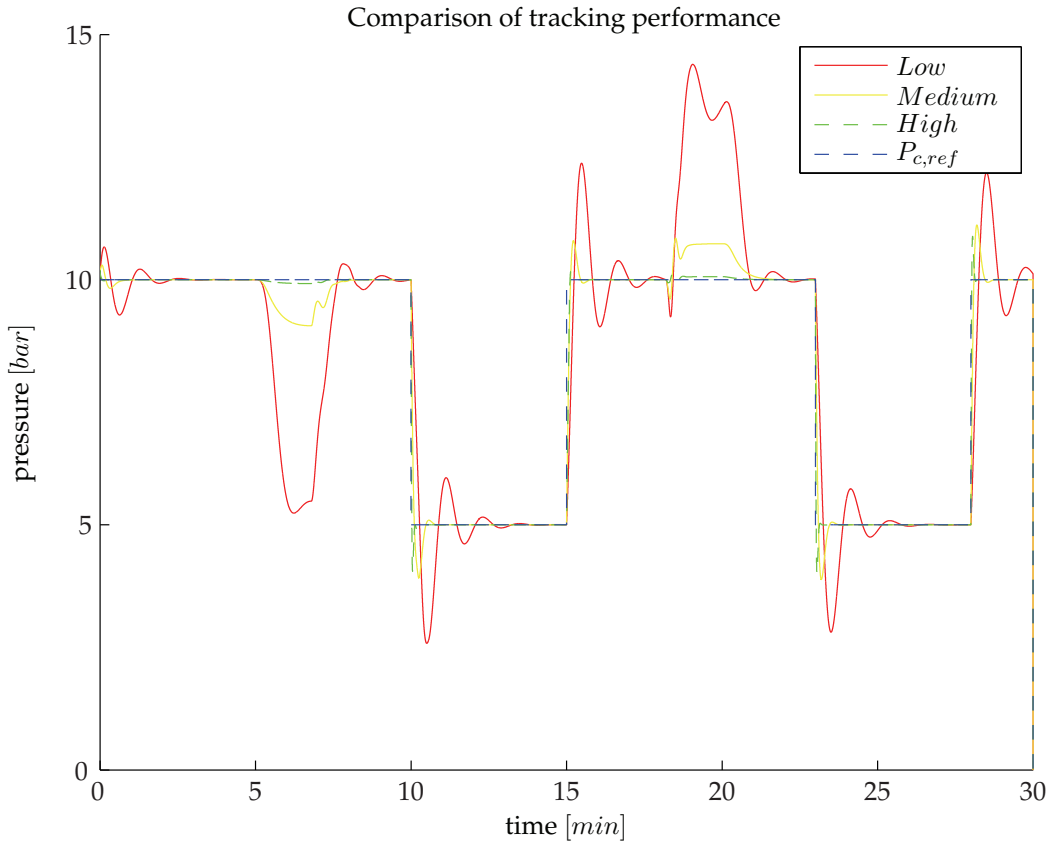

Figure B.11: Tuning of PI controller: Tracking performance. The Low setting equals $K_c = 10$, Medium is $K_c = 2$ and High is $K_c = 0.5$

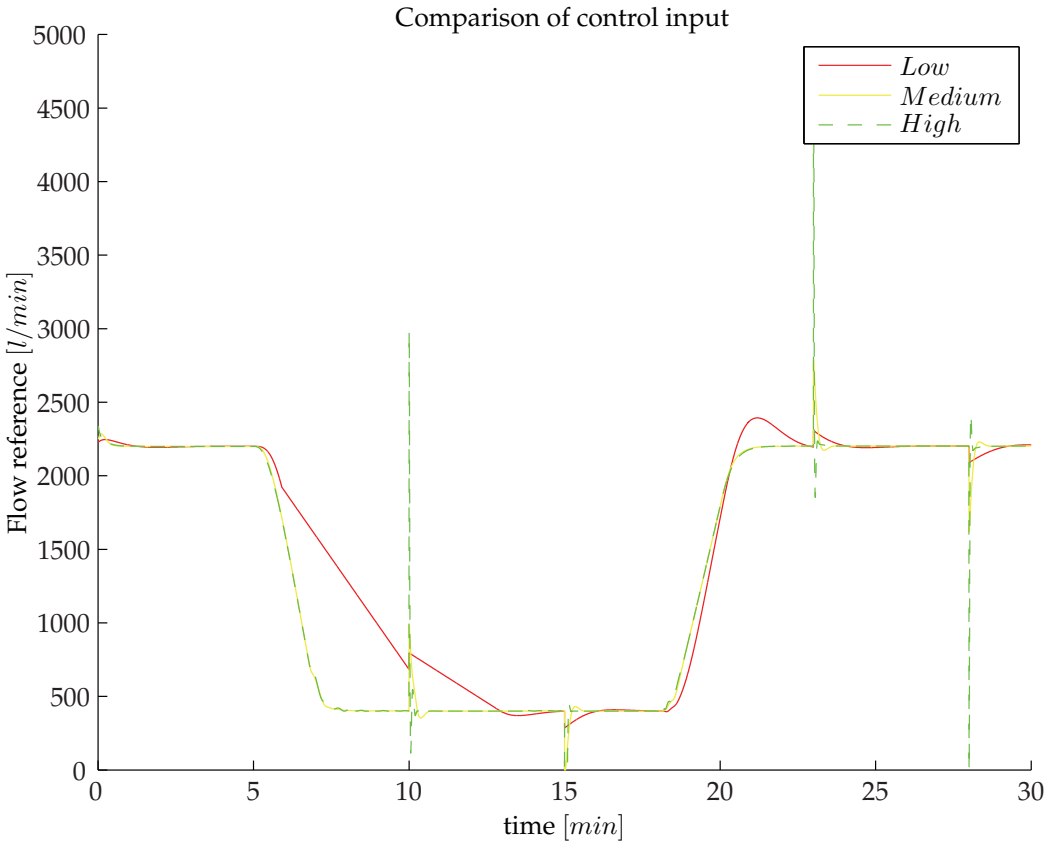

Figure B.12: Tuning of PI controller: Control input usage. The Low setting equals $K_c = 10$, Medium is $K_c = 2$ and High is $K_c = 0.5$

We try simulating with these values in the connection scenario, where we have both reference changes and disturbances to evaluate performance.

We see from figure B.11 and B.12 that for the lowest setting for K_c we get very good following and disturbance rejection, but we also have very large peaks in the control input. The highest value for K_c results in very poor tracking and disturbance rejection. The medium value gives acceptable tracking and rejection, and at the same time it has a much more sensible control input usage and is therefore selected. We also know that it offers more robustness. The same procedure was done for the bottomhole control structure. The model parameters and control gains are summarized in table B.6 and B.7.

Table B.6: Skogestad Tuning - Bottomhole: First order plus time delay model

Operating point	τ	θ	Δy	Δu	k
$q_{c,h} = 2200$ [l/min]	30	0	19.01 [bar]	200 [l/min]	$-5.70 \cdot 10^8$
$q_{c,l} = 400$ [l/min]	30	0	18.26 [bar]	200 [l/min]	$-5.48 \cdot 10^8$

Table B.7: Skogestad Tuning - Bottomhole: Gain Table

τ_c	0.5	2	10
$K_{c,h}$	$-1.05 \cdot 10^-7$	$-2.63 \cdot 10^{-8}$	$-5.26 \cdot 10^{-9}$
$T_{i,h}$	2	8	30
$K_{c,l}$	$-1.10 \cdot 10^{-7}$	$-2.74 \cdot 10^{-8}$	$-5.48 \cdot 10^{-9}$
$T_{i,l}$	2	8	30

Appendix C

Simulations

C.1 Simulation Overview

A wide array of simulations was tested for the system and only the most important plots are included in this thesis. However, the simulation data and additional figures are available on the compact disk. A simulation overview of the data available is given in table C.1 and C.2.

Table C.1: Topside simulations

Scenario	PI	MRAC	$\mathcal{L}_1$ low k	Slow MRAC	$\mathcal{L}_1$
Connection	✓	✓	✓	✓	✓
Noisy Connection	✓	✓	✓	-	-
Power Loss	✓	✓	✓	-	-
Mud loss high flow	✓	✓	✓	-	-
Mud loss low flow	✓	✓	✓	-	-
Kick	✓	✓	✓	-	-
Fast ΔP term	-	-	-	-	-
Friction	-	-	-	-	-
Inner dynamics	✓	✓	✓	-	-
Inner dynamics slow	✓	✓	✓	✓	-
Inner dynamics slower	✓	✓	✓	✓	-
Changing β_a	✓	✓	✓	✓	-
Sampling 0.1 $[sec]$	-	-	✓	-	-
Sampling 0.5 $[sec]$	✓	✓	✓	-	-
Sampling 1.0 $[sec]$	✓	✓	✓	-	-
Sampling 2.0 $[sec]$	✓	✓	✓	-	-
Sampling 1.0 $[sec]$ and added inner dynamics	✓	✓	✓	-	-
Sampling 0.5 $[sec]$, hold for 0.5 $[sec]$ and added dynamics	✓	✓	✓	-	-
Drift	-	✓	✓	-	-
Drift with modifications	-	✓	-	-	-
Saturation	✓	✓	✓	-	-
Saturation with mod.	✓	✓	✓	-	-
Reference trajectory	✓	✓	✓	-	-
Observer / trajectory	✓	✓	✓	-	-
Tuning adaptive gains	-	✓	✓	-	-
Tuning initial values	-	✓	✓	-	-
Tuning gains	✓	-	-	-	-
Tuning reference model	-	✓	✓	-	-
High gain changing β_a	-	-	✓	-	-

Table C.2: Bottomhole simulations

Scenario	PI	$\mathcal{L}_1$ low k	$\mathcal{L}_1$
Connection	✓	✓	-
Noisy Connection	-	-	-
Power Loss	-	-	-
Mud loss	-	-	-
Kick	-	-	-
Fast ΔP term	-	-	-
Friction	-	-	-
Inner dynamics	✓	✓	-
Inner dynamics slow	✓	✓	-
Inner dynamics slower	-	-	-
Changing β_a	✓	✓	-
Changing ρ	✓	✓	-
Sampling 0.1 $[sec]$	-	-	-
Sampling 0.5 $[sec]$	-	-	-
Sampling 1.0 $[sec]$	-	-	-
Sampling 2.0 $[sec]$	-	-	-
Sampling 1.0 $[sec]$ and added inner dynamics	-	-	-
Sampling 0.5 $[sec]$, hold for 0.5 $[sec]$ and added dynamics	-	-	-
Drift	-	-	-
Drift with modifications	-	-	-
Saturation	-	-	-
Saturation with mod.	-	-	-
Reference trajectory	-	-	-
Observer / trajectory	✓	✓	-
Tuning adaptive gains	-	-	-
Tuning initial values	-	-	-
Tuning gains	✓	-	-
Tuning reference model	-	-	-
High gain changing β_a	-	-	-

Bibliography

AtBalance (2008), 'Managed Pressure Drilling - Pressure Control', `http://www.atbalance.com/TE_mpd_system.html`. Fetched 2008-10-12.

Azar, J. J. & Samuel, G. R. (2007), *Drilling Engineering*, 1st edn, PennWell Corporation.

Butler, H. (1992), *Model Reference Adaptive Control - From Theory to Practice*, 1st edn, Prentice-Hall, Inc.

Cao, C. & Hovakimyan, N. (2006*a*), Design and Analysis of a Novel $\mathcal{L}_1$ Adaptive Controller, Part I: Control Signal and Asymptotic Stability, *in* 'Proceedings of the 2006 American Control Conference'.

Cao, C. & Hovakimyan, N. (2006*b*), Design and Analysis of a Novel $\mathcal{L}_1$ Adaptive Controller, Part II: Guaranteed Transient Performance, *in* 'Proceedings of the 2006 American Control Conference'.

Cao, C. & Hovakimyan, N. (2007*a*), Guaranteed Transient Performance with $\mathcal{L}_1$ Adaptive Controller for Parametric Strict Feedback Systems, *in* 'Proceedings of the 2007 American Control Conference'.

Cao, C. & Hovakimyan, N. (2007*b*), Guaranteed Transient Performance with $\mathcal{L}_1$ Adaptive Controller for Systems with Unknown Time-varying Parameters and Bounded Disturbances: Part I, *in* 'Proceedings of the 2007 American Control Conference'.

Cao, C. & Hovakimyan, N. (2007*c*), $\mathcal{L}_1$ Adaptive Output Feedback Controller for Systems with Time-varying Unknown Parameters and Bounded Disturbances, *in* 'Proceedings of the 2007 American Control Conference'.

Cao, C. & Hovakimyan, N. (2007*d*), $\mathcal{L}_1$ Adaptive Output Feedback Controller to Systems of Unknown Dimension, *in* 'Proceedings of the 2007 American Control Conference'.

Cao, C. & Hovakimyan, N. (2007*e*), Stability Margins of $\mathcal{L}_1$ Adaptive Controller: Part II, *in* 'Proceedings of the 2007 American Control Conference'.

Cao, C. & Hovakimyan, N. (2008*a*), 'Design and Analysis of a Novel $\mathcal{L}_1$ Adaptive Control Architecture With Guaranteed Transient Performance', *IEEE Transactions on Automatic Control* **53**(2).

Cao, C. & Hovakimyan, N. (2008*b*), $\mathcal{L}_1$ Adaptive Controller for a Class of Systems with Unknown Nonlinearities: Part I, *in* '2008 American Control Conference'.

Cao, C. & Hovakimyan, N. (2008*c*), $\mathcal{L}_1$ Adaptive Controller for Multi-Input Multi-Output Systems in the Presence of Unmatched Disturbances, *in* '2008 American Control Conference'.

Cao, C. & Hovakimyan, N. (2008*d*), $\mathcal{L}_1$ Adaptive Controller for Nonlinear Systems in the Presence of Unmodelled Dynamics: Part II, *in* 'Proceedings of the 2008 American Control Conference'.

Cao, C. & Hovakimyan, N. (2008*e*), '$\mathcal{L}_1$ adaptive controller for systems with unknown time-varying parameters and disturbances in the presence of non-zero trajectory initialization error', *International Journal of Control* **81**(7), 1147 – 1161.

Cao, C. & Hovakimyan, N. (2009), '$\mathcal{L}_1$ Adaptive Output-Feedback Controller for Non-Strictly-Positive-Real Reference Systems: Missile Longitudinal Autopilot Design', *Journal of Guidance, Control and Dynamics* **32**(3).

Cao, C., Hovakimyan, N., Kaminer, I., Patel, V. V. & Dobrokhodov, V. (2007), Stabilization of Cascaded Systems via $\mathcal{L}_1$ Adaptive Controller with Application to a UAV Path Following Problem and Flight Test Results, *in* 'Proceedings of the 2007 American Control Conference'.

Dozal-Mejorada, E. J. & Ydstie, B. E. (2007), Adaptive Control with Model Based Supervision and Non-convex Parameter Estimation. Results presented at DYCOPS 2007 in Cancún, México. Submitted for review in Automatica.

Godhavn, J.-M. (2009), Control Requirements for High-End Automatic MPD Operations, *in* 'SPE/IADC Drilling Conference and Exhibition'.

Hannegan, D. (2006), Case Studies - Offshore Managed Pressure Drilling, *in* 'SPE Annual Technical Conference and Exhibition'.

Hannegan, D. M. (2006-2007), 'Managed Pressure Drilling - A new way of looking at drilling hydraulics, Overcoming conventional drilling challenges'.

Hovakimyan, N. (2008), 'Robust Adaptive Control - UIUC MechSE 598'. Lecture Notes.

Ioannou, P. A. & Sun, J. (1996), *Robust Adaptive Control*, 1st edn, Prentice-Hall, Ltd.

Jahn, F., Cook, M. & Graham, M. (2008), *Hydrocarbon Exploration and Production*, 2nd edn, Elsevier.

Kaasa, G.-O. (2007), A Simple Dynamic Model of Drilling for Control..., Technical report, Hydro Oil and Energy, Porsgrunn Research Centre.

Kaasa, G.-O. (2008), 'Well drawing'.

Li, D., Patel, V. V., Cao, C., Hovakimyan, N. & Wise, K. (2007), Optimization of the Time-Delay Margin of $\mathcal{L}_1$ Adaptive Controller via the Design of the Underlying Filter, *in* 'AIAA Guidance, Navigation and Control Conference and Exhibit'.

Patel, V. V., Cao, C., Hovakimyan, N., Wise, K. A. & Lavretsky, E. (2007), $\mathcal{L}_1$ Adaptive Controller for Tailless Unstable Aircraft, *in* 'Proceedings of the 2007 American Control Conference'.

Pedersen, T. (2008), Experimental Evaluation of Model-Reference Adaptive Control for Managed Pressure Drilling. Master's Project, NTNU.

Skogestad, S. (2003), 'Simple analytic rules for model reduction and PID controller tuning', *Journal of Process Control* **13**, 291–309.

Skogestad, S. & Postlethwaite, I. (2007), *Multivariable Feedback Control*, 2nd edn, John Wiley & Sons, Ltd.

Stamnes, Ø. N. (2007), Adaptive Observer for Bottomhole Pressure Drilling, Master's thesis, NTNU.

Åström, K. J. & Wittenmark, B. (1995), *Adaptive Control*, 2nd edn, Addison-Wesley Publishing Company, Inc.

Tsakalis, K. S. & Ioannou, P. A. (1993), *Linear Time-Varying Systems: Control and Adaptation*, 1st edn, Prentice-Hall, Inc.

van Riet, E., Reitsma, D. & Vandecraen, B. (2003), Development and Testing of a Fully Automated System to Accurately Control Downhole Pressure During Drilling Operations, *in* 'SPE/IADC Middle East Drilling Technology Conference & Exhibition'.

Wise, K. A., Lavretsky, E. & Hovakimyan, N. (2008), 'Robust and Adaptive Control Workshop'. Course notes from workshop held at the StatoilHydro Porsgrunn Research Centre in July 2008.